Interaction Partners of the Postsynaptic Protein Sharpin: Involvement in Protein Degradation in *Rattus norvegicus* and a Human Cell Line

Ph.D. Thesis

submitted by

Gwendlyn Kollmorgen

University of Hamburg

Faculty of Biology

2007

Genehmigt vom Department Biologie
der Fakultät für Mathematik, Informatik und Naturwissenschaften
an der Universität Hamburg
auf Antrag von Herrn Priv.-Doz. Dr. H.-J. KREIENKAMP
Weiterer Gutachter der Dissertation:
Herr Professor Dr. H. BRETTING
Tag der Disputation: 09. November 2007

Hamburg, den 26. Oktober 2007

Professor Dr. Reinhard Lieberei
Leiter des Departments Biologie

Abbreviations

aa	amino acids
AAA-ATPase	ATPases associated with diverse cellular activities
Abi-1	Abelson interacting protein1
Abp1	actin binding protein
Ala	alanine
AMP	ampicillin
Ank	ankyrin
AP-2	clathrin adaptor protein 2
AraC	Cytosine-β-D-Arabinofuranoside
Asp 58	aspartate residuein position 58 of ubiquitin
Asp58Ala	aspartate 58 of ubiquitin mutated to Ala
B27	B27 Supplement
BSA	bovine serum albumin
c	centi
cdpm	chronic proliferative dermatitis
c-myc	cellular myc protooncogene
CP	core particle
C-terminus	carboxy-terminus
ºC	degrees Celsius
CUE	coupling of ubiquitin conjugation to endo-plasmic reticulum-associated degradation
DAPI	4',6-diamidino-2-phenylindole
DIV	days *in vitro*
DMEM	Dulbecco's Modification of Eagle's Medium
dMM	1-deoxymannojirimycin
DMSO	dimethylsulfoxide
DNA	deoxyribonucleic acid
dNTP	deoxyribonucleotide triphosphate
DTT	Dithiothreitol
E. coli	Escherichia coli
E1	ubiquitin activating enzyme
E2	ubiquitin conjugating enzyme
E3	ubiquitin ligase
E4	multiubiquitinating enzyme
ECL	enhanced chemiluminescence
EDD1	E3 ligase p100 kDa
EDTA	ethylenediamine tetraacetic acid
eEF1A	elongation factor 1 A
EGFP	enhanced green fluorescence protein
EM	electron microscopy

Eps15	epidermal growth factor receptor pathway substrate 15
ER	endoplasmic reticulum
ERAD	endoplasmic reticulum-associated degradation
FCS	fetal calf serum
g	gram
GABA	γ-aminobutryic acid
GKAP	guanylate kinase-associated protein
GKAP sepharose	peptide IYIPEAQTRL coupled to sepharose
Gly76	glycine amino acid residue of ubiquitin
GST	glutathione S-transferase
h	hour
H_2O_2	hydrogen peroxide
HBSP	Hepes buffer solution phosphate
HBSS	Hanks balanced salt solution
HCl	hydrogen chloride
HECT	Homologous to E6AP Carboxy Terminus
HEK293	human embryonic kidney fibroblast cell line
HPLC	high-performance liquid chromatography
HRP	horse radish peroxidase
IL	interleukine
Ile 44	isoleucine residue in position 44 of ubiquitin
Ile44Ala	isoleucine 44 of ubiquitin mutated to Ala
IMD	IRSp53/MIM homology domain
IP3R	inositol trisphosphate receptor
IPTG	Isopropyl β-D-1-thiogalactopyranoside
IRSp53	Insulin Receptor Substrate p53
K	potassium
KCl	potassium chloride
K_d	binding constant
kDa	kilodalton
krpm	kilo revolutions per minute
l	liter
LB	Luria-Bertani broth
LiCl	lithium chloride
LT	lymphotoxin
Lys	lysine
Lys48, Lys63	lysine residues in position 48 and 63 of ubiquitin, respectively, often used for chain linkage

m	meter
M	molar
MAGUK	membrane-associated guanylate kinases
MG132	Carbobenzoxy-L-leucyl-L-leucyl-L-leucinal
mGluR1	metabotropic glutamate receptors
min	minute
MIU	motif interacting with ubiquitin
mRNA	messenger RNA
MVE	multivesicular endosome
NaAc	sodium acetate
NaOH	sodium hydroxide
NFκB	nuclear factor-kappa B
NIK	NF-κB-inducing kinase
NH_4	ammonium
NHS	N-hydroxysuccinimide
nm	nanometer
NMDA	N-methyl d-aspartate
NMR	Nuclear magnetic resonance
Npl4	nuclear protein localization 4
N-terminus, NT	amino-terminus
NZF	Npl4 zinc finger
OD_{600}	optical density at 600 nanometers
OS-9	upregulated in osteosarcoma 9
p62	sequestosome 1/p62
PAA	polyacrylamide
PAGE	polyacrylamide gel electrophoresis
PBS	Phosphate Buffered Saline
PCR	polymerase chain reaction
PDZ	PSD-95/SAP-90 Discs-large ZO-1 homology
PEG	polyethyleneglycol
PFA	paraformaldehyde
PSD	postsynaptic density
PSD-95	postsynaptic density-95 protein
QDO	quadruple drop-out medium
RBCK	RING finger, B-box and coiled-coiled protein interacting with PKC1
RH	RBCK homology
RIP	serine/threonine kinase receptor interacting protein 1
RING	Really Interesting New Gene
RP	regulatory particle
Rpm	revolutions per minute

Rpn	Regulatory particle non-ATPase subunit
Rpt	Regulatory particle AAA-ATPase subunit
RT	room temperature
s	second
S	Svedberg unit
S^{35}	sulfur 35
SAM	sterile alpha motif
SAPAP	SAP90/PSD-95-associated proteins
SDS	Sodium dodecyl sulfate
SEM	standard error of the mean
SH3	Src-homology 3
SUMO	small ubiquitin-like modifier
TBST	tris buffered saline
TDO	triple drop-out medium
TE	tris-EDTA
TNF	tumor necrosis factor α
TNFR	tumor necrosis factor α receptor
TRAF	TNF-receptor-associated factor
TRADD	TNFR-associated death domain protein
tris	trishydroxymethylaminomethane
TTX	tetrodotoxin
UBA	ubiquitin associated
Ubc	ubiquitin-conjugating enzyme
UBD	ubiquitin binding domain
Ubi, Ub	ubiquitin
Ubl	ubiquitin-like domain
U-box	UFD2 homology domain
UFD2	ubiquitin fusion degradation
UIM	ubiquitin-interacting motif
UPS	ubiquitin-proteasome system
V	volt
v/v	volume per volume
w/v	weight per volume
WAVE2	Wiskott-Aldrich syndrome-related protein
X-gal	5-bromo-4-chloro-3-indolyl-beta-D-galacto-pyranoside
yOS-9	yeast homolog of OS-9
YPDA	yeast medium

ZMNH	Zentrum für Molekulare Neurobiologie
Zn	zinc
ZnF	zinc finger
α	anti
μ	micro
Ø	diameter
Δ	delta, deleted

Chapter 1 Introduction

1.1. Composition and Function of the Neuronal Synapses

1.1.1. Synapses

In 1897, Charles Sherrington first coined the term synapse. Since then it has been used to describe the area where signal transmission from one neuron to another occurs (Zigmond *et al*., 1999). The synapse is composed of presynaptic and postsynaptic terminals. In the 1950's, using electron microscopy De Robertis and Bennett (1954) and Palay (1958) visualized these terminals and the "thickened and denser" region of the postsynaptic terminal – the postsynaptic density (PSD) – was described by Palay (1958). In the chemical synapse the active zone of the presynaptic terminal releases a neurotransmitter, which binds to a receptor located in the postsynaptic membrane. There are two kinds of neuronal synapses: excitatory and inhibitory. The neurotransmitters γ-aminobutryic acid (GABA) and glycine are present in inhibitory synapses. Excitatory synapses in the central nervous system contain the neurotransmitter glutamate. The postsynaptic side of these glutamatergic synapses is where the PSD is located in dendritic protrusions called spines (Zigmond *et al*., 1999).

The thick dense region of the PSD that is visible in electron microscopy (EM) is due to the intense concentration of protein in that area. By implementing scanning transmission EM, Chen *et al*. (2005) have described the PSDs purified from rat forebrain to have a mean diameter of 360 nm and a molecular mass of approximately 1 giga dalton. Recently, two groups have analyzed purified PSD preparations by nanoflow high performance liquid chromatography (HPLC) coupled to electrospray tandem mass spectrometry. Jordan *et al*. (2004) identified 452 and Peng *et al*. (2004) identified 374 different proteins that were present in the PSD. Many of these proteins are multiply present. By utilizing EGFP-based calibration experiments, Sugiyama *et al*. (2005) have estimated that PSD-95, GKAP (guanylate kinase-associated protein), together with Shank and Homer compose 27% of total protein in the PSD. Moreover, the number of molecules in a single PSD was estimated for the MAGUK (membrane-associated guanylate kinases like PSD-95), Shank, Homer, and GKAP families of proteins to be approximately 270, 300, 340, and 170, respectively.

The Shank family consists of proteins of large molecular weight that interact with many partners, thereby forming a sort of scaffold that is the backbone of the PSD. There are three known Shank proteins: Shank1, Shank2, and Shank3. As expected of scaffold proteins, they have many protein interaction domains. At the N-terminus there are multiple Ankyrin repeats, followed by an SH3 (Src-homology 3) domain, a PSD-95/SAP-90 Discs-large ZO-1 homology (PDZ) domain, a large proline-rich domain, and a sterile alpha motif (SAM) domain at the very C-terminus of the protein (Sheng and Kim, 2000). A brief description of the known Shank interaction partners is given in the following paragraphs.

Lim *et al*. (2001) and Boeckers *et al*. (2001) have reported that the Ankyrin repeats of Shank interact with Sharpin and Fodrin, respectively. Sharpin will be discussed further below. Fodrin, a member of the spectrin protein family, has been described to be involved in axon transport, synaptic vesicle tethering in nerve terminals, as well as in F-actin cross-linking (Bennett and Baines, 2001; Aunis and Bader, 1988). In addition, Mameza (2003) has shown that a region located in the N-terminal sequence of Shank (72-174 aa) can also form an intra-molecular complex with the Ankyrin repeats. This intramolecular interaction may be a mechanism, which regulates the binding of other proteins to the Ankyrin repeat domain of Shank.

The SH3 domain of the Shank family of proteins has been shown by Quitsch *et al*. (2005) to be involved in Densin-180 binding through a bipartite interaction. Parts of the C-terminal end of Densin-180 bind to the SH3 domain as well as a section of the proline-rich region of Shank proteins. Overexpression of Densin-180 in neurons leads to abnormal dendritic branching, which is mediated by the leucine-rich repeats located at its N-terminus. Coexpression of Shank with Densin-180 hinders this morphological change in neurons, most likely as a result of a conformational change in the structure of Densin-180, when it interacts with Shank.

The PDZ domain of the Shank family of proteins has been described to interact with the PEAQTRL amino acid sequence at the very C-terminal end of the PSD proteins SAPAP1-4/GKAP (SAP90/PSD-95-associated proteins) (Boeckers *et al*., 1999; Naisbitt *et al*., 1999;

Yao *et al*., 1999). This interaction is necessary for the recruitment of Shank1 to the dendritic spine as shown by Romorini *et al*. (2004). The SAPAP/GKAPs have also been described to associate with the guanylate kinase domain of PSD-95 (Takeuchi *et al*., 1997) and PSD-95 in turn interacts with the cytoplasmic region of the NMDA receptor (Kornau *et al*., 1995). Hence, through its interaction with GKAP, Shank is linked to PSD-95 and thereby indirectly also to the NMDA (N-methyl d-aspartate) receptor located in the membrane of the dendritic spine. The PDZ domains of Shank1 and Shank2, which is also known as cortactin-binding protein 1, interact directly with the C-terminus of somatostatin receptor subtype 2 (Zitzer *et al*., 1999a; Zitzer *et al*., 1999b). Furthermore, Tobaben *et al*. (2000) have shown the PDZ domains of all three Shank proteins interact with the G protein-coupled α-latrotoxin receptor CL1. Finally, Zhang et al. (2005) have also shown that the long C-terminal splice variant of the L-type Ca^{2+} channel subunit $Ca_V1.3a$ interacts with the PDZ domains of Shank1 and 3.

The proline-rich domain of Shank has been shown to interact with many different proteins. Part of the proline-rich region of Shank1-3 is bound by the SH3 domain of the insulin receptor substrate p53 (IRSp53) (Soltau *et al*., 2002; Bockman *et al*., 2002). IRSp53 has been shown to mediate F-actin bundling through its IRSp53/MIM homology domain (IMD) in a small GTPase regulated process (Yamagishi *et al*., 2004). Other proteins that interact with the proline-rich region of Shank are the actin binding protein (Abp1) and cortactin (Qualmann, 2004; Du *et al*., 1998). Abp1 has been shown by Kessels *et al*. (2001) to be involved in the endocytic process, by linking the actin cytoskeleton to functional proteins involved in endocytosis. Cortactin is also involved in the endocytic process (Olazabal and Machesky, 2001) as well as in the regulation of the actin cytoskeleton (Huang *et al*., 1997). In addition, Abi-1 (Abelson interacting protein-1) has been shown to interact through its SH3 domain with the proline-rich region of Shank3. Abi-1 has been described to act in a Rac-GTPase dependent manner as regulator of the formation and activity of the WAVE2 (Wiskott-Aldrich syndrome-related protein) signaling complex. Together activated WAVE2 and actin-related protein (Arp) 2/3 promote actin assembly (Proepper *et al*., 2007; Innocenti *et al*., 2005). Yet another protein that binds to the proline-rich region of Shank is Homer1b (Tu *et al*., 1999). Homer is known to interact with the group 1 metabotropic glutamate receptors (mGluR1a and mGluR5) (Brakeman *et al*., 1997), as well as with the intracellular IP3R (inositol trisphosphate receptor), which is integrated in the endoplasmic reticulum

(ER) membrane. Thus, the simultaneous interaction with Shank and IP3R allows Homer dimers to bridge mGluRs to intracellular stores of calcium in the ER (Tu *et al*., 1998). This indirect interaction between Shank and the mGluRs via Homer on the one hand and the indirect interaction between Shank and the NMDA receptor via PSD-95 and SAPAP/GKAP on the other hand allows Shank to link both of these glutamate receptors (Tu *et al*., 1999). A schematic diagram of a synapse depicting some of the proteins decribed above to interact with the Shank family of proteins is shown in Figure 1.1.

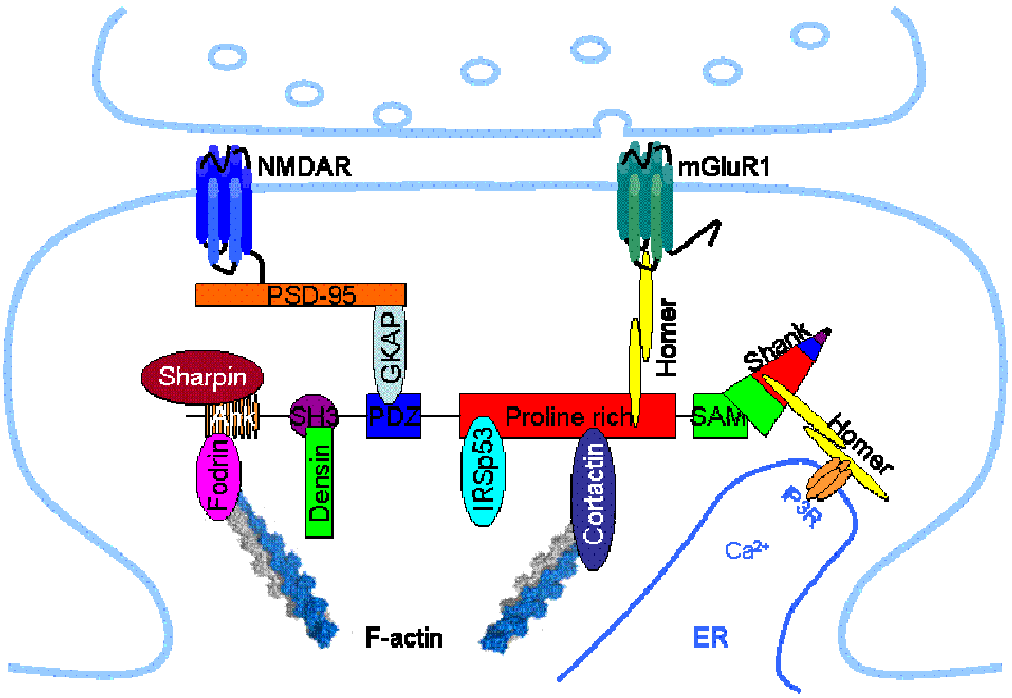

Figure 1.1 Schematic Diagram of a Synapse
A typical excitatory synapse is depicted. The Shank family of proteins is located at the core of the postsynaptic side of the synapse. These scaffolding proteins form an important link between the mGlu and NMDA receptors, as well as a link between the PSD membrane-associated proteins and proteins involved in actin dynamics at the base of the spine.

SAM domains of Shank3 have been shown to interact with each other (Naisbitt *et al*., 1999). They form helices that stack together side by side in parallel generating a sheet-like structure (Baron *et al*., 2006). This SAM domain sheet structure may actually constitute the architectural backbone for the PSD. The authors show that refolding the SAM sheets in the presence of Zn^{2+} results in high structural order in the newly folded SAM sheets. Thus, they

propose that the presynaptic terminal release of Zn^{2+} in neuronal activity leads to the structured arrangement of Shank3 in the PSD.

The majority of the work in this thesis concentrates on Sharpin, another protein that interacts with Shank, and on new Sharpin interacting proteins. Sharpin is a 45 kDa protein, whose role in the cell is not well defined. As already mentioned, it binds to the Ankyrin repeat domain of Shank, which consists of seven Ankyrin repeats. Each repeat is composed of 33 amino acids, which take on a typical fold of two antiparallel α-helices separated by a short loop. As adjacent repeats are connected by a β-hairpin loop, these repeats form a parallel stack (Devi *et al*., 2004). Binding of Sharpin to this stack of ankyrin repeats is mediated by the amino acids 172-305 of Shank1 (Lim *et al*., 2001). Based on its 45 % sequence similarity to RBCK1 (RBCC protein interacting with PKC 1), the region of Sharpin that interacts with Shank has been described by the same authors as part of a RBCK homology (RH) domain (aa 172 to 381). While RBCK1 itself is well known to interact with protein kinase C isoforms, the authors were unable to show a similar interaction for Sharpin. *In silico* analysis using Motif Scan determines part of the RH domain of Sharpin (aa 218-287) to have similarity with type 2 ubiquitin like (Ubl) domains. There are two types of Ubl domains: Type 1 Ubl domains are present in small ubiquitin-like modifiers like SUMO (small ubiquitin-like modifier) that can be attached to substrate proteins in a similar manner as ubiquitin. Consequently, sumoylation represents another type of posttranslational modification of proteins that has in part similar functions, yet is completely separate from ubiquitination. Type 2 Ubl domains on the other hand are functional protein/protein interaction motifs that cannot be attached to substrate proteins. They have been found in ubiquitin binding proteins like Rad23 and are believed to play a role for regulatory interactions between different components of the ubiquitination machinery.

The N-terminal part of Sharpin (aa 1-172) that does not participate in the Shank interaction contains a coiled-coil structure and its function has yet to be determined. Finally, the C-terminus of Sharpin has been described, based on homology, to have an Npl4 zinc finger (NZF) structure. Npl4 (nuclear protein localization 4) is involved in the removal of proteins from the ER in the process of endoplasmic reticulum-associated degradation (ERAD). Meyer *et al*. (2002) have shown that Np14 contains a zinc finger that is capable of binding

ubiquitin. Thus, based on the Ubl and the NZF domain homologies, this thesis investigated the hypothesis that Sharpin is involved in ubiquitin signaling.

Synaptic proteins that are involved in ubiquitination, recognition of ubiquitin, or the ubiquitin-proteasome system (UPS) have recently become a focus of research, since several studies demonstrated the importance of the ubiquitination process in the formation and plasticity of the synapse. Synaptic plasticity refers to the ability of the synapse to change; the connection between the neurons can be either strengthened or weakened. On the postsynaptic side, NMDA receptor activation regulates the conductance of AMPA receptors or their number in the synaptic membrane, thereby strengthening (more AMPA receptor influx) or weakening (less AMPA receptor influx) synaptic efficiency (Abbott and Nelson, 2000; Colledge *et al*., 2003). Colledge *et al*. (2003) show that removal of the AMPA receptor from the postsynaptic membrane requires activation of the NMDA receptor as well as NMDA-induced proteasome degradation of PSD-95.

In addition to PSD-95, a number of other PSD proteins, including Shank and GKAP, have recently been described to be degraded by the proteasome system (Ehlers, 2003). In the study by Ehlers, cultured cortical neurons were treated with bicuculline, a $GABA_A$ receptor antagonist; this treatment increases excitatory synaptic activity by preventing the inhibitory action of the GABAergic synapses – so that neurons are exposed to a long excitatory phase. Alternatively, the author hindered neuronal activity by treating samples with tetrodotoxin (TTX), a Na^+ channel blocker. By comparing both treatments to untreated controls Ehlers found that neurons treated with bicuculline showed specific decreases in protein expression of the PSD that were the exact opposite of the changes seen in the TTX treated PSD analysis. For example the relative levels of Shank and GKAP to the control were approximately two-fold higher in PSD preparations from TTX-treated neurons, whereas they were reduced in preparations treated with bicuculline. The reduction of GKAP and Shank is due to the UPS, as there was no decrease in PSD preparations from neurons that were treated with bicuculline plus proteasome inhibitors (MG132, lactacystine, or epoxomicin).

However, UPS degradation is not only involved in maintaining synaptic plasticity. Studies in *Drosophila* and *C. elegans* demonstrate that there is also a role for this system in the

formation of synapses. For instance, the loss of function of an E3 ubiquitin ligase, a protein involved in ubiquitination, leads to an abnormal number and morphology of synapses in these organisms (DiAntonio *et al*., 2001; Liao *et al*., 2004). This demonstrates the importance of the UPS in the formation and maintenance of synapses.

1.1.2. Ubiquitination

Since its discovery in the 1970s, ubiquitin has been shown to be a key regulatory element of many eukaryotic cellular processes such as: the cell cycle, membrane transport, cell migration, ERAD, NFκB (nuclear factor-kappa B) transcription factor activation, neuronal remodeling, DNA repair, as well as targeted protein degradation (Finley *et al*., 1994; Staub and Rotin, 2006; Wang HR *et al*., 2003; Kostova and Wolf, 2003; Chen, 2005; Ehlers, 2003; Schauber *et al*., 1998; Ciechanover *et al*., 1984). Ubiquitin is present in all eukaryotic cells; it consists of 76 aa residues and has a molecular weight of 8.5 kDa (Stryer *et al*., 1995). Ubiquitin can be covalently attached to lysine residues of other proteins thereby ascertaining their participation in appropriate cellular processes. In an energy dependent step ubiquitin must be activated, before it can be covalently linked to target proteins. This activation is facilitated by a ubiquitin-activating enzyme, an E1 enzyme, in a two step process (see Figure 1.2A). In the first step of this activation the E1 enzyme, by the hydrolysis of ATP, converts ubiquitin to a C-terminal ubiquitin adenylate. In the second step of activation, the ubiquitin adenylate is transferred to a cysteine residue present in the active site of the enzyme. The resulting high energy E1-ubiquitin thiol ester can donate ubiquitin, by transacylation, to a specific cysteine residue in a ubiquitin conjugating enzyme (E2). Then with the help of a ubiquitin ligase (E3), ubiquitin is transferred to the ε-amino group of a lysine residue in the target protein forming an isopeptide bond (see Figure 1.2B). There are two families of E3 ligases, the HECT (Homologous to E6AP Carboxy Terminus) family of ligases, and the RING (Really Interesting New Gene) ligases. The difference between the two groups lies in how the ligase is involved in the transfer of ubiquitin. A cysteine residue from the HECT family of ligases receives ubiquitin from the E2 conjugating enzyme, thereby, forming a thiol ester with ubiquitin. The HECT E3 ligase then transfers ubiquitin to a lysine residue of the target protein. In comparison the RING family of E3 ligases acts rather only as a scaffold for the ubiquiting conjugating enzyme and the target protein. In this group of ligases, ubiquitin is never transferred from the E2 enzyme to the E3 ligase, rather it is transferred to

the substrate directly by the E2 enzyme (Pickart, 2004; Pickart and Eddins, 2004; Hershko, 1988; Hicke *et al*., 2005).

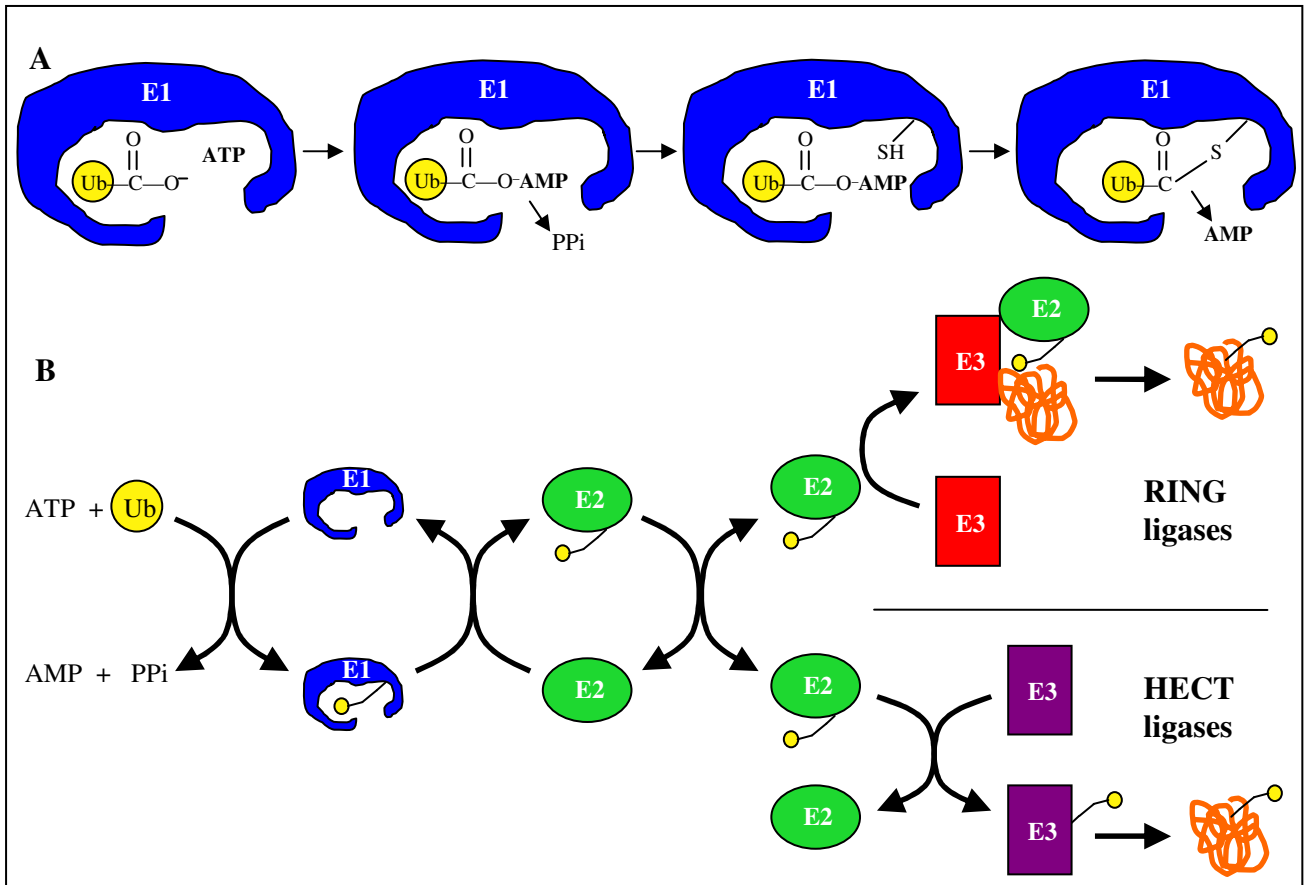

Figure 1.2 Ubiquitin Activation and Ubiquitination
Ubiquitin is activated in an energy consuming two-step reaction (**A**) the ubiquitin activating enzyme (E1) induces the formation of a ubiquitin C-terminal adenylate by ATP hydrolysis. The activated ubiquitin is then transferred to a specific cysteine residue of the E1 enzyme, forming a thiol ester. (B) The transfer of ubiquitin to a specific cysteine residue of the ubiquitin conjugating enzyme (E2) by transaceylation. The following step in the ubiquitination process depends on the type of E3 ligase family that the E2 enzyme interacts with: HECT or RING ligase families. If the E2 interacts with a HECT ligase then ubiquitin is transferred from the E2 to a specific cysteine of the E3 ligase, and the E3 alone attaches ubiquitin to the ε-amino group of a lysine residue in the target protein by an isopeptide bond. The other family that contains the RING ligases acts as a scaffold for the E2 enzyme and the target protein. Ubiquitin is then tranferred directly from the E2 enzyme to the ε-amino group of a lysine residue in the substrate by an isopeptide bond.

Koegl *et al*. (1999) have discovered another enzyme, E4 to be involved in ubiquitin modification of proteins. The E4 enzymes contain a modified version of the RING finger domain that is named UFD2 homology domain (U-box). The E4 enzymes in concert with E1 and E2 enzymes can extend the length of the ubiquitin chains on target proteins, but they require an initial ubiquitin moiety to be attached to their substrates by an E3 ligase. Recognition of the substrates for ubiquitination is determined by E3 ligases in tightly controlled regulatory steps. Some of the known regulatory mechanisms for substrate recognition involve the following: N-end rule pathway (recognition of a permissive amino acid at the N-terminus of a protein), peptide-induced allosteric activation of the E3 ligase, phoshorylation of the substrate, the E3 ligase or both, and recognition of unfolded substrates (Glickman and Ciechanover, 2002).

Ubiquitin can be attached to substrate proteins as monomer or polymers – monoubiquitination or polyubiquitination. When more than one monomer is attached to different lysine residues of a protein this is referred to as multimonoubiquitination. Monoubiquitination of target proteins can regulate many different cellular processes like: receptor endocytosis, endosomal sorting, histone regulation, DNA repair, virus budding, and nuclear export. Multimonoubiquitination has also been shown to regulate endocytosis. The attachment of ubiquitin polymers to target proteins is more complex. Ubiquitin contains seven lysine residues that can be used to form polyubiquitin chains: Lys6, Lys11, Lys27, Lys29, Lys33, Lys48, and Lys63. Of these seven different chain types, the Lys48 and Lys63 chains are the best described. Lys48 chains were the first polyubiquitin chains to be characterized; proteins ubiquitinated with Lys48 chains are targeted for degradation by the proteasome. The modification of target proteins with Lys63 ubiquitin chains on the other hand has been shown to be a necessary regulatory step in processes such as DNA repair, endocytosis, and activation of protein kinases (Haglund and Dikic, 2005).

The ubiquitination of target proteins is specifically recognized by proteins that contain ubiquitin binding domains (UBD). The first ubiquitin binding domain was discovered in the proteasomal subunit S5a, which contains a ubiquitin-interacting motif (UIM) (Hicke *et al*., 2005). Since then sixteen other UBDs have been described and the heterogeneity between the structures of these domains is great. Structurally, the domains can be divided into three

general groups: helical, zinc-finger, and Ubc-related ubiquitin binding domains. Recent studies have shown that ubiquitin presents two interfaces for interaction with its recognition domains. One interface encompasses the area around Ile44, the other interface is centered around Asp58. UBDs generally have low binding affinities for monoubiquitin; the binding constant (K_d) of these interactions is only on the order of 100 µM. This weak affinity is compensated for by the fact that a long chain of ubiquitin molecules provides many points for interaction, making sure that dissociated UBDs can immediately reassociate. Furthermore, adjacent residues of a polyubiquitin chain or neighboring monoubiquitin residues in a multiubiquitinated protein augment the binding affinity by simultaneously interacting with tandem UBDs within a single ubiquitin recognizing protein. Binding affinity can also be strengthened by the fact that more than one interface of the UBD can bind to different ubiquitin moieties of a single poly- or multiubiquitinated target protein at the same time. Dimerization of UBDs from different ubiquitin recognizing proteins represents yet another potential mechanism for strengthening the interaction, since dimers can interact with the different binding surfaces of a single ubiquitin molecule (Hurley *et al*., 2006; Lee *et al*., 2006; Hicke *et al*., 2005, Wang B. *et al*., 2003).

As previously mentioned, Sharpin is predicted to have a NZF ubiquitin binding domain. More than 100 proteins have been found to contain the following consensus sequence for NZF domains: x(4)-Trp-x-Cys-x(2)-Cys-x(3)-Asp-x(6)-Cys-x(2)-Cys-x(5) (whereby x represents any amino acid, see also Figure 1.3). The four highly conserved cysteine residues complex a single zinc ion. Among the NZF domain containing proteins are Npl4 (nuclear protein localization 4) and the nuclear pore protein RanBP2. Although both proteins contain the consensus sequence outlined above, Npl4 interacts with ubiquitin, whereas RanBP2 does not. By comparing the amino acid sequences of NZF domains known to interact with ubiquitin with the sequence of RanBP2, Alam *et al*. (2004) discovered that there were certain amino acids that were conserved in those proteins that interact with ubiquitin, namely tryptophan 13, phenylalanine 14, and methionine 25 (other hydrophobic aliphatic residues can be substituted at position 25). In the structural organization of NZF domains conserved tryphophan and aspartate residues stabilize the four short β-strands in the interior of the finger by hydrophobic interactions and hydrogen bonding, respectively. (Alam *et al*., 2004; Meyer *et al*., 2002; Wang B. *et al*., 2003). NMR experiments by Wang B. *et al*. (2003) show

that the conserved hydrophobic residues of the NZF domain interact with ubiquitin at the hydrophobic surface region surrounding Ile44. This region of ubiquitin also includes the residues Leu8, Val70, Leu71, and Leu73. Further hydrophilic interactions surrounding this hydrophobic interface appear to be an integral factor for orientation and specificity of ubiquitin binding. In Figure 1.3, amino acid sequences of the NZF domain of Npl4 and Sharpin are aligned and the residues corresponding to the consensus sequence are highlighted. The criteria for a ubiquitin binding sequence are perfectly matched by Sharpin; a schematic diagram of the proposed NZF finger of Sharpin is also depicted.

A

Npl4 Zinc Finger: **TSAMWACQHCTFMNQPGTGHCEMCSLPRT**
Sharpin Zinc Finger: **PQPGWSCPSCTFINASANPGCEMCSTQRP**

B

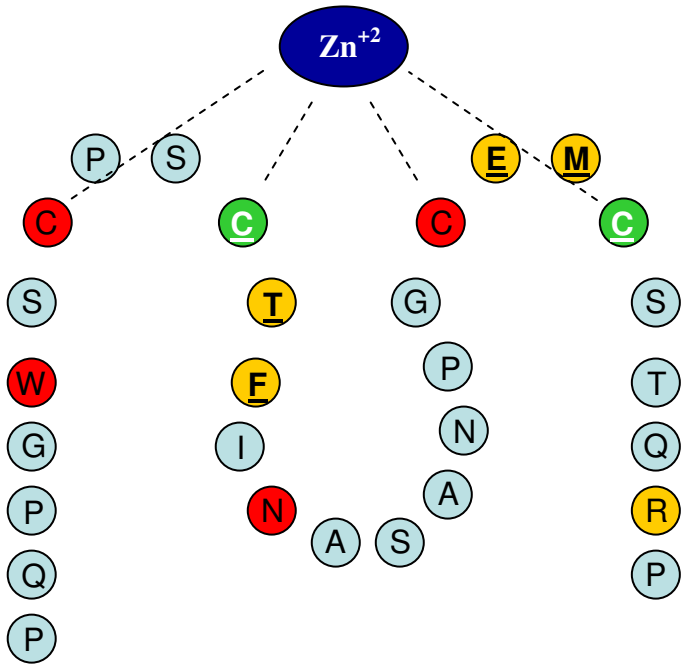

Figure 1.3 Sharpin Zinc Finger Alignment and Schematic Diagram
(A) Alignment of the zinc finger domains from Npl4 and Sharpin. The four cysteine residues that bind to the zinc ion are underscored. Red and green residues are highly conserved, and residues coloured in yellow are moderately conserved. B) Schematic diagram of the NZF finger structure of Sharpin. Yellow and green residues predicted to contact ubiquitin are underlined and shown in boldface (Meyer *et al*., 2002; Alam *et al*., 2004).

The recognition of ubiquitinated substrates by a UBD containing protein may trigger various downstream processes. A functional role for UBD containing proteins is well described in the endocytic pathway. The surface availability of many membrane receptors, transporters, and channels, has been shown to be controlled by ubiquitin-dependent internalization. Modification of a membrane protein by monoubiquitination or Lys63-linked diubiquitin chains is a signal for ubiquitin receptor proteins to bind. Members of the Epsin family of proteins, for example, are capable of interacting with ubiquitin through their UIM domains and with the endocytic machinery by their clathrin and clathrin adaptor protein 2 (AP-2) binding motifs. The ubiquitinated membrane protein is then internalized through endocytosis and an early endosome is formed. At this stage, the internalized proteins can be deubiquitinated and recycled to the membrane. However, if the ubiquitinated membrane protein is recognized by a ubiquitin receptor its fate is quite different. In yeast, when the ubiquitin residue of an internalized plasma membrane protein is recognized by the UIM of Vps27, it is prevented from entering the recycling pathway and is instead sorted into the multivesicular endosome (MVE). Vps27 transfers the targeted protein to the UEV (ubiquitin conjugating enzyme variant) domain of Vps23 which in turn delivers it to the NZF domain of Vps36, another component of the endosomal sorting complex. Before being finally sequestered in a MVE vesicle the cargo proteins are deubiquitinated. By fusing with a lysosome the MVE delivers its cargo protein to the lysosomal lumen, where the proteins are degraded (Hicke *et al*., 2005; Aguilar and Wendland, 2003; Hicke, 2001). A similar cargo sorting pathway with homologous protein components functions also in mammalian cells.

Proteasome degradation is the best described of the cellular effects regulated by ubiquitination. The 26S proteasome is composed of a 20S core particle (20S CP) and two 19S regulatory particles (19S RP), one at each end of the cylindrical core (see Figure 1.4). The following gives an overview based on what is known about the yeast proteasome, but this is also applicable to mammalian proteasomes due to their high evolutionary conservation among eukaryotes. The 14 different subunits (α1-7, β1-7) that build the 20S CP assemble into four rings that are stacked in the order α1-7, β1-7, β1-7, α1-7. The peptidase activity of the proteasome is attributed to the β-rings, specifically subunits β1, β2, and β5. The 19S RP on the other hand is composed of approximately 17 subunits that constitute a base and a lid structure. The base structure consists of three Rpn (regulatory

particle non-ATPase) subunits (Rpn1, -2, -10) and six Rpt (regulatory particle triple A ATPase) subunits (Rpt1-6). The Rpt subunits consist of ATPases associated with diverse cellular activities (AAA-ATPases) and are postulated to form a hexameric ring. The lid structure of the 19S RP is composed of eight non-ATPase subunits (Rpn3, -5, -6, -7, -8, -9, -11, -12) (Miller and Gordon, 2005; Glickman and Ciechanover, 2002; Pickart, 2000). The attachment of Lys48-linked ubiquitin chains to lysine residues of target proteins acts as the signal for protein degradation by the proteasome. Ubiquitin conjugated to substrate proteins in this way is recognized by a ubiquitin receptor for the proteasome. There are two scenarios for shuttling ubiquitinated proteins to the proteasome. In one scenario, ubiquitinated proteins are directly recognized by the UIMs of certain subunits of the 19S RP, like Rpn10 and Rpt5 or the mammalian homologues S5a and S6´, respectively. The other scenario involves ubiquitin receptor proteins such as Rad23 that contain both UBA (ubiquitin associated) and Ubl domains. In addition to binding ubiquitinated proteins through their UBA domains, these proteins can also interact with the proteasome via their Ubl domains (Elsasser and Finley, 2005; Miller and Gordon, 2005). Once the uniquitinated protein reaches the 19S RP of the proteasome, it is either recognized by Rpn10 or the ubiquitin receptor is recognized by Rpn1 or Rpn2. The substrate is then deubiquitinated most likely by Rpn11. In ATP-consuming reactions, the substrate is unfolded by the ATPases of the hexameric ring and then channeled into the central barrel of the 20S CP. The substrate is cleaved by β1, β2, and β5 subunits in the core particle, which results in short peptides with an average length of 7-9 aa (Elsasser, *et al*., 2004; Miller and Gordon, 2005; Glickman and Ciechanover, 2002).

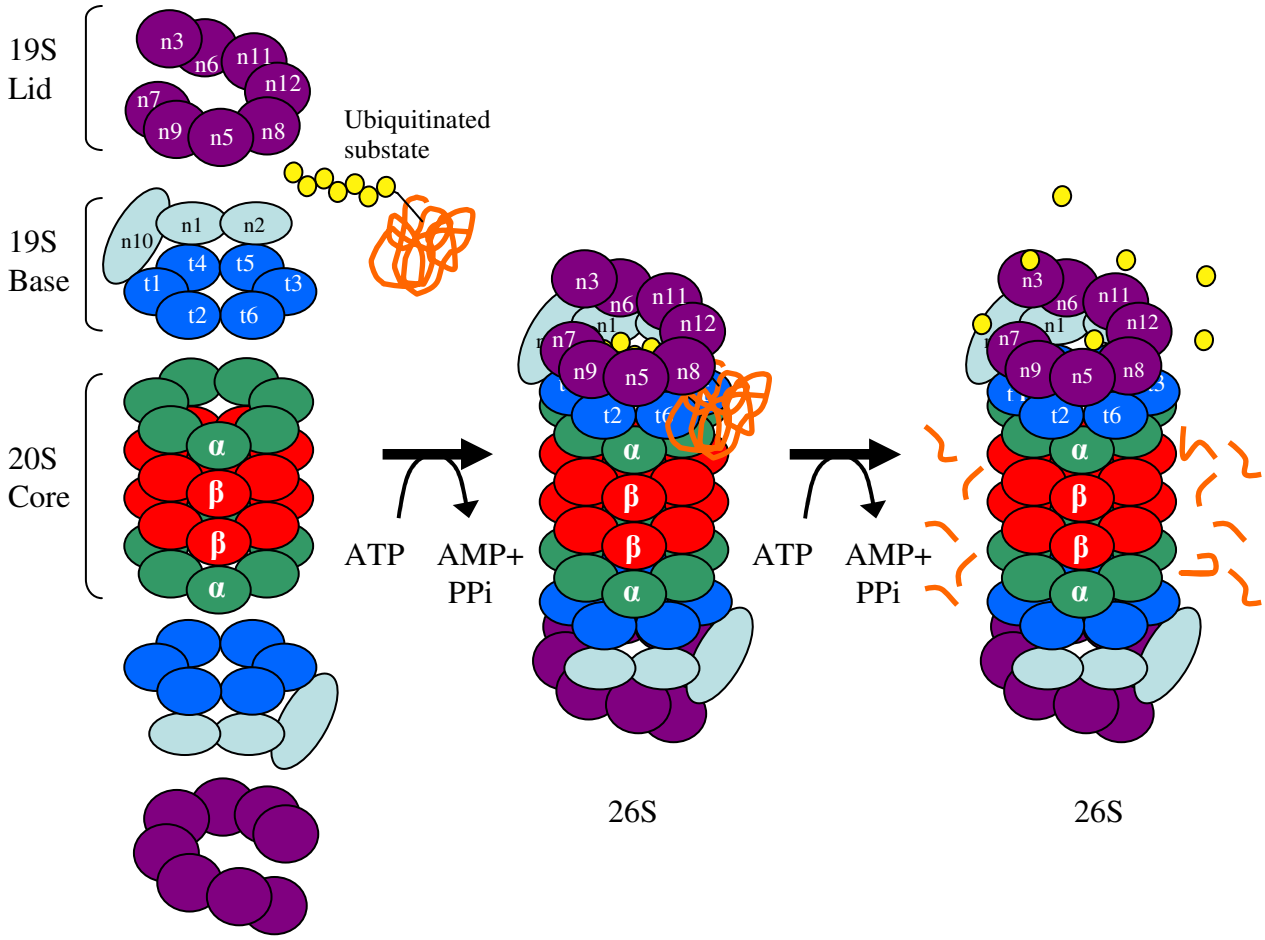

Figure 1.4 Schematic Diagram of the Yeast 26S Proteasome
Outlined above is a representation of the proteasome. Depicted in red and green is the 20S core particle that contains four stacked septuplet rings. The outer rings are composed of α1-7 subunits and enclose the catalytic core made up of the β1-7 subunits. The base and the lid components of the 19S particle are depicted in blue and purple. The six dark blue ATPase subunits of the base form a hexameric ring, while the non-ATPase componets (shown in light blue) recognize ubiquitinated substrates. Finally, the lid structure of the 19 S particle is composed of eight subunits, which are involved in deubiquitination of the substrate. Formation of the 26 S proteasome from the 19S and 20S particles, as well as the unfolding of the ubquitinated substrate requires energy in the form of ATP. Once the deubiquitinated, unfolded substrate reaches the β-subunits of the catalytic core it is cleaved into small peptides.

An important cellular process that has been tied to protein degradation by the proteasome is ERAD. Newly synthesized secretory and membrane proteins are glycosylated and recognized by chaperone proteins of the ER lumen (Lodish *et al*., 2001). Chaperones, like calnexin, calreticulin, BiP and yOS-9, bind to nascent proteins in order to ensure their correct folding (Meusser *et al*., 2005; Bhamidipati *et al*., 2005). Only correctly folded proteins can exit the ER to the Golgi apparatus, and this progression is mediated by changes in glycosylation. Proteins that are unable to fold and transit to the Golgi apparatus are recognized by chaperones that target them to the ER membrane for retrotranslocation. Recently, yOS-9 has been identified to play a key role in this process (Bhamidipati *et al*., 2005). Although the molecular mechanism of retrotranslocation is not fully understood, it has been hypothesized that recognized misfolded proteins are retrotranslocated through an import pore like Sec61 (Meusser *et al*., 2005). Another hypothesis is that Derlin1 is involved in this process (Lilley and Ploegh, 2004; Ye *et al*., 2004). Recently, Wahlman *et al*. (2007) have shown that Derlin1 is responsible for the retrotranslocation of the small unmodified protein, Δgpαf. The process of retrotranslocation requires energy in order to export the misfolded protein; this energy is provided by the AAA-ATPase Cdc48p (also known as p97 or VCP) (Ye *et al*., 2001). Once the protein reaches the cytosol, it is ubiquitinated by the E3 ligase, Hrd1p, which has been shown to be essential for the degradation of several retrotranslocated proteins in ERAD (Bays, 2001). The ubiquitinated ERAD substrates are then shuttled to the proteasome, where they are degraded (Meusser *et al*., 2005).

Although originally discovered solely in the context of protein degradation, it has meanwhile become increasingly clear that the ubiquitination of proteins by E3 ligases and the removal of ubiquitin from modified proteins by deubiquitinating enzymes demonstrate as post-translational modifications the same capacity for cellular signaling as protein phosphorylation.

1.1.3. The Ubiquitin Proteasome System at the Synapse

Many neurodegenerative diseases have recently been linked to the UPS. The best example is autosomal recessive juvenile parkinsonism, a disease that has been attributed to mutations in a gene named parkin (Kitada *et al*., 1998). Shimura *et al*. (2000) described this gene to encode an E3 ligase and the parkin gene product was indeed demonstrated to have ubiquitin-

protein ligase activity. Subsequently, Imai *et al*. (2000) found the parkin mRNA to be up-regulated during unfolded protein stress. Furthermore, the E3 ligase activity of Parkin was demonstrated to protect cells from cell death induced by unfolded protein stress. The Angelman syndrome is another example of a UPS deficiency that leads to neurodegeneration. Mutations in the gene coding for the ubiquitin ligase Ube3a have been shown to cause this syndrome (Kishino *et al*., 1997). Deficiencies in the UPS have in fact been implicated in many neurodegenerative diseases. Accumulation of ubiquitin conjugates, often in inclusion bodies, is the hallmark of neurodegenerative diseases, like Alzheimer's disease, Parkinson's disease, and Huntington's disease (Ciechanover and Brundin, 2003). Understanding the role of the UPS in the formation and maintenance of the brain may aid in the discovery of new therapeutical agents for these diseases.

The UPS has been a recent focus of many aspects of neurobiology like brain development, cell migration, axon outgrowth and guidance, synapse development, pre- and postsynaptic function, as well as postsynaptic remodeling and plasticity (Patrick, 2006; Yi and Ehlers, 2005). A study by Ehlers (2003) has demonstrated the importance of the UPS in changing the protein composition in the PSD in response to synaptic activity. In addition, Bingol and Schuman (2006) have shown that in response to KCl stimulation proteasomes translocate from the dendritic shafts into the synaptic spines, and that this translocation can be inhibited by the NMDA receptor antagonist AP5. The importance of UPS function for synaptic plasticity is also underscored by the work of Zhao *et al*. (2003). These authors have shown by measuring excitatory postsynaptic potentials that in cultured sensory and motor neurons from *Aplasia californica* proteasome inhibition increases the strength of the sensory-motor synapse. In addition, treatment of these neurons with proteasome inhibitor resulted in an increase in their glutamate-evoked postsynaptic potential; this response is characteristic of an increase in either the number of glutamate receptors or their responsiveness. Finally, inhibition of the proteasome in these neurons also led to an increase in the length of neurite outgrowths as well as an increase in the number of synaptic contacts formed compared to non-treated controls (Zhao *et al*., 2003; Cline, 2003).

Effects of the UPS on the internalization of mGluRs in cultured hippocampal neurons have been demonstrated by Patrick *et al*. (2003). Under normal conditions, treatment with the

glutamate agonist AMPA causes internalization of mGluRs in neurons. This effect was diminished, when the neurons were pretreated with proteasome inhibitor. Moreover, the mGluR internalization in response to AMPA was also diminished, when the cells were infected with a Sindbis virus encoding the ubiquitin chain-elongation mutant Ub Lys48Arg. This ubiquitin mutant prevents the elongation of Lys48 ubiquitin chains, but allows for the synthesis of alternative linkages, like Lys63-linked chains. This demonstrates that internalization of mGluRs depends specifically upon the synthesis of Lys48-linked ubiquitin chains, and therefore suggests a role of the UPS. In a time course of inhibition, internalization of these receptors was prevented by a 2.5 min preincubation with proteasome inhibitor, indicating that local protein degradation must occur in the synapse. Even though local protein degradation by the UPS at both sides of the synapse has become a focal point of research lately, little is known about the role of specific UPS components at the synapse. Here, I provide evidence that Sharpin may be involved in the local protein degradation by the UPS in the PSD. I found that Sharpin interacts with ubiquitin and binds to ubiquitinated proteins. I also identified novel interaction partners of Sharpin that suggest a role for Sharpin as part of the UPS in neurons.

Chapter 2 Materials and Methods

2.1. Materials

2.1.1. Chemicals

The chemicals used in the experiments described here were of analytical grade and purchased from Sigma, Merck, or Roth unless otherwise stated. All solutions were prepared with deionized water.

2.1.2. Microbial Strains, Cell Line and Laboratory Animals

Table 2.1 summarizes the organisms and cell line used for this work as well as their sources.

Bacterial Strain	*Escherichia coli* TOP' 10	Stratagene
Bacterial Strain	*Escherichia coli* BL21	Stratagene
Yeast Strain	*S. cerevisiae* AH109	Clontech
Cell Line	Human Embryonic Kidney 293 (HEK293)	ATCC
Laboratory Animals	*Rattus norvegicus* (Wistar Rat)	Animal facility at the University of Hamburg Eppendorf (UKE)

Table 2.1 Organisms and cell line used in this study

2.1.3. Plasmid DNAs

2.1.3.1. Bacterial Vectors

The following vectors were transformed into BL21 cells in order to produce and purify GST fusion proteins.

Vector	Notes
pGEX from Amersham	Unfused Glutathione S-Transferase
GST-S5a	The proteasomal subunit S5a cloned into pGEX-6P1
GST-Ubiquitin	Ubiquitin cloned into pGEX-4T2

Table 2.2 Vectors used for Glutathione S-Transferase Fusion Protein Production

2.1.3.2. Yeast Vectors

The vectors summarized in the table below were transformed into yeast in order to detect protein-protein interactions using a yeast two hybrid system.

Vector	Notes
pACT (Invitrogen)	Prey vector
pACT Ubiquitin	Ubiquitin cDNA derived from a construct provided by the ZMNH
pACT Ubi I44A	Ubiquitin with isoleucine (Ile) residue 44 mutated to alanine (Ala)
pACT Ubi D58A	Ubiquitin with aspartate (Asp) residue 58 mutated to alanine (Ala)
pACT Ubi I44A D58A	Ubiquitin containing both the Ile/Ala and Asp/Ala mutation
pACT M (Sharpin)	Encoding only the middle region of Sharpin (aa 171-304)
pGBKT7 (Invitrogen)	Bait vector
pGBKT7 CT (Sharpin)	Encoding only the C-terminal end of Sharpin (aa 304-381)
pGBKT7 M (Sharpin)	Encoding only the middle region of Sharpin (aa 171-304)

Table 2.3 Vectors used for Yeast Two Hybrid Interactions

2.1.3.3. Mammalian Vectors

In order to perform protein-protein interaction studies in living cells, HEK293 cells or primary cortical neurons were transiently transfected with the plasmids listed in table 2.4.

Vector	Notes
pcDNA 3.1 (Invitrogen)	Mammalian expression vector
Sharpin FL	Sharpin cloned into pcDNA 3.1, Sharpin with C-terminal c-myc tag
OS-9	OS-9 cloned into pcDNA 3.1, OS-9 with C-terminal c-myc tag
pCMV 3b (Stratagene)	N-terminal c-myc tag
pCMV NT PDZ	The PDZ domain from Shank1 cloned into pCMV 3b, in order to generate a N-terminally c-myc tagged PDZ fusion protein.
Sharpin PDZ	Sharpin cloned behind the PDZ tag in the pCMV NT PDZ vector; this construct has in addition an N-terminal c-myc tag.

Table 2.4 Vectors used for Protein Expression in Mammalian Cells

2.1.4. Antibodies

Table 2.5 summarizes the antibodies and their respective working concentrations used for Western blotting and/or immunocytochemistry experiments performed in the course of the work presented here.

Working Concentration			
Primary Antibody	Western Blot	Immunocytochemistry	Source
α-c-myc, mouse	1:5000	1:1000	Sigma
α-Ubiquitin, mouse	1:2000	-	Chemicon
α-PSD-95, mouse	1:10000	-	Upstate Biotechnology
α-tubulin, mouse	1:10000	-	Abcam
α-Adaptin γ, mouse	1:5000	-	Transduction Labs
α-EAA1, mouse	1:2500	-	BD Biosciences
α-GAPDH, mouse	1:10000	-	Ambion
α-Sharpin, rabbit	1:5000	1:1000	Eunjoon Kim, Pusan National University
α-Shank, rabbit	1:5000	1:400 (Aff. Purified)	Our Laboratory
α-beta-COP, rabbit	1:1000	-	Affinity BioReagents
α-proteasome, rabbit	1:1000	-	Biomol
α-Shank3, guinea pig	-	1:1000	Tobias Böckers, University of Ulm
Secondary Antibody	Western Blot	Immunocytochemistry	Source
HRP-coupled α-mouse IgG	1:2000	-	Amersham Biochemicals
HRP-coupled α-rabbit IgG	1:2000	-	Amersham Biochemicals

Table 2.5 Antibodies used for Western Blotting and Immunocytochemistry

2.2. Methods

2.2.1. Molecular Biology Techniques

2.2.1.1. Polymerase Chain Reaction (PCR)

Genes of interest were amplified by PCR technology. The pfu DNA polymerase used in these reactions was obtained from Stratagene. A typical reaction was performed in a volume of 50 µl with 0.1-1 µg of template. The final concentrations of the different reagents were 1x for the reaction buffer (Stratagene), 10 pmol of each primer, 1.25% of Dimethylsulfoxide (DMSO, Merck), 0.2 mM of each dNTP (Fermentas) and 1 unit of pfu DNA polymerase. The annealing temperature of each primer was calculated using the following formula: Tm = 4(G+C) + 2(A+T).

The reactions were performed either in the T-Gradient PCR machine from Biometra or the GeneAmp 2400 Thermocycler from Perkin Elmer. A standard PCR reaction format is listed in the following table, however, annealing temperatures and elongation times were calculated specifically for each reaction.

Step	Temperature	Time
Initial denaturation	94ºC	3 min
Denaturation	94ºC	30 s
Annealing	(Calculated Tm) - 5 ºC	30 s-1 min
Elongation	72 ºC	1 min per 1000 bases
	4 ºC	∞

Table 2.6 Typical PCR cycling

If the PCR product generated was subsequently used for cloning, the entire reaction was loaded on a gel and the template DNA and primers were separated from the PCR product by gel electrophoresis. The PCR product was excised from the gel and purified prior to restriction enzyme digest (see sections 2.2.1.2 and 2.2.1.4).

2.2.1.2. Restriction Digest

In order to clone existing DNA or newly synthesized PCR products, restriction digests were performed as described by Sambrook *et al*. 1989. Endonucleases were obtained from either

New England Biolabs or Fermentas. The digests were set up according to the manufacturers instructions and were incubated for 1h at 37 ºC, unless the enzyme required a different temperature.

2.2.1.3. Agarose Gel Electrophoresis

Separation of DNA fragments from PCR reactions or restriction digests was achieved by horizontal gel electrophoresis carried out in agarose gel chambers (Amersham Biosciences). Agarose (Invitrogen) was melted in 1xTAE (100mM Tris/Actetate, 5 mM EDTA, pH8). Agarose concentrations between 1 and 2% were used depending on DNA fragment size. Prior to pouring the gel, 0.5 µg/ml of ethidium bromide (Merck) was added. To assist in gel loading and front monitoring the DNA sample was mixed with 6x gel loading buffer (10 mM Tris HCl, 0.25% (w/v) xylene cyanol FF, 30 % glycerol (v/v)). After loading the samples and DNA Markers (Lambda DNA/EcoR1+HindIII, Gene Ruler™ 100bp DNA Ladder, Fermentas), the fragments were separated in 1xTAE buffer by applying a constant voltage of between 50 and 150 V, depending on the desired separation time. After separation the DNA fragments were visualized using a UV transilluminator (UVT 2035, Herolab).

2.2.1.4. DNA Extraction from Agarose Gel

Under UV light, the DNA band was excised from the agarose gel using a scalpel and placed in a 1.5 ml tube. The DNA was purified from the gel using the QIAEX Gel Extraction Kit from Qiagen as described in the handbook.

2.2.1.5. DNA Ligation

In order to create the desired plasmid constructs, insert and vector fragments with compatible ends were ligated to each other. A typical 10 µl reaction contained vector and insert in a ratio of 1:3, respectively, 1x ligase buffer and 1 unit of T4 DNA Ligase (both Fermentas). The reaction was allowed to proceed either at room temperature (RT) for a minimum of 30 min or at 16 ºC overnight.

2.2.1.6. Preparation of Competent Bacteria (KCM Method)

The preparation was carried out according to Klebe *et al.* (1983). 200 ml of LB Broth (1.0% (w/v) Bacto-Tryptone (Difco), 0.5% (w/v) Yeast Extract (Difco), 1.0% (w/v) NaCl (Merck) adjusted to pH 7.0 and autoclaved) was inoculated with an overnight starter culture of

TOP10' bacteria. The culture was incubated at 37 ºC with shaking until an optical density of 600 nm (OD_{600}) of 0.3-0.6 was achieved. Upon removal of the cultures from the incubator, they were placed on ice. The cells were then harvested by centrifugation at 5000 rpm for 5 min at 4 ºC in a tabletop centrifuge (Eppendorf 5415). The pellet was resuspended in 20 ml of ice-cold TBS (1x LB broth (pH 6.1) diluted from a 5x stock solution, 10 % (w/v) Polyethylene glycol 3300 (PEG 3300), 5 % (w/v) DMSO, 10 mM $MgCl_2$, 10 mM $MgSO_4$). After incubating for 10 min on ice, the cell suspension was aliquoted in 500 µl portions into 1.5 ml tubes using a pre-chilled 10 ml Stripette. The aliquots were immediately snap-frozen in liquid nitrogen and stored at -70 ºC until use.

2.2.1.7. Transformation of Competent Bacteria

An aliquot of competent bacteria was thawed on ice. Meanwhile, the DNA to be transformed was mixed with 5x KCM (500 mM KCl, 150 mM $CaCl_2$, 250 mM $MgCl_2$) in a 1.5 ml tube and brought to a total volume of 100 µl with sterile water. The DNA dilution was placed on ice and 100 µl of the thawed competent cells were added, the tube was flicked to mix the content and then incubated for 10-20 min on ice. To induce uptake of the plasmid by the bacteria, the tube was transferred to 37 ºC for 5 min. After the addition of 800 µl of LB, the tube was inverted to ensure mixture and then again incubated at 37 ºC for 20-30 min to initiate expression of the resistance genes. The bacteria were pelleted by centrifugation at 10.5 krpm for 2 min, 800 µl of the supernatant were removed and the pellet was resuspended in the remaining LB. The suspension was plated out on LB-Agar plates containing the appropriate antibiotic. The inverted plates were incubated at 37 ºC overnight.

2.2.1.8. Mini Preparation of Plasmid DNA Bacterial Clones

A single bacterial colony was inoculated in 3 ml of LB containing either 50 mg/ml of Ampicillin or 30 mg/ml of Kanamycin in a sterile culture tube. The culture was grown overnight at 37 ºC with shaking (225 rpm), after which 1.5 ml of the culture was transferred to an Eppendorf tube. The bacteria were collected by centrifugation and the pellet was resuspended in 200 µl of P1 Buffer (50 mM Tris-Cl (pH 8.0), 10 mM EDTA, 100 µg/ml RNase A). Alkyline lysis of the bacteria was performed by adding 200 µl of P2 Buffer (200 mM NaOH, 1 % SDS (w/v)) and mixing the tubes by inversion. After a short incubation at RT, 200 µl of P3 Buffer (3.0 M K Acteate (pH 5.5)) was added and the tubes were again inverted to mix. Removal of the precipitated proteins from the lysate was achieved by a 5

min centrifugation step at 14 krpm. The supernatants were transferred to new 1.5 ml tubes and 400 µl of isopropanol were added. The Plasmid DNA was precipitated by centrifugation at 13 krpm for 5 min. DNA pellets were washed once with 70 % (v/v) ethanol, allowed to dry, and reconstituted in TE or water with RNase. Plasmids were analyzed by restriction digests. If the plasmid was to be sequenced the plasmid was reprecipitated using $1/10^{th}$ vol. of 3 M Na Acetate (pH 5.5) and 2.5 vol. of 100 % ethanol. After a 5 min centrifugation at 14 krpm, the pellets were washed with 70 % ethanol, dried and resuspended in water containing 0.1 mg/ml RNase A.

2.2.1.9. DNA Sequencing

In order to verify that the reading frame and the nucleotide sequence of cloned cDNAs were correct, DNA sequencing analysis was performed. A 0.5 µl aliquot of the reprecipitated plasmid was placed in a 0.5 ml tube, along with 10 pmol of the sequencing primer and 2 µl of Big Dye (ABI). In a thermocycler the 10 µl reaction was subjected to the following sequencing program cycle.

Step	Temperature	Time
Initial denaturation	96 ºC	1 min
Denaturation	96 ºC	20 s
Annealing	50 ºC	5 s
Elongation	60 ºC	4 min
	4 ºC	∞

Table 2.7 Thermocycler program used for sequencing.

After completion of the reaction, the DNA was precipitated by adding $1/10^{th}$ vol. of 3 M Na Acetate (pH 5.5) and 2.5 vol. of ethanol, and centrifuging for 30 min at 14 krpm. After a 70% (v/v) ethanol wash, the pellets were dried and sent for further analysis.

2.2.1.10. Midi Preparation of Plasmid DNA

Applications like mammalian cell transformation with plasmids require highly pure and intensely supercoiled DNA. To achieve this quality of plasmid DNA, it was prepared using the NucleoBond® Xtra Midi Plasmid DNA Purification Kit from Macherey and Nagel. In short, an overnight culture of bacteria (200 ml) containing the desired plasmid was collected

by centrifugation. The pellet was resuspended in 8 ml of RES Buffer, then 8 ml of LYS Buffer were added, and the contents were gently mixed. After a brief incubation for 5 min, 8 ml of NEU Buffer were added, and the contents were again gently mixed. The lysate was poured onto an equilibrated NucleoBond® Xtra column containing a filter. After all of the lysate passed through the column, a wash step with 5 ml of EQU Buffer was performed and the filter was removed. The column was also washed with 8 ml of WASH Buffer, before the DNA was eluted with 5 ml of ELU Buffer and precipated by adding 4 ml of isopropanol. The DNA pellet was washed with 70% (v/v) ethanol, dried and resuspended in water.

2.2.2. Yeast Two Hybrid Techniques

2.2.2.1. Yeast Transformation

A single, well isolated colony of *Saccharomyces cerevisiae* AH109 grown on YPDA agar (for agar plates 20 g/l Bacto Agar was added to YPDA medium composed as described below) was inoculated into 3 ml of YPDA medium (20 g/l Difco peptone, 10 g/l Difco yeast extract, 2 % (w/v) glucose (Merck), 0.2 % (w/v) adenine hemisulfate (SIGMA), 10 mg/ml kanamycin; (pH 5.8)). After overnight incubation, a flask with 50 ml YPDA medium was inoculated with the starter culture and the yeast were grown at 30 ºC to an OD_{600} of 0.4-0.5. The cells were collected by centrifugation with 3 krpm for 5 min and washed once with 25 ml of sterile water. The cell pellet was resuspended in 1ml of a 100 mM LiCl, transferred to a sterile 1.5 ml tube, and quickly pelleted again at 13 krpm for 15 s in a minifuge. Finally, the pelleted cells were resuspended in 400 µl of 100 mM LiCl. Meanwhile, salmon sperm DNA (2 µg/ µl) was heat denatured by placing it in a boiling water bath for 5 min and then quickly transferring it to ice in order to preserve its single-stranded state. For each transformation reaction, 50 µl of yeast cell suspension were placed in a 1.5 ml tube and quickly spun down. The following solutions were layering on top of the pellet in the order given here: 240 µl of 50 % (w/v) PEG 3300, 30 µl of 1 M LiCl, 50 µl of single stranded salmon sperm DNA, 0.1-10 µg plasmid DNA in a total volume of 34 µl. After resuspending the cell pellet by vortexing, the reaction was placed at 30 ºC for 30 min. Plasmid uptake was assisted by a 30 minute heat shock at 42 ºC, before the cells were collected at 1000 rpm for 15 s. Finally, the cells were resuspended in 500 µl of sterile water and 100-200 µl aliquots of the suspension were plated out on the appropriate Synthetic Defined (SD) selection plate

(6.7 g/l Yeast nitrogen base without amino acids (Clontech), 20 g/l bacto-agar, 2 % (w/v) glucose, and the appropriate dropout supplement mixture (Qbiogene), 10 μg per ml kanamycin; (pH 5.8)). The plates were incubated at 30 ºC until colonies appeared.

2.2.2.2. Yeast Two-Hybrid Screening

A yeast two-hybrid screen, using the middle domain of Sharpin as bait, was performed according to Clontech's Matchmaker™ Pretransformed Library User Manual. Amino acids 171-304 of the rat Sharpin gene were cloned into the pGBTK7 vector and transformed into the AH109 strain as described above. A single transformed colony was used to inoculate 50 ml of SD-Trp medium and grown to an OD_{600} of 0.8. The cells were collected by centrifugation at 1,000 x g for 5 min, and resuspended in 5 ml of SD-Trp medium. An aliquot of 1 ml of the *S. cerevisiae* Y187 strain pretransformed with the rat pACT Library was thawed at RT. After a 10 μl aliquot of the library was removed for library titration, the rest of was combined with the 5 ml pGBKT7 Sharpin suspension in a 2 l flask containing 45 ml of 2 x YPDA liquid medium. Mating was propagated at 30 ºC for 26 h with slow shaking (40 rpm). The diploid cells were harvested by 10 min centrifugation at 1000 x g, residual cells were collected from the flask by rinsing with 50 ml of 0.5 x YPDA and this solution was used to wash the pelleted cells. After pelleting by centrifugation, the cells were resuspended in 10 ml of 0.5x YPDA, and 200 μl aliquots were plated out onto 25 SD/-Ade/-His/-Leu/-Trp (QDO) plates (∅15 cm) and 25 SD/-Ade/-His/-Trp +10 mM 3-AT (TDO) plates (∅15 cm). The inverted plates were kept at 30 ºC until colonies appeared.

2.2.2.3. β-Galactosidase Colony-Lift Filter Assay

To verify positive clones obtained from the screen, each colony was restreaked into one box of a grid on a fresh QDO plate (∅10 cm), and returned to 30 ºC to grow. When a lawn had grown, the plates were removed from the incubator and sterile 10 cm Whatman #5 filter paper was laid over the colonies, smoothened out with forceps, and marked by poking a pattern of holes with a sterile needle. The filter was removed and laid in liquid nitrogen to permeabilize the cells. Meanwhile, fresh filters were soaked on a tray with Z Buffer (60 mM Na_2HPO_4, 40 mM NaH_2PO_4, 10 mM KCl, 1 mM $MgSO_4$, 0.27 % (v/v) β-mercaptoethanol, 0.334 mg/ml 5-bromo-4-chloro-3-indolyl- β-D-galactopyranoside (X-Gal); (pH 7.0)). The frozen filters were placed upon the soaked ones and incubated at RT to allow β-Galactosidase released from the yeast cells to hydrolyze the X-Gal and form a blue

precipitate. Colonies that turned blue were inoculated from the grid plate into 3 ml of liquid SD-Leu medium and incubated at 30 ºC with shaking for 48 h.

2.2.2.4. Plasmid Isolation from Yeast

The 3 ml cultures from confirmed positive clones were collected by centrifuging the culture tubes at 3 krpm for 5 min. 100 µl of STET Buffer (50 mM Tris/HCl, 50 mM EDTA, 8 % (w/v) sucrose, 5 % (v/v) Triton X-100; (pH 8.0)) were used to resuspend the pellet. The suspension was transferred to a 1.5 ml Eppendorf tube and the amount of glass beads (425-600 microns, SIGMA) that fits into the top of a 0.5 ml tube was added to each cell suspension. Mechanical shearing was achieved by placing the 1.5 ml Eppendorf tubes in a multi-tube vortex mixer and shaking vigorously for 5 min. Then another 100 µl of STET Buffer were added. In order to heat denature their contents, the tubes were placed in a boiling water bath for 5 min, and then put on ice to cool. After centrifugation for 10 min at 14 krpm, 180 µl of each supernatant were transferred to a fresh 1.5 ml tube, 90 µl of 7.5 M NH_4 acetate were added, and the tubes were chilled at -80 ºC for 1h. Precipitated proteins were removed by centrifugation with 14 krpm for 30 min at 4 ºC; again 180 µl of the supernatant were transferred to fresh 1.5 ml tubes. Two volumes of 100 % ethanol were added and the DNA was allowed to precipitate at -80 ºC for 30 min. The precipitated DNA was collected by centrifuging with 14 krpm for 30 min at 4 ºC. The pellet was washed with 70 % ethanol, dried, and dissolved in 100 µl of water. To further purify the DNA it was bound to QIAEX matrix as described by the corresponding QIAGEN manual for DNA purification. Eluted plasmids were then transformed into competent *E. coli*, the amplified plasmid DNA was isolated from the bacteria and sequenced as described above.

2.2.3. Cell Biology Techniques

2.2.3.1. Culture of HEK293 Cells

Human Embryonic Kidney 293 (HEK293) cells were cultivated in Dulbecco's Modified Eagle's medium (DMEM, Cambrex) containing 10 % (v/v) Fetal Calf Serum (SIGMA), penicillin (100 U per ml) and streptomycin (100 µg per ml). Proper growth was ensured by incubation in a 37 ºC humidified atmosphere with 5 % CO_2. The cells were regularly spilt to maintain optimal growth. Splitting was performed as follows: the medium was aspirated from the plates, the cells were washed once with PBS (137 mM NaCl, 8.8 mM Na_2HPO_4,

2.7 mM KCl 0.7 KH_2PO_4; (pH 7.4)). 1ml of PBS was then added to the plate along with 0.5 ml of 1x trypsin (Invitrogen), which was diluted in Versene Buffer (137 mM NaCl, 8.8 mM Na_2HPO_4, 2.7 mM KCl, 0.7 KH_2PO_4, 1 mM EDTA; pH 7.4). As soon as the cells had detached from the plate, 3 to 5 ml of DMEM with 10 % FCS was added to stop the trypsinization, the cells were resuspended well and appropriately diluted for further culture. If the cells were just to be maintained in culture, the suspension was plated out directly, whereas if the cells were to be subsequently transfected, the trypsin/EDTA solution was completely removed from the cells by centrifugation and resuspension of the cells in fresh medium.

2.2.3.2. Transient Transfection of HEK293 Cells

In order to transiently express a gene of interest in HEK293 cells, they were seeded onto plates at about 70-80% confluency. Note that transfection was done concomitantly with the seeding. While the cells were being centrifuged to remove the trypsin, 10 µg of purified plasmid DNA were placed in a sterile 1.5 ml tube, along with 426 µl of sterile water, and 64 µl of 2 M $CaCl_2$. The mixture was pipetted into 0.5 ml of 1xHBSP (1.5 mM Na_2HPO_4, 10 mM KCl, 280 mM NaCl, 12 mM glucose, 50 mM HEPES; (pH 7.0); sterile filtered) in a 15 ml conical tube, while the tube was being vortexed. Precipitates were allowed to form for ~5 min, while the cells were plated out. Prior to adding them onto the cells, the precipitates were briefly pipetted up and down. Each plate was tilted so that all medium collected on one side and the precipitates were directly pipetted into the pooled medium.

2.2.3.3. Cortical Neuron Preparation and Culture

Preparation and cultivation of rat cortical neurons were performed according to Blichenberg *et al*. (1999). Rat embryos (E18-E20) were removed from a euthanized Wistar Rat. The brains of the embryos were dissected and collected in 1x HBSS (10x HBSS from Invitrogen diluted to 1x with water and 1.2g HEPES/1 liter; (pH 7.3); sterile filtered) with 1x penicillin/streptomycin. The hindbrain was separated from the cortex, as the meninges were removed using dissection forceps. The hippocampus was detached from the cortex and both were separately collected in fresh HBSS.

Using dissection scissors, the collected cortices in HBSS were cut into small pieces. The pieces were transferred to a 50 ml conical tube with a 10 ml stripette. The volume was adjusted to 36 ml with HBSS and 4 ml of 10x trypsin-EDTA was added (approximately 4

ml/10 cortices). Parafilm was wrapped around the lid to prevent water from reaching the underside of the lid, and then the conical tube was submersed and immobilized in a 37 ºC water bath. After incubating for 30 min, the 50 ml tube was sprayed well with 70 % ethanol and the parafilm was removed. Gravity was used to collect the pieces of cortex tissue at the bottom of the tube. They were then collected with a 10 ml Stripette and transferred to a fresh conical tube. The trypsin solution was diluted by addition of Plating Medium (DMEM containing 10 % (v/v) FCS and 3 % (v/v) glucose (Merck)) to a final volume of approximately 40 ml. This dilution of the trypsin was repeated a total of three times, before the pieces were finally collected in as small a volume as possible. The tissue was dissociated by vigorously pipetting it up and down first with a 10 ml pipette, then with a long, fire-polished glass pipet and lastly with a long, fire-polished, drawn out glass pipet so that the opening diameter was further reduced by about half. The volume of the cell suspension was adjusted to 45 ml with Plating Medium and it was passed through a cell strainer to remove connective tissue and cell aggregates. One day prior to the neuron preparation, 10 cm plates or glass cover slips in 12 well dishes were already coated with 1 mg/ml poly-L-lysine (SIGMA) in 0.1 M Borate buffer and washed three times with water. Plating medium was added to the coated dishes before 10^6 neurons were seeded on each 10 cm plate. $2x10^5$ cells in Plating Medium were dispensed in each well of the coated 12 well dishes. After the neurons had attached to the plates, the Plating Medium was replaced with Neurobasal Medium (Invitrogen) supplemented with 0.5 % B27 (Invitrogen), 0.5 mM L-glutamine (Invitrogen) and 25 µM Glutamate (Merck). To prohibit the proliferation of contaminating fibroblasts, 5 µM Cytosine-β-D-Arabinofuranoside (Ara C; SIGMA) was added directly to the medium on the plates.

2.2.3.4. Transfection of Cortical Neurons

On day seven of culture, the neurons were transfected by the calcium phosphate method. In the following brief description of the procedure, the first value given is the amount used for 2 wells of a 12 well dish and the second value corresponds to the amount used for one 10 cm dish. Plasmid DNA (2.5 µl, 37.5 µl) and an equal volume of 1 µg/ µl salmon sperm DNA were placed in a 1.5 ml tube. Sterile water (95 µl, 675 µl) was added along with 2.5 M $CaCl_2$ (10 µl, 75 µl). BBS Buffer (100 µl, 750 µl) was pipetted into a (1.5 ml tube, 15 ml conical tube), the DNA containing solution was pipetted into the BBS Buffer while vortexing. Calcium phosphate precipitates were allowed to form for 20 min and were then added to the

neurons. After incubating for 2-4 hours, the cells were washed three times with HBSS or Versene Buffer in order to remove the excess precipitates. Fresh Neurobasal medium was added and the neurons were maintained under normal cell culture conditions until fixation for immunohistochemistry.

2.2.3.5. Immunocytochemistry

In order to visualize the intracellular localization of overexpressed or endogenous proteins, transfected or untransfected cells grown on glass coverslips were fixed at 4 ºC for 10 min with 4 % (w/v) paraformaldehyde (PFA) in PBS. After removal of unreacted PFA by washing three times with PBS, cell membranes were permeablized by incubation with 0.1 % (v/v) Triton X-100 in PBS for 5 min. Following incubation in 5 % (v/v) horse serum as blocking solution for one hour, the coverslips were inverted and placed in a dampened chamber onto 60 µl drops of primary antibody solution diluted in 5 % horse serum. After overnight incubation at 4 ºC, the coverslips were returned to the 12-well dishes and washed 3 times for 5-10 min with PBS. Next the coverslips were incubated with a 1:400 dilution of the appropriate species-specific secondary antibody coupled to a fluorescent dye. For this 30 min at RT with secondary antibody, the coverslips were again inverted and placed in a dampened and darkened chamber onto 60 µl drops. After the 30 min incubation, the coverslips were returned to the 12 well dishes and washed three times with PBS and finally once with water. Using gelatine (SIGMA) the coverslips were mounted onto glass slides and dried flat at 4 ºC. Immunofluorescence staining was observed with a Zeiss Axiovert 135 microscope and documented using a C4742-95-12NRB CCD camera (Hamamatsu) and the OpenLab 2.2.5 software (Improvision). Adobe Photoshop 6.0 software was used for further processing of the image files.

2.2.4. Biochemical Techniques

2.2.4.1. Microtiter Format Protein Concentration Assay

A standard curve was prepared with the following volumes of a 1 mg/ml BSA solution: 0, 2, 4, 6, 10, 15, and 20 µl. Aliquots of the protein samples to be analysed were pipetted into separate wells of the microtiter plate. Protein standard and sample wells were brought up to 20 µl final volume with H_2O. 180 µl of Bradford reagent were added to each well. The absorbance at 600 nm was measured in a microtiter plate reader (Titertek Multiscan Plus,

Flow Laboratories) and the protein concentration of the unknown protein samples was backcalculated from the linear range of the standard curve.

2.2.4.2. SDS-Polyacrylamide-Gel-Electrophoresis (SDS-PAGE)

Proteins were separated based upon their molecular weight by resolving them on discontinuous gels according to Laemmli (1970). The upper third of each gel consisted of the so-called stacking gel, which contained only 5 % (v/v) polyacrylamide (PAA). The lower two thirds of each gel consisted of the so-called resolving gel, which depending upon the molecular weight of the proteins of interest contained between 6 and 15 % PAA. All gels were cast and run using the PROTEAN II or III system from BioRad. Prior to loading the protein samples on the gel, they were completely denatured by boiling for 5 min at 95 ºC in 1 x Laemmli Buffer (10 % (v/v) glycerol, 20 mM DTT, 1.5 % (w/v) SDS, 60 mM Tris/HCl, 0.05 % Coomassie G-250; (pH 6.8)). The buffer reservoirs of the electrophoresis apparatus were filled with SDS Running Buffer (25 mM Tris, 192 mM glycine, 0.1 % (w/v) SDS). After loading the wells with the samples and a molecular weight standard (Full Range Rainbow Marker, Amersham Biosciences), proteins were electrophorised by applying a constant voltage of 150-200 V.

2.2.4.3. Western Blotting

After PAA gel electrophoresis, proteins were transferred to nitrocellulose (PROTRAN, Schleicher & Schuell). Electrotransfer was performed in a Mini-transfer-Blot Apparatus (BioRad) filled with Blotting Buffer (20 % (v/v) methanol, 192 mM glycine, 25 mM Tris, 0.02 % (w/v) SDS) with 100 V constant voltage for 1h at 4 ºC. After the transfer, the nitrocellulose membranes were washed with water and stained with Ponceau S (SIGMA). Blocking was done with a buffer consisting of 5 % (w/v) skim milk powder in TBST (150 mM NaCl, 50 mM Tris, 0.02 % (v/v) Tween 20; pH 7.9). Primary antibodies were diluted in this same Blocking Buffer as specified in table 2.5, and incubated for either for 1h at RT or overnight at 4 ºC. Unbound primary antibody was washed away with three changes of TBST. Then secondary antibody coupled to horseradish peroxidase (HRP) was added at 1:5000 dilution in TBST and incubated with the membranes for 30 min. After another three washes with TBST, the HRP coupled secondary antibody was detected using enhanced chemiluminescence (ECL) (see below). X-Ray film (Cronex 5 Medical) was exposed to the membranes and developed.

The ECL solution was made in the lab according to Haas et al., (2005). Solution A consists of 0.1 M Tris-HCl (pH 8.6) and 0.25 mg/ml Luminol (SIGMA) and Solution B contains p-Coumaric Acid dissolved (1.1 mg/ml) in DMSO. Just prior to use, the solutions were mixed with 35 % H_2O_2 in the following ratios: 1000 µl Solution A: 0.3 µl H_2O_2 : 100 µl Solution B; The ECL solution was incubated with the membranes for 1 min.

2.2.4.4. Expression and Purification of GST Fusion Proteins

For the synthesis of proteins of interest in bacteria, the corresponding genes were cloned in frame downstream of the coding sequence for glutathione S- transferase (GST) in the bacterial expression vectors pGEX-4T2 or pGEX-6P1. Plasmids with the correct in-frame sequences were transformed into BL21 cells and transformants were inoculated into a 3 ml overnight culture. After transferring this starter culture into 200 ml LB-AMP, the bacteria were grown while shaking at 37 ºC until an OD_{600} of 0.8 was reached. Then Isopropyl-β-D-thio-galactopyranoside (IPTG) was added to an end concentration of 0.5 % (v/v) to induce expression of the fusion protein for 2 h with shaking at 37 ºC. The bacteria were collected by centrifugation at 6000 rpm for 20 min and resuspended in 10 ml of STE Buffer (150 mM NaCl, 10 mM Tris (pH 8.0),1 mM EDTA). Lysozyme (1 mg/ml final concentration) was added to digest the bacterial cell wall. The protease inhibitors Pepstatin A and PMSF at end concentrations of 1 µg/ml and 0.1 mM, respectively, were used to prevent protein degradation. Cell membranes and bacterial DNA were sheared by sonification on ice (5 x 10 s; with maximum intensity) and Triton X-100 was added at 1.6 % (v/v) final concentration. Cell debris was removed by centrifugation for 25 min at 16 krpm in a Sorvall A8.24 rotor, then the supernatant was collected and mixed with 1 ml of packed volume of washed Glutathione Sepharose 4B beads (Amersham Biosciences). The GST fusion protein was allowed to bind to the Glutathione Sepharose at 4 ºC with inversion for at least 30 min. The beads were then washed three times with STE Buffer and either stored in an equal volume of STE or the proteins were eluted from the beads by addition of 1 ml of Elution Buffer (10 mM glutathione, 50 mM Tris/HCl (pH 8.0)) and then stored in frozen aliquots.

2.2.4.5. GKAP Affinity Purification

Taking advantage of the fact that the C-terminal amino acids PEAQTRL of the protein GKAP have high affinity for the PDZ domain of Shank1, one can selectively pull down proteins containing this domain from cell lysates by using sepharose beads covalently

coupled with a peptide of this sequence. Plasmids containing the PDZ domain of Shank1 either as N-terminal or as C-terminal tag were used to clone genes of interest. After transfection of HEK293 cells with these plasmids, the PDZ fusion proteins were transiently expressed for 24 to 48h. The cells were washed once with icecold PBS and were lysed on ice with 1 ml per 10cm plate of RIPA Buffer (50 mM Tris-HCl (pH 8.0), 150 mM NaCl, 1% (v/v) NP-40, 0.5 % (w/v) Na-deoxycholate, 5 mM EDTA, 0.1 % SDS, 100µM PMSF, 1 µg/ml Pepstatin A, 10 µg/ml leupeptin). After 15 min incubation, the lysates were collected and cell debris was removed by centrifugation with 14 krpm for 5 min at 4 ºC. A 30 µl aliquot of each supernatant was saved for expression control and the rest was transferred to a fresh 1.5 ml tube and 40 µl of a 50% slurry (washed) of the GKAP peptide coupled to NHS-sepharose (see below) were added. On a rotator wheel, the tubes were incubated at 4 ºC for at least 1h, after which the beads were washed three times with RIPA Buffer. Finally, the beads were resuspended in 15 µl of 5 x Laemmli Buffer.

2.2.4.6. Peptide Coupling to NHS Sepharose

In order to immobilize peptides for affinity purification, they were coupled to N-hydroxy-succinimide (NHS)-activated sepharose 4 Fast Flow (Amersham Biosciences). A peptide with the sequence IYIPEAQTRL was custom synthesized by Biogenes. Polyubiquitin chains for coupling were obtained from Boston Biochem. 0.3 mg of the peptides were reconstituted in Coupling Buffer (0.1 M $NaHCO_3$, 0.5 M NaCl (pH 7.5-8.0)). Meanwhile, 1 ml of the packed NHS sepharose was washed three times with ice cold 1 mM HCl to prevent hydrolysis of the active ester groups. After addition of the peptide solution to the washed NHS beads, the activated ester group on the sepharose can attack the primary amino group of the peptide, thereby forming a stable amide linkage. After rotating the reaction either at RT for 4 h or at 4 ºC overnight, the remaining non-reacted coupling groups were blocked by incubating the beads in Buffer 1 (0.1 M Tris-HCl (pH 8.0) 0.5 M NaCl) for 30 min with rotation. Finally to ensure complete blockage, the beads were washed three times successively with 14 ml of Buffer 1 and with 14 ml of Buffer 2 (0.1 M NaAc (pH 4.0), 0.5 M NaCl). The washed beads were stored at 4°C in Coupling Buffer with 20 % (v/v) isopropanol.

2.2.4.7. Postsynaptic Density Preparations

Postsynaptic densities (PSD) of cortical neurons were prepared according to Ehlers (2003) (http://www.ehlerslab.org/protocols/psdprep.html) with some modifications. Neurons were cultivated on 10 cm plates and the cells were collected from the plates by scraping in a 1 ml volume of HEPES-buffered sucrose (0.32 M sucrose, 4 mM HEPES (pH 7.4) 1 tablet of Complete™ protease inhibitors (Roche) 50 ml buffer, 2 mM EDTA, 50 mM NaF, 20 mM β-glycerophosphate, 1mM activated odium orthovanadate). After homogenization with a glass-teflon homogenizer and centrifugation at 1000 x g for 10 min at 4 ºC, the supernatants were collected in a fresh tube. Another 1 ml aliquot of HEPES-buffered sucrose was used to wash the 10 cm plate and this wash was used to resuspend the above pellet homogenized and centrifuged as before. After taking an aliquot input, the supernatants were combined and centrifuged for 15 min at 10,000 x g. The pellets were resuspended in 1 ml HEPES-buffered sucrose and spun at 10,000 x g for 15 min. Following resuspension of the pellets in 1 ml of ice cold 4 mM HEPES (pH 7.0) with Complete™ protease inhibitors and phosphatase inhibitors the suspensions were homogenizedin small glass-teflon homogenizers, and then incubated at 4 ºC with rotation for 30 min. The synaptic membranes were collected by centrifugation at 20,000 x g for 30 min and resuspended in 500 µl of ice cold 50 mM HEPES (pH 7.4) plus Complete™ protease inhibitors and phosphatase inhibitors. After homogenization small glass-teflon homogenizers, Triton X-100 was added to 0.5 % (v/v) and incubated at 4 ºC for 15 min on a rotator. Finally, the PSDs were collected by centrifugation at 32,000 x g for 20 min; the pellets were resuspended in 100-500 µl of 50 mM HEPES (pH 7.4) plus Complete™ protease inhibitors and phosphatase inhibitors, and homogenized as described before. If proteasome inhibitor was added to the neurons in culture it was also added to each solution in the preparation, because MG132 is a reversible inhibitor.

2.2.4.8. In vivo labeling of Proteins with [S^{35}]-Methionine

In order to determine protein stability, HEK293 cells overexpressing full-length Sharpin were plated onto 6 cm dishes coated with poly-D-Lysine (SIGMA). One hour prior to labeling, the cells were washed three times with PBS and then incubated in starvation medium (DMEM with dextrose, without glutamine, without methionine (Catalog # 1642254; MP Biochemicals Inc), with 0.1 % BSA and 1 x Glutamax (Invitrogen)). Cellular proteins

were labeled by incubating the cells in 37 ºC incubator with 5 % CO_2 for 1 h in starvation medium containing 50 µCi [S^{35}]-Methionine per 700 µl medium. To minimize radioactive contamination of the incubator, the cell culture plate with the labeling medium was placed inside a 15 cm plate lined with charcoal filters on the lid. After this 'pulse' labeling, the radioactive medium was removed and the plates were washed once with PBS. The 'chase' was initiated by giving 1 ml of Chase Medium (DMEM, 10 % (v/v) FCS, 0.25 µg/ml non-radioactive methionine) to each plate and incubating for various time periods. Immediately after the labeling period, those plates chosen as labeling controls were washed three times with PBS and lysed in RIPA buffer as described before. After removal of cell debris, the supernatants were stored frozen at -20 ºC until the samples of the chase reactions had also been collected. For the chase kinetic, the cells were incubated in Chase Medium for 1.5, 3 and 6 h, respectively. After each time point, cells of the corresponding sample were lysed and frozen as described above for the labeling controls. When the samples for all of the time points had been gathered, they were thawed together, given 40 µl of Protein A/G Plus Agarose (Santa Cruz) pre-washed three times with RIPA buffer, and rotated for 1h at 4 ºC. This incubation served to deplete proteins that unspecifically bound to Protein A/G Plus Agarose. The beads were spun down and the precleared supernatants were transferred to fresh 1.5 ml tubes. After adding 5 µl of anti-c-myc antibody to each tube and rotating the samples for 1 h at 4 ºC, 40 µl of pre-washed Protein A/G agarose were added to capture the antibody and the rotation was continued for another 30 min. After that the beads were washed once with 1 ml of Wash Buffer 1 (1x PBS, 0.6 M NaCl, 0.1 % (v/v) SDS, 0.05 % NP 40), then with 1 ml of Wash Buffer 2 (1 x PBS, 1 % (v/v) Triton X-100, 2 M KCl) and finally twice with Wash Buffer 3 (0.1 x PBS, 15mM NaCl). The beads were then boiled in Laemmli Buffer. Note that for Sharpin immunoprecipitation DTT was omitted from the Laemmli Buffer, because the reduced heavy chains of the antibody run at the same height as Sharpin and the specific signal for Sharpin is then compromised. After separating the samples by SDS-PAGE, the gels were dried and exposed to a phosphoimager screen capable of detecting S^{35}.

2.2.4.9. DNA Fragmentation Assay

HEK293 cells and neurons were treated with or without proteasome inhibitor (MG132) overnight. Cells were lysed in 500 µl of TTE Buffer (10 mM Tris-HCl, 10 mM EDTA, 0.2 % (v/v) Triton X-100; pH 7.4) and the cell debris was removed by centrifugation with 14

krpm for 5 min at 4 ºC. Supernatants were then extracted twice with phenol-chloroform (1:1 mixture). To the extracts 1/10th vol. of 3 M sodium acetate, 1 µg/µl glycogen (SIGMA), and 2.5 volumes of 100 % ethanol were added, and DNA precipitation was enhanced by incubating for 30 min at -70 ºC. Precipitated DNA was collected by centrifugation with 10 krpm for 15 min at 4 ºC, washed once with 70 % (v/v) ethanol and dried. The DNA was resuspended in water containing 0.1mg/ml RNase A, and incubated for 1 h at 37 ºC to digest all RNA. Fragmentation analysis was done on a 2 % Agarose gel.

2.2.4.10. Subcellular Fraction by Sucrose Gradient Centrifugation

The cell lysate was fractionated by a modified version of the protocol used by Wente *et al*. (2005). HEK293 cells overexpressing c-myc, OS-9, and PDZ-Sharpin constructs were treated overnight with proteasome inhibitor. After 16 h of treatment, the cells were harvested by scraping them in 1 ml of isotonic buffer (20 mM Hepes-HCl (pH 7.4), 1 mM $MgCl_2$, 1 mM EGTA, 250 mM sucrose). The cells were disrupted with ten strokes of a glass-teflon homogenizer. Centrifugation with 1100 x g at 4ºC for 5 min removed the nuclei and cellular debris. 1.6 mg of the supernatant were applied to the top of 11 ml of a discontinuous sucrose gradient (0.6-2.0 M sucrose in isotonic buffer). After centrifugation with 100,000 x g for 20 h at 4ºC, 1 ml aliquots of the gradient were removed successively from the top. The fractions were analyzed by Western blotting.

Chapter 3 Results

3.1. Novel Protein Binding Partners of Sharpin

3.1.1. Yeast Two-Hybrid Screen with the Central Domain of Sharpin

One series of experiments performed in the course of this work was aimed at identifying novel interaction partners of Sharpin that could potentially shed some light on its cellular function. In order to elucidate the role of Sharpin in the cell, the central ubiquitin-like domain of Sharpin was used as bait to perform a yeast-two hybrid screen. Employing the rat brain pretransformed library from Clontech, 3.1 x 10^6 clones were screened for interaction with Sharpin. Ten of the 33 different confirmed positive clones listed in Table 3.1 were found more than once. The most frequently found protein was OS-9, which had originally been identified due to the fact that it is highly expressed in osteosarcomas. OS-9 is a protein with a signal peptide and has been described extensively in yeast with regard to its role in endoplasmic reticulum associated degradation (ERAD) (Friedmann *et al*., 2002). In mammals, OS-9 has not yet been shown to play a similar role in ERAD, but rather seems to be involved in the hypoxic response, since it interacts with hypoxia-inducible factor 1α and HIF-1α prolyl hydroxylases. Litovchick *et al*. (2002) showed that one isoform of mammalian OS-9 is localized in the peripheral membrane of the ER and described a role for it in the secretory pathway.

Another multiply found protein that bound to the middle region of Sharpin as bait was the E3 ligase EDD1. It is a HECT (Homologous to E6-Assoicated Protein C-Terminus) domain E3-ligase that is mainly localized in the nucleus of cells, probably due to its interaction with importin α. It has been shown to upregulate progesterone receptor transcription activity (Henderson *et al*., 2002). Altered expression of EDD1 has been described in many different types of cancers and this is attributed to its role in the activation of the DNA damage checkpoint kinase (Henderson *et al*., 2006). The interactions with OS-9 (upregulated in osteosarcoma protein 9) and EDD1 (E3 Ubiquitin-protein ligase, 100 kDa protein) were chosen for further investigations as potentially having physiological relevance for the cellular function of Sharpin.

Identified Interacting Partner	# of clones	Accession #
upregulated in osteosarcoma OS-9	9	BC085907
stathmin-like 3 Stmn 3	4	NM_024346
succinate dehydrogenase complex subunit B, iron sulfur	4	XM_216558
EDD100 kDa protein E3 ligase	3	X64411
glyceraldehyde 3-phosphate dehydrogenase	3	NM_017008
PREDICTED dynactin 6	3	XM_214362
S100 protein, beta polypeptide	2	BC087026
plectrin 1 (Plec 1)	2	NM_022401
MUS81 endonuclease	2	BC098853
translocase of inner mitochondrial membrane 50 homolog	2	BC010303
PREDICTED sperm associated antigen 8	1	XM_432826
PREDICTED similar to KB07 protein	1	XM_344580
NADH dehydrogenase (ubiquinone) Fe-S protein	1	BC082067
superoxide dismutase 2,mitochondrial	1	BC070913
mitochondrial genome	1	MIRNXX
calcitonin gene-related peptide-receptor component protein	1	BC059117
ATP synthase, H+ transporting, mitochondrial	1	BC059139
PREDICTED similar to FAD104	1	XM_226988
mitochondrial genome	1	MIRNXX
PREDICTED similar to SERTA	1	XM_234301
PREDICTED poly (rC) binding protein 4	1	XM_343468
Nicotiana tabacum mRNA for MAP kinase	1	NTA302651
Mus musculus ES cells DNA	1	AK082773
Similar to RIKEN cDNA B230219D22	1	XM_573984
PREDICTED: palmitoylated 6 (MAGUK p55 subfamily member 6) (predicted) (Mpp6_predicted)	1	BC070913
general transcription factor	1	NM_212501
Translation elongation factor 1 alpha	1	NM_175838
guanine nucleotide binding protein gamma 3	1	AK032646
autophagy protein 5	1	AM087012
cartilage acidic protein 1	1	BC089944
Pals-beta splice variant	1	AF199010

Table 3.1 Proteins that Interacted with the Central Domain of Sharpin

Gene products identified in a yeast two-hybrid screen are listed with the number of clones found for each candidate and the NCBI accession number of the corresponding nucleotide sequence as reference.

3.1.2. Sharpin/OS-9 Interaction

3.1.2.1. MG132-Induced Sharpin/OS-9 Interaction in HEK293 Cells

Under normal cellular conditions, it was difficult to detect an interaction between OS-9 and Sharpin in HEK293 cells. As both proteins may play roles in protein degradation, one possible explanation was that complexes between OS-9 and Sharpin only exist transiently and are dissociated or degraded rapidly after fulfilling their role in the UPS. In order to determine whether such complexes could be stabilized, when the UPS does not operate normally, the proteasome inhibitor MG132 was added to transfected cells prior to cell lysis.

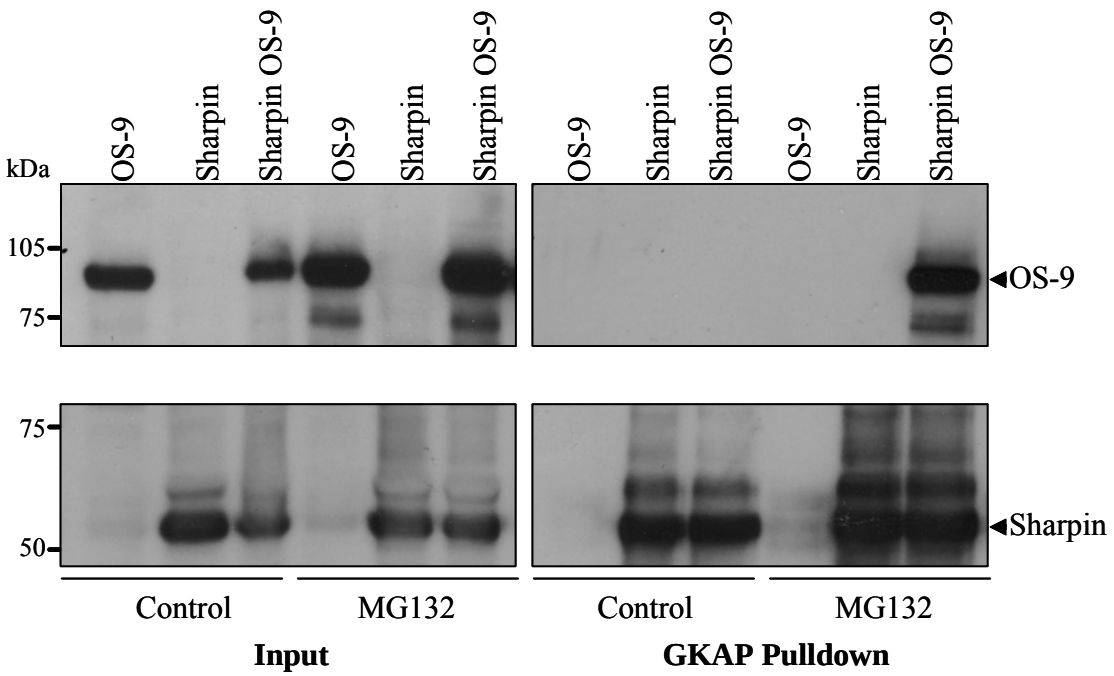

Figure 3.1 OS-9 Coprecipitation with PDZ-tagged Sharpin
HEK293 cells were transfected with c-myc-tagged OS-9 and PDZ-tagged Sharpin constructs. After overnight expression the cells were equally split onto two plates. 24 h post-transfection, 10 µM MG132 was added for 16 h prior to lysis. The lysates were incubated with GKAP-coupled sepharose and the bound proteins were eluted in Laemmli buffer. OS-9 was detected with the α-c-myc antibody and Sharpin with the α-Sharpin antibody

Under these conditions OS-9 clearly coprecipitated with PDZ-tagged Sharpin in pull-downs with GKAP-coupled sepharose. In the course of this work, it became apparent that for reasons unknown PDZ- and EGFP-tagged Sharpin molecules are more stable in HEK293 cells than the myc-tagged.

3.1.2.2. No Effect of ER or Oxidative Stress on Sharpin/OS-9 Interaction

In addition to inhibiting the proteasome, MG132 has been shown to also have secondary effects in cells in particular it induces ER and oxidative stress. Yeast OS-9 and mammalian OS-9 have been described to play a role in both of these MG132-induced stresses. Trying to further pinpoint the "stimulus" regulating the Sharpin/OS-9 interaction, HEK293 cells were treated with known ER and oxidative stressors. As a disulfide reducing agent, DTT increases the number of reduced and hence misfolded proteins in the ER lumen, which promotes ER stress. Thapsigargin causes ER-stress by triggering the release of calcium from the lumen of the ER (Shang *et al*., 2002). Oxidative stress was evoked by the addition of H_2O_2 (Gosslau *et al*., 2001). HEK293 cells transfected overnight with PDZ-tagged Sharpin and c-myc-tagged OS-9 constructs were treated with the reagents mentioned above and analyzed for Sharpin/OS-9 interaction. As shown in Figure 3.2 on page 40, OS-9 only coprecipitated with Sharpin in GKAP sepharose pull-downs from the sample that was treated with MG132. None of the other stress-inducing agents tested here could promote complex formation between the two proteins to any detectable extent. Because neither DTT nor Thapsigargin nor H_2O_2 treatment resulted in enhanced binding of Sharpin and OS-9, it appears that this interaction is indeed a specific result of proteasome inhibition and not due to secondary effects of MG132 treatment like induction of ER or oxidative stress.

3.1.2.3. No Effect of ERAD Inhibition on OS-9/Sharpin Interaction

As shown in the previous section, oxidative or ER stress did not induce OS-9/Sharpin complex formation, whereas adding MG132 to cells in culture did. Since proteasome inhibitors, like MG132, disrupt not only normal cellular protein degradation but also ERAD, it seemed plausible that ERAD inhibition could actually be the stimulus for OS-9/Sharpin interaction, especially given that yeast OS-9 had already been shown to play a role in ERAD. The non-competitive mannosidase I inhibitor 1-deoxymannojirimycin (dMM) is known to block the degradation of misfolded ER-proteins by inhibiting the ERAD pathway (Farinha and Amaral, 2005).

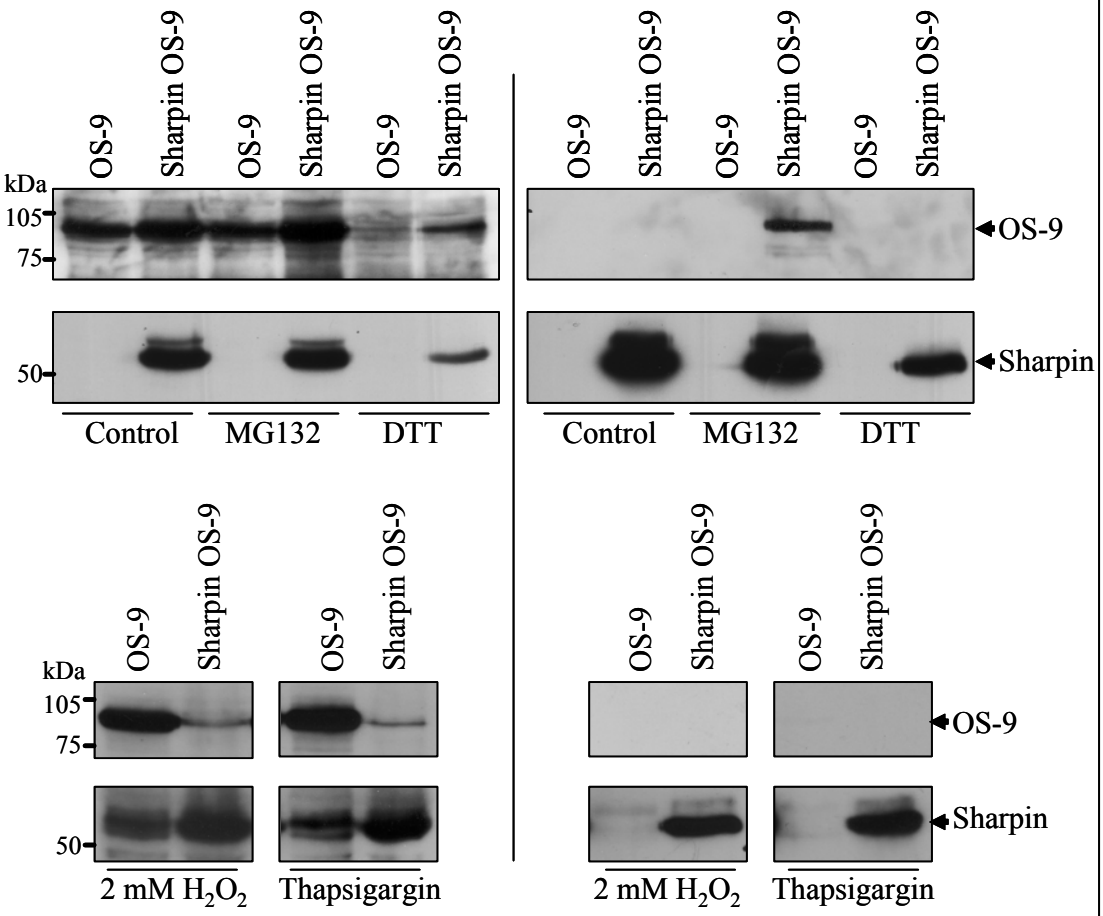

Figure 3.2 ER and Oxidative Stressors do not Promote Sharpin-OS-9 Interaction

HEK293 cells were transfected with c-myc-tagged OS-9 and PDZ-tagged Sharpin constructs. Prior to lysis the cells were treated with either MG132 overnight or thapsigargin for 1 h or H_2O_2 for 4 h or DTT for 1 h. PDZ-Sharpin was precipitated from cell lysates with GKAP-coupled sepharose. Proteins eluted from the beads with Laemmli buffer were analyzed by Western blotting. OS-9 coprecipitated with Sharpin only in the presence of proteasome inhibitor.

In order to determine whether ERAD inhibition is sufficient to induce the OS-9/Sharpin interaction, HEK 293 cells overexpressing PDZ-tagged Sharpin and c-myc-tagged OS-9 were treated overnight with dMM. In parallel with the dMM treatment, lactacystine, another proteasome inhibitor, was tested to further confirm that the complex formation between OS-9 and Sharpin is triggered by inhibition of the UPS. In contrast to MG132, lactacystine is a non-reversible inhibitor, therefore, unlike MG132, it was only added to the cells, but not to the lysis buffer.

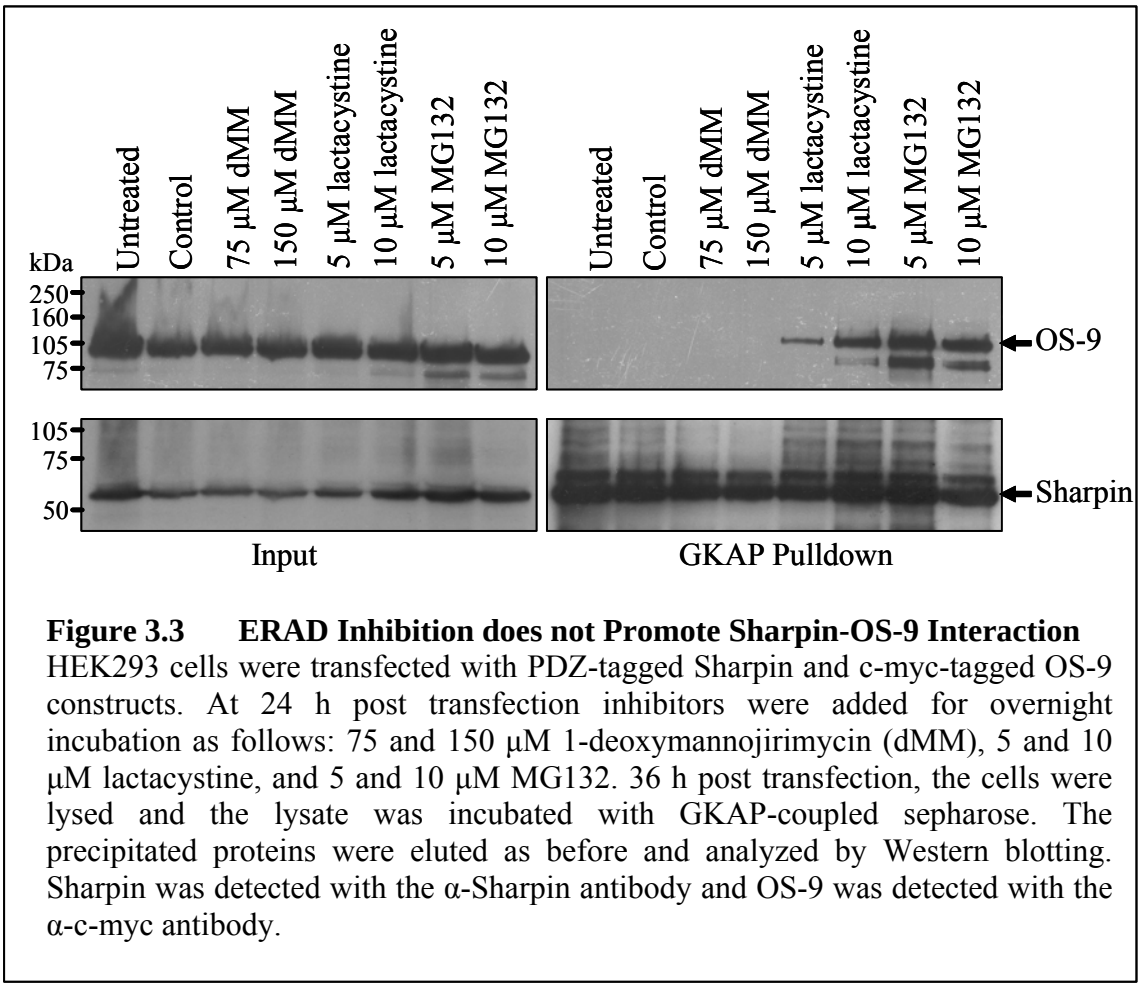

Figure 3.3 ERAD Inhibition does not Promote Sharpin-OS-9 Interaction
HEK293 cells were transfected with PDZ-tagged Sharpin and c-myc-tagged OS-9 constructs. At 24 h post transfection inhibitors were added for overnight incubation as follows: 75 and 150 µM 1-deoxymannojirimycin (dMM), 5 and 10 µM lactacystine, and 5 and 10 µM MG132. 36 h post transfection, the cells were lysed and the lysate was incubated with GKAP-coupled sepharose. The precipitated proteins were eluted as before and analyzed by Western blotting. Sharpin was detected with the α-Sharpin antibody and OS-9 was detected with the α-c-myc antibody.

As seen in Figure 3.3, the ERAD inhibitor dMM was not capable of inducing any detectable coprecipitation of OS-9 with Sharpin. On the other hand lactacystine as well as MG132 were both able to promote this interaction. This result clearly shows that the interaction between OS-9 and Sharpin is directly related to the inhibition of the proteasome and not caused by blocking ERAD.

3.1.2.4. Subcellular Fractionation Analysis of the Sharpin/OS-9 Interaction

As mentioned above, mammalian OS-9 has been described to be subcellularly localized to the cytoplasmic side of the ER membrane. Given that the Sharpin/OS-9 interaction occurs only in the presence of proteasome inhibitor, one possible explanation was that different subcellular localizations of Sharpin and OS-9 prevent their interaction in non-treated cells. In order to determine, where this interaction occurs, a subcellular fractionation was performed on HEK 293 cells overexpressing c-myc-tagged OS-9 and PDZ-tagged Sharpin.

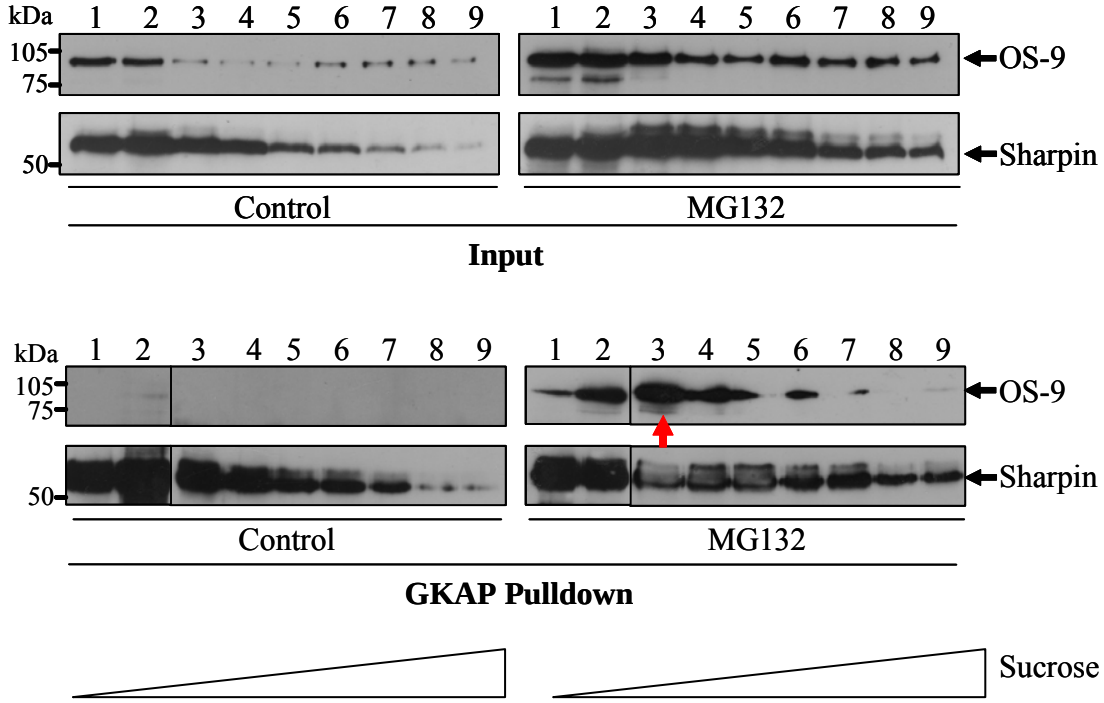

Figure 3.4 OS-9 and Sharpin Interaction analyzed by Sucrose Gradient Cellular Fractionation

HEK293 cells were transfected overnight with c-myc-tagged OS-9 and PDZ-tagged Sharpin constructs. At 24 h post transfection, DMSO or 10 µM MG132 was added for another 16 h. Then cells were homogenized and supernatants free of nuclei and cellular debris were loaded onto discontinuous sucrose gradients. After equilibration centrifugation, the gradients were fractionated and 80 µl of each gradient fraction were retained for Western blotting (top panel). Pull downs with GKAP sepharose (bottom panel) were done with the remaining 500 µl of each fraction. The precipitated proteins were analyzed by Western blotting. Sharpin was detected with the α-Sharpin antibody and OS-9 was detected with the α-c-myc antibody. The red arrow depicts the fraction with the highest extent of OS-9/ Sharpin coprecipitation.

A change in the distribution of both, Sharpin and OS-9, in the different fractions of the gradient was observed, when cells were treated with proteasome inhibitor. In the DMSO treated samples, Sharpin was seen predominately in the first four fractions and OS-9 primarily in the first two fractions, but also to a lesser extent in fractions 6-8. In comparison, the samples treated with MG132 showed an increase in the amounts of both proteins in all fractions of the gradient. This could mean that upon proteasome inhibition these proteins become part of a higher molecular weight complex thereby changing their intracellular localization. To eludicate in which of the different fractions complex formation between Sharpin and OS-9 occurred, each fraction was submitted to a GKAP pull-down assay and the precipitated proteins were analyzed by Western blotting.

As shown in Figure 3.4, dependence of the OS-9/Sharpin interaction on proteasome inhibition was once again confirmed. Complexes of these two proteins were mainly found in the fractions with lower sucrose concentration (fractions 1-7) and a clear peak of coprecipitation was seen in fraction 3. In order to determine where different subcellular organelles migrate in the sucrose gradient, aliquots of the input fractions were also probed with available antibodies directed against subcellular markers. The antibodies available for

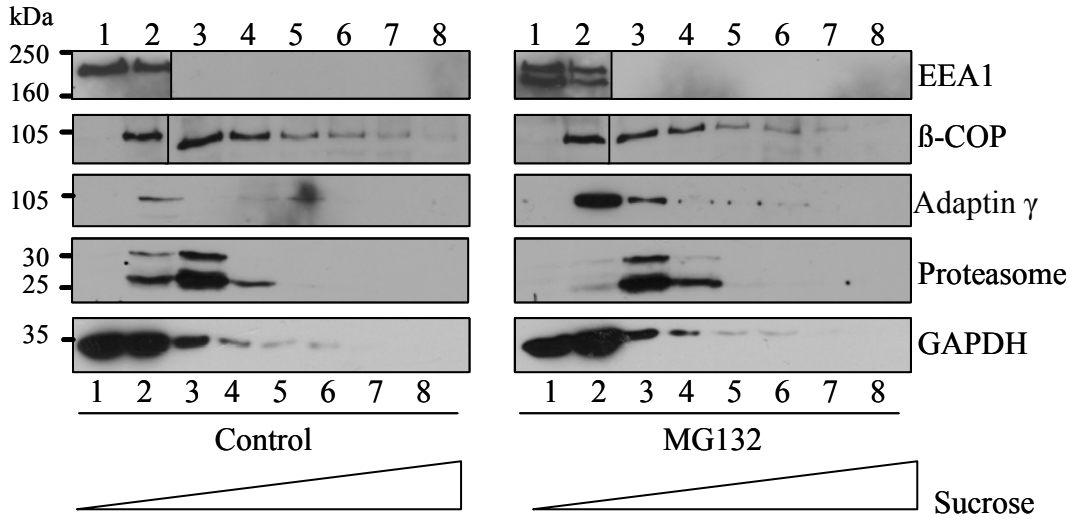

Figure 3.5 Sucrose Gradient Fractionation Analysis
Aliquots from each fraction of a gradient were separated by SDS PAGE and probed with antibodies against the following subcellular marker proteins: β-COP, EEA1, Adaptin γ, 20S proteasome subunit, and GAPDH.

detecting the Golgi apparatus (directed against GM130 and 58 K proteins) and the endoplasmic recticulum (directed against GRP 78) gave no signal in Western blots (data not shown), which is most likely due to low sensitivity or poor quality of the antibodies. However, antibodies recognizing β-cop (a marker for retrograde COP1 vesicle transport from the ER to the Golgi), EEA1 (an early endosome marker), adaptin γ (a protein involved in the sorting between the TGN and endosomes), the 20 S proteasome subunit, and the soluble cytosolic marker protein GAPDH, all gave reliable results. As indicated by the α-GAPDH Western blot in Figure 3.5, the majority of the cytosolic proteins are located in fractions 1 and 2 and progressively lesser amounts occur in the fractions 3 to 6. Given that the peak of Sharpin/OS-9 interaction is detected in fractions 2 to 4, it seems that the interaction does not primarily occur in the cytosol. Furthermore, the Western blots show that β-COP is most prominently found in fractions 2 to 4 and that the 20S proteasome subunit is found exclusively in fractions 3 and 4. So the distribution patterns of both proteins overlapped with that of the Sharpin-OS-9 complexes, whereas the distribution patterns of the endosomal markers EEA1 and adaptin γ correlated poorly. Interestingly, fraction 3 contained the highest amounts of both Sharpin/OS-9 complexes as well as 20S proteasome subunit.

3.1.2.5. Sharpin/OS-9 Colocalization in MG132-Treated Cortical Neurons

In order to see, whether proteasome inhibitor-induced complex formation between Sharpin and OS-9 also occurs in a more physiologically relevant cell type, tagged constructs for both proteins were cotransfected into primary cortical neurons and their subcellular localization was analyzed by immunocytochemisty. When the cells were left untreated, Sharpin staining was concentrated in the nucleus, whereas OS-9 staining was largely cytoplasmic with the highest intensity in the vicinity of the nucleus. In contrast, when the neurons were treated with proteasome inhibitor, the majority of the Sharpin staining was seen in the cytoplasm, especially around the nucleus, and this cytoplasmic distribution coincided largely with that of OS-9. The colocalization of Sharpin and OS-9 in neurons after proteasome inhibition strongly suggests that also in this cell type complex formation is induced by blocking the UPS.

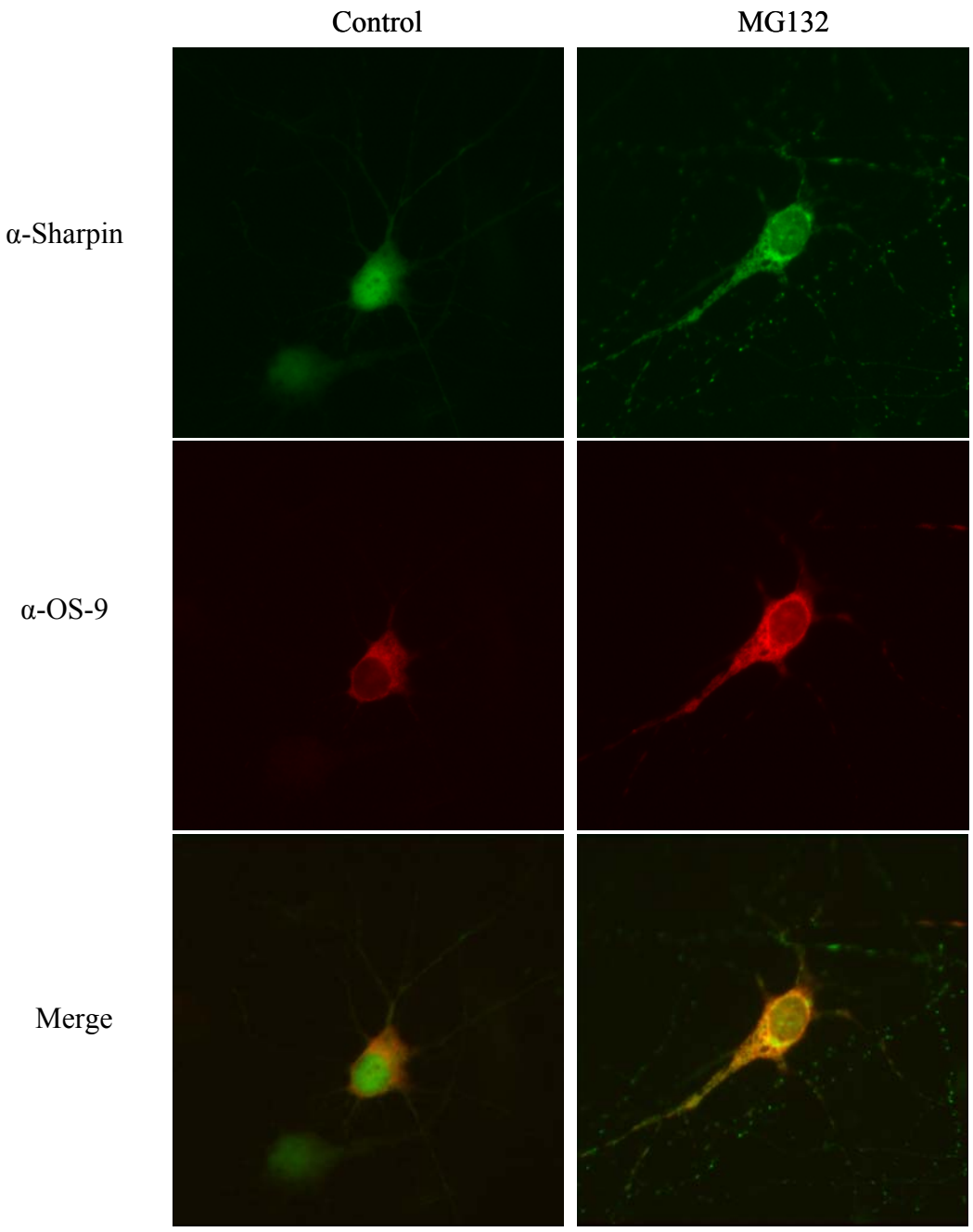

Figure 3.6 Colocalization of Sharpin and OS-9 upon Proteasome Inhibition

Flag-tagged Sharpin and c-myc tagged OS-9 were cotransfected in cortical neurons (DIV 7), proteasome inhibitor was added on day 8 and the cells were finally fixed in 4% PFA on day 9. Sharpin was detected using α-Sharpin primary antibody and an α-rabbit Alexa 488 (green) secondary antibody. OS-9 was detected with α-c-myc primary antibody and an α-mouse Cy3 (red) secondary antibody.

3.1.3. Sharpin/Rpt1 Interaction

To better understand the dependence of the Sharpin/OS-9 interaction on proteasome inhibition, it was investigated, whether Sharpin bound directly to components of the proteasome. Enenkel *et al.* (1998) described the generation of an EGFP-tagged subunit of the 19S proteasome regulatory particle Rpt1, an ATPase that forms part of the hexameric ring in the 19S particle. In this construct, the Rpt1 cDNA had been cloned in frame behind the green fluorescent protein. The fusion protein was still incorporated into the 19S complex and also into functional 26S proteasomes. Therefore, it seemed possible to create a PDZ-tagged Rpt1 protein that can still be integrated into the 26S proteasome. Using GKAP-coupled sepharose, intact proteasomes could then be precipitated from lysates of cells overexpressing PDZ-tagged Rpt1.

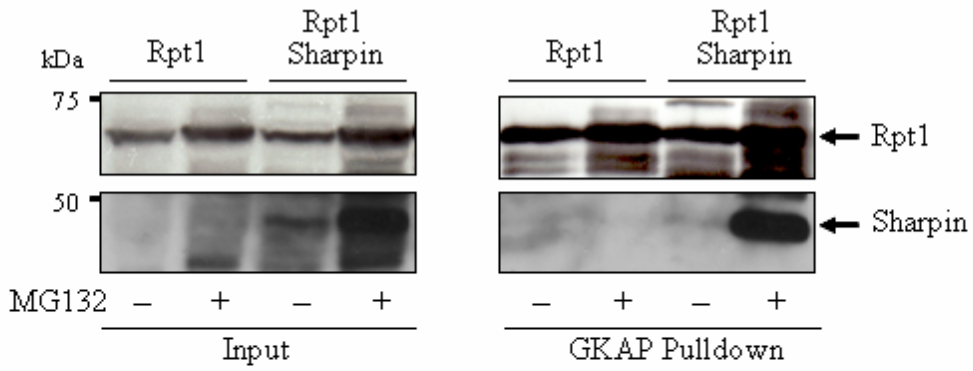

Figure 3.7 Sharpin Coprecipitates with Rpt1, a 19S Proteasome Subunit
HEK293 cells were transfected with PDZ-tagged Rpt1 and c-myc-tagged Sharpin constructs. The cells were treated with MG132 or left untreated. After cell lysis, Rpt1 was pulled down with GKAP-coupled sepharose. Precipitated proteins were eluted as before and analyzed by Western blot. Sharpin was detected with α-c-myc antibody and Rpt1 was detected with α-PDZ antibody.

Figure 3.7 shows that Sharpin massively coprecipitates with the PDZ-tagged 19S proteasome subunit upon proteasome inhibition. This effect was confirmed in three more, independently performed experiments. However, antibodies directed against S5a, another protein in the 19S particle, and against the 20S proteasome subunit did not detect these proteins in the pull-down, suggesting that the interaction of Sharpin and Rpt1 does not

require the structural context of an intact proteasome. So while it is clear that complexes of Sharpin and Rpt1 formed only in the presence of proteasome inhibitor, it cannot be concluded from these experiments that the transient nature of this interaction in the absence of MG132 is due to rapid degradation of the complex or one of the binding partners by intact proteasomes also present in the complex.

3.1.4. Sharpin/EDD1 Interaction

In the yeast two-hybrid screen with the middle region of Sharpin as bait, EDD1 had been found as a Sharpin binding protein. This is particularly interesting with regard to a possible role of Sharpin in the UPS. To test whether the interaction between Sharpin and the E3 ligase EDD1 could be confirmed in mammalian cells, Sharpin and EDD1 were co-overexpressed in HEK293 cells. Using the GKAP pull-down assay described before, PDZ-tagged Sharpin was precipitated from cell lysates and blotted for the presence of EDD1.

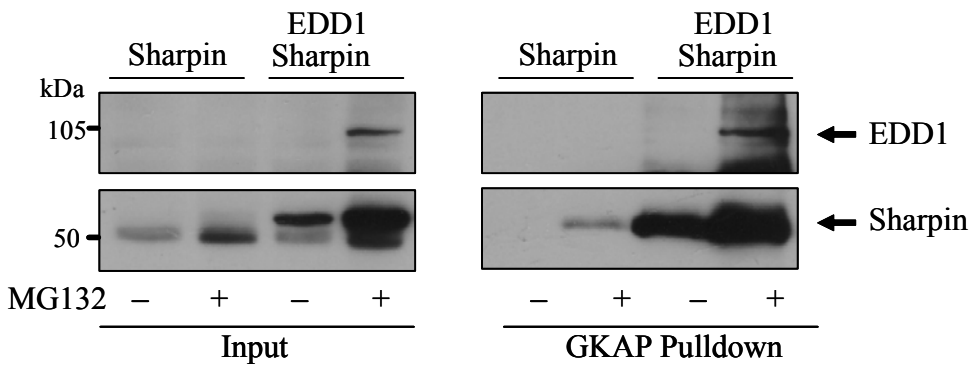

Figure 3.8 Sharpin Coprecipitates with the E3 Ligase EDD1
HEK293 cells were transfected with PDZ-tagged Sharpin and c-myc-tagged EDD1 constructs. The cells were left untreated or treated with MG132 overnight. After cell lysis, Sharpin was precipitated using GKAP-coupled sepharose. Coprecipitating proteins were eluted as before and analyzed by Western blot. Sharpin and EDD1 were both detected with α-c-myc antibody, as the Sharpin construct used in addition to the PDZ-tag also had a c-myc tag.

Figure 3.8 shows that EDD1 indeed coprecipitated with Sharpin, but again the interaction was only seen in the presence of proteasome inhibitor.

3.2. Association of Sharpin with Components of the Ubiquitin Proteasome System

3.2.1. Sharpin/Ubiquitin Interaction

3.2.1.1. Ubiquitin Binding via Sharpin's NZF Domain

Proteins containing Npl4 zinc finger domains (NZF) homologous to Sharpin's zinc finger domain have previously been shown to bind ubiquitin (Alam *et al*., 2004). In order to determine whether or not Sharpin is also capable of ubiquitin binding, a GST-ubiquitin fusion protein was synthesized in *E. coli* and bound to glutathione sepharose. These ubiquitin beads were then incubated with a lysate of HEK293 cells overexpressing Sharpin. As a positive control for Sharpin binding, a GST fusion protein of the ankyrin repeat domain of Shank1 was used, while beads coated only with GST served as negative control.

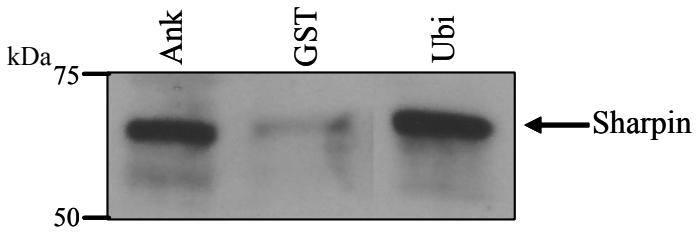

Figure 3.9 GST-Ubiquitin Pull-down
A c-myc Sharpin tagged construct was overexpressed in HEK293. Different aliquots of the same cell lysate were incubated with GST-Ankyrin repeats (Ank), GST, or GST-ubiquitin (Ubi) fusion proteins bound to glutathione sepharose beads. Sharpin bound to the beads was eluted and immunoblotted with α-c-myc antibody. Sharpin bound to GST-ubiquitin equally well as to GST-Ankyrin repeats, whereas it did not bind to plain GST. The Sharpin band in this blot runs at a higher molecular weight than usual, because it contains a portion of PSD-95 besides the c-myc-tag.

As shown in Fig. 3.9, Sharpin indeed strongly interacted with the GST-ubiquitin fusion protein. The amount of pull-down was similar to that seen with a fusion protein containing the Ankyrin repeats of Shank. The fact that GST without a fusion moiety did not detectably bind Sharpin shows that the interactions detected were not mediated by the GST portion of the fusion proteins.To verify that the C-terminal NZF domain of Sharpin was responsible for

its interaction with ubiquitin, the yeast two hybrid system was employed. The part of the Sharpin cDNA encoding the NZF domain was cloned into the yeast-two hybrid bait vector pGBTK7, thereby generating a fusion protein with the DNA binding domain (BD) of the Gal4 protein that is a transcription activator. The ubiquitin cDNA was cloned into the prey vector pACT, which allows for the translation of a fusion protein with the activation domain (AD) of the Gal4 protein. If an interaction between Sharpin and ubiquitin occurs, yeast clones should grow on minimal agar plates without adenine, histidine, tryptophan, and leucine (quadruple drop-out (QDO) plates) due to transcription of the corresponding auxotrophy genes. When a single yeast colony containing both plasmids was serially diluted and spotted onto QDO plates, growth was observed even at a 10^{-4} dilution confirming that the interaction between Sharpin and ubquitin is indeed quite strong.

The majority of interactions between UBDs and ubiquitin occur through the isoleucine 44 residue of ubiquitin, which sits on one side of the ubiquitin molecule (Hicke *et al*., 2005). Recently, however, a novel interaction between an UBD and ubiquitin has been described. Penengo *et al*. (2006) have shown that one of the UBDs from Rabex-5 (Rab5 guanine-nucleotide-exchange factor) interacts with the aspartate 58 residue of ubiquitin, which is located on the opposite side of the ubiquitin molecule. A single UBD bound to Asp 58 does not simultaneously make contacts with the Ile 44 residue. In the same study, it was shown that two Rabex-5 molecules can interact with the same ubiquitin molecule. The A20 zinc finger of one Rabex-5 molecule interacts with the Asp 58 residue, while the other binds to the classical Ile 44 residue of ubiquitin with a MIU domain (motif interacting with ubiquitin), which is the second type of UBD in Rabex-5. In an attempt to elucidate the role of these two different ubiquitin residues for complex formation with Sharpin, the following point mutations were introduced in the pACT-ubiquitin construct: Ile44Ala, Asp58Ala, and an Ile44Ala/Asp58Ala double mutation. The yeast strain AH109 was then cotransformed with the plasmid coding for the C-terminal NZF domain of Sharpin (pGBTK7) and the plasmids for these different ubiquitin mutants. As summarized in Table 3.2, no difference was seen in the extent of auxotrophic growth due to the interaction of Sharpin with either wild-type ubiquitin or one of the two different single point mutants. However, the interaction between the double point mutant and Sharpin's NZF domain was clearly weaker. This result suggests that the NZF domain of Sharpin can bind with comparable affinities to Asp 58 and

Ile 44 of ubiquitin, but in the absence of both residues its binding to ubiquitin is considerably diminished.

Plasmids cotransformed with the Sharpin NZF domain (pGBKT7)	Growth
pACT Ubi	+++
pACT Ubi Ile 44 Ala	+++
pACT Ubi Asp 58 Ala	+++
pACT Ubi Ile 44 Ala + Asp 58 Ala	+

Table 3.2 NZF domain of Sharpin Interacting with Ubiquitin variants

Plasmids containing the cDNA for Sharpin's NZF domain as bait and wildtype or point mutated ubiquitin as prey were cotransformed in AH109 cells. From each cotransformation single colonies (∅ 1 mm) were serially diluted. An aliquot of each dilution was plated onto QDO and analyzed for growth.

3.2.1.2. Sharpin Pull-Down with K48- and K63-Linked Ubiquitin Chains

As shown above, Sharpin interacts with GST-ubiquitin monomers. In cells, ubiquitination comes in different forms: mono-, multimono-, and polyubiquitination. The latter can be further divided into groups based upon which lysine residue is used in the isopeptide bonds (Hicke *et al*., 2005). Ubiquitin has seven lysine residues that have been shown to form linked ubiquitin chains; Lys6, Lys11, Lys27, Lys29, Lys33, Lys48, and Lys63 (Peng *et al*., 2003). The functions of Lys11, Lys27, and Lys33-linked ubiquitin chains are unclear to date, Lys6-linked chains have been associated with DNA repair, and Lys29-linked chains are involved in proteasome degradation (Pickart and Fushman, 2004). The best studied forms are Lys48- and Lys63-linked chains. The majority of proteins targeted for proteasome degradation are modified with Lys48-linked ubiquitin chains (Finley *et al*., 1994). Proteins ubiquitinated with Lys63-linked chains have been shown to be involved in receptor endocytosis and subcellular sorting, DNA damage repair, stress response, translation, as well as the NFκB signaling pathway (Hicke, 1997; Sun and Chen, 2004; Arnason and Ellison, 1994; Spence *et al*., 2000; Deng *et al*., 2000). In order to determine, whether Sharpin preferentially binds to a certain type of polyubiquitin chains, pull down experiments with Lys48- and Lys63-linked ubiquitin chains coupled to NHS-sepharose were performed. Some representative results are shown in Figure 3.10 on the next page.

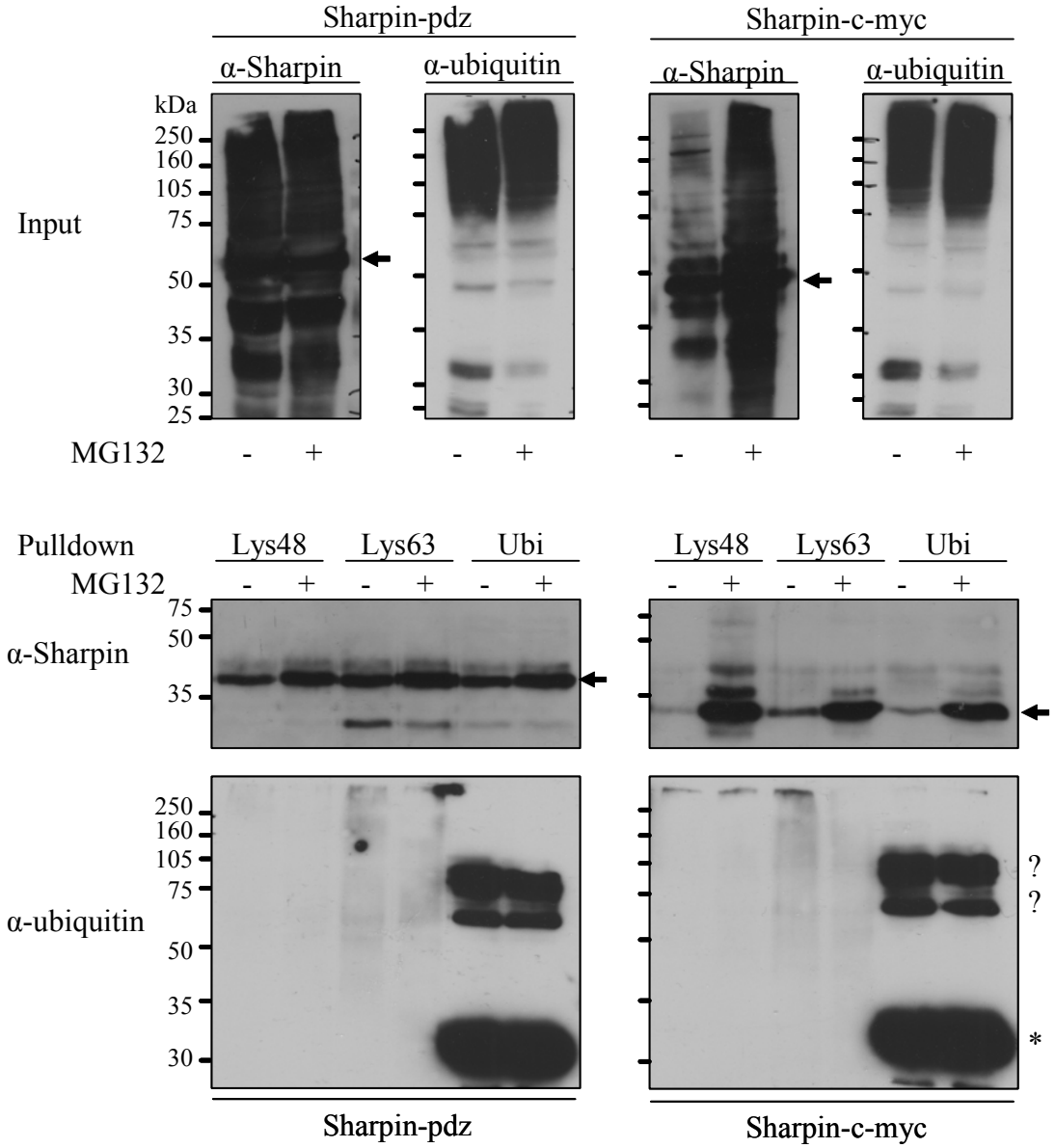

Figure 3.10 Sharpin Coprecipitates with K48- and K63-linked Ubiquitin Chains

HEK293 cells were transfected with c-myc-tagged and PDZ-tagged Sharpin constructs and treated with MG132 as before. Cell lysates were equally divided in three portions. One was incubated with Lys48-linked polyubiquitin beads and another with Lys63-linked polyubiquitin beads. A control fraction was incubated with monoubiquitin-GST bound to glutathione beads. After washing the beads, attached proteins were eluted with Laemmli buffer and analyzed by Western blotting with α-Sharpin and α-ubiquitin antibodies. The position of the Sharpin band is marked by an arrow. Question marks label two unknown proteins that were prominently found in the ubiquitin-GST pull-downs. The asterisk denotes the band representing the GST-ubiquitin fusion protein itself.

For these experiments, HEK293 cells were transfected with a c-myc-tagged as well as with a PDZ-tagged Sharpin construct; the cells were split and treated with MG132 as described above. The lysate was equally divided in three portions and 40 µl of Lys48-linked polyubiquitin beads were added to one fraction, while another one was mixed with 40 µl of the Lys63-linked polyubiquitin beads. As positive control 10 µl of GST-ubiquitin bound to glutathione sepharose beads were added to the third fraction. It is evident from Figure 3.10 that Sharpin coprecipitated with Lys48- and Lys63-linked ubiquitin chains as well as with monoubiquitin. However, especially when comparing the lanes with samples that were not treated with proteasome inhibitor, it appears that the interaction of Sharpin with Lys63-linked polyubiquitin chains was the strongest. Two different Sharpin constructs were tested in these experiments: one resulting in Sharpin that was fused to the PZD domain of Shank1 and one encoding C-terminally c-myc-tagged Sharpin. Comparing the intensities of the Sharpin bands in the left (PDZ-tagged Sharpin) and the right (c-myc-tagged Sharpin) panels of the figure above, suggests that the Sharpin-PDZ fusion protein is either expressed at a higher level or is more stable in cells than c-myc-tagged Sharpin; the reason for this is presently unclear. In addition to the primary band of the expected molecular weight for Sharpin, the α–Sharpin antibody also detected additional bands of higher molecular weight that could represent variously ubiquitinated forms of Sharpin. However, when the membranes were probed with the α-ubiquitin antibody, these same bands were not detected, indicating that they do not represent polyubiquitinated Sharpin. However, it cannot be ruled out that the antibody used is not sensitive enough for detection of multimonoubiquitinated Sharpin.

3.2.2. Sharpin/Rad23 Interaction

Polyubiquitinated proteins are translocated to the active proteasome by ubiquitin receptor proteins that contain ubiquitin binding motifs and at the same time interact with the proteasome. Rad23 is such a carrier protein. It contains two ubiquitin-associated (UBA) motifs that bind polyubiquitinated proteins and it also has an ubiquitin-like element through which it binds to the proteasome (Chen *et al*., 2001; Chen and Madura, 2002). To test binding of Sharpin to these UBA domains, pull-down experiments were done with a commercially available kit that utilizes beads coated with Rad23-derived UBA motifs for enrichment of ubiquitinated proteins. Lysate of HEK293 cells transiently overexpressing

Sharpin-EGFP was incubated with 40 µl of these beads. Proteins in the pull-down were separated by SDS PAGE and immunodetected with α-Sharpin antibody.

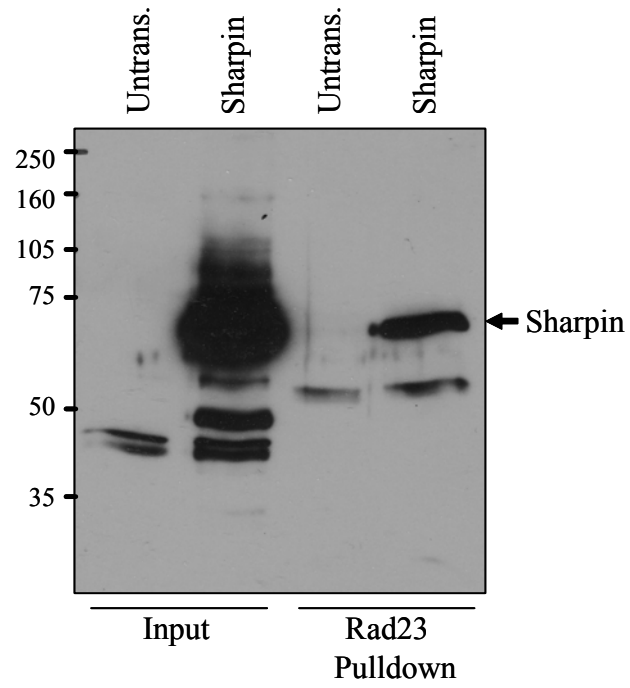

Figure 3.11 Pull-down with UBA domain of Rad23
An EGFP-tagged Sharpin was overexpressed in HEK293 cells for 36 h. Lysates of untransfected or Sharpin-overexpressing cells were incubated with 40 µl of beads coated with GST-Rad23 Ubiquitin-associated (UBA) domains. Bound proteins were eluted with Laemmli buffer and immunoblotted with α-Sharpin antibody.

Sharpin clearly coprecipitated with the Rad23 beads. However, coprecipitated Sharpin ran as a single sharp band, whereas proteins that normally coprecipitate with Rad23 show a typical broad smear towards higher molecular weight due to the heterogeneity of their degree of polyubiquitination. Since Sharpin bound to Rad 23 domains was apparently not polyubiquitinated, it might have also indirectly bound to Rad23 by interacting with other proteins in the lysate that were in turn then captured by the Rad 23 UBA beads due to their polyubiquitination.

3.2.3. Sharpin/S5A Interaction

The proteasome subunit S5a is another ubiquitin receptor and contains two ubiquitin interaction motif (UIM) domains. These domains belong to the same helical UBD structure group as the UBA domains from Rad23, but they have a slightly different tertiary structure. In order to test interaction of Sharpin with this second kind of UBD, the coding region for human S5a was amplified from HEK293 cDNA and cloned into the pGEX6P1 vector. S5a-GST fusion protein immobilized on glutathione beads was then used, as described, to isolate ubiquitinated proteins from cell lysates.

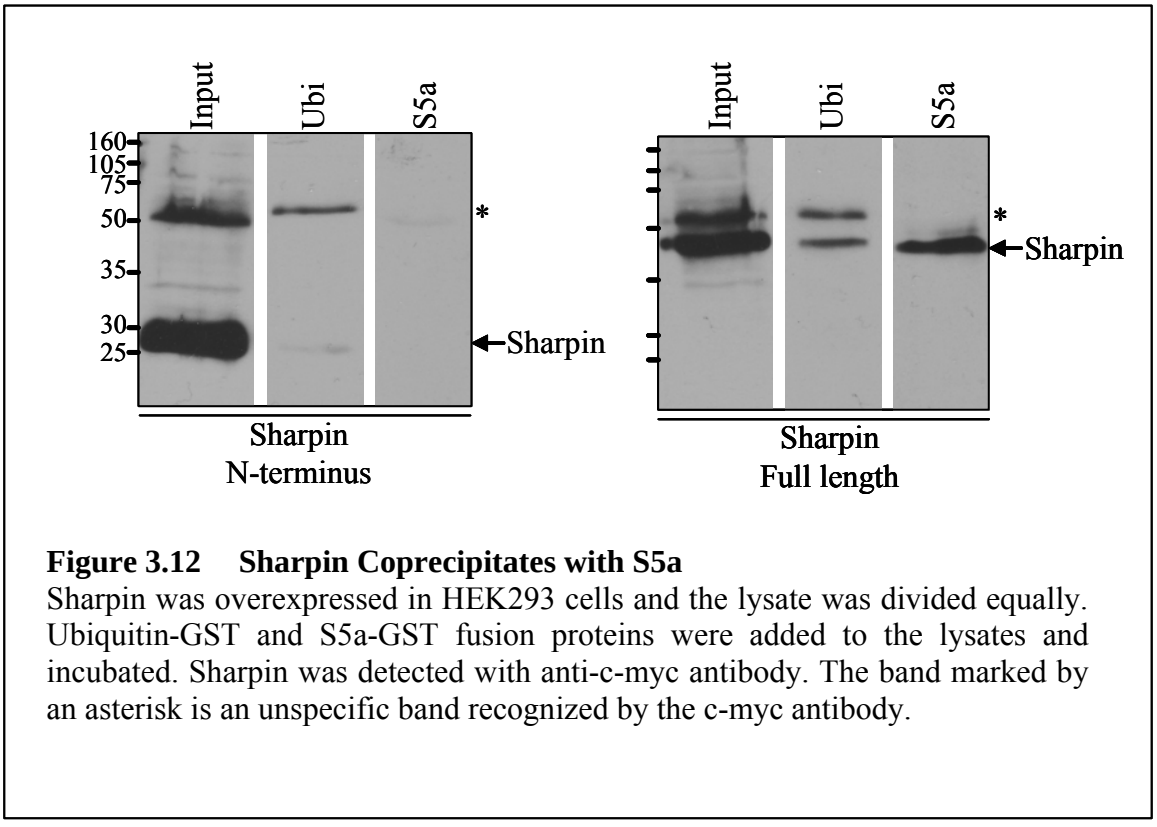

Figure 3.12 Sharpin Coprecipitates with S5a
Sharpin was overexpressed in HEK293 cells and the lysate was divided equally. Ubiquitin-GST and S5a-GST fusion proteins were added to the lysates and incubated. Sharpin was detected with anti-c-myc antibody. The band marked by an asterisk is an unspecific band recognized by the c-myc antibody.

Figure 3.12 shows that GST-S5a, like the RAD23-derived fusion protein, was able to pull down Sharpin from lysates. As before, Sharpin that was precipitated with the ubiquitin binding protein gave a discrete single band in the western blot indicating again that it was not polyubiquitinated. Therefore, Sharpin may only interact indirectly via binding to other polyubiquitinated proteins with S5a. An attempt was made to clarify, whether Sharpin interacts directly or indirectly with ubiquitin receptors, like Rad23 and S5a, by using the yeast two-hybrid system. Full length Sharpin cDNA and truncated constructs coding for only

the N-terminus (aa 1-170), the middle part (aa 171-304) or the C-terminus (aa 305-381) were cloned into the bait vector pGBKT7. The S5a cDNA was cloned into the prey vector pACT. After cotransfection into the AH109 yeast strain and appropriate selection, a single colony was serially diluted and spotted onto QDO-Agar. There was no interaction between S5a and any of the deletion mutants of Sharpin. However, whether or not full length Sharpin interacts with S5a could not be determined, because expression of full length Sharpin alone in the test strain was sufficient to activate the galactose operon that controls all auxotrophy markers.

3.2.4. Intramolecular Regulation of Sharpin/UPS Interactions

According to Kang *et al.* (2007) some proteins containing both a ubiquitin-like (Ubl) and a ubiquitin binding domain (UBD) form an intramolecular complex between these two domains thereby regulating their binding to ubiquitin. As Sharpin contains both of these domains, such an intramolecular interaction could also occur in Sharpin.

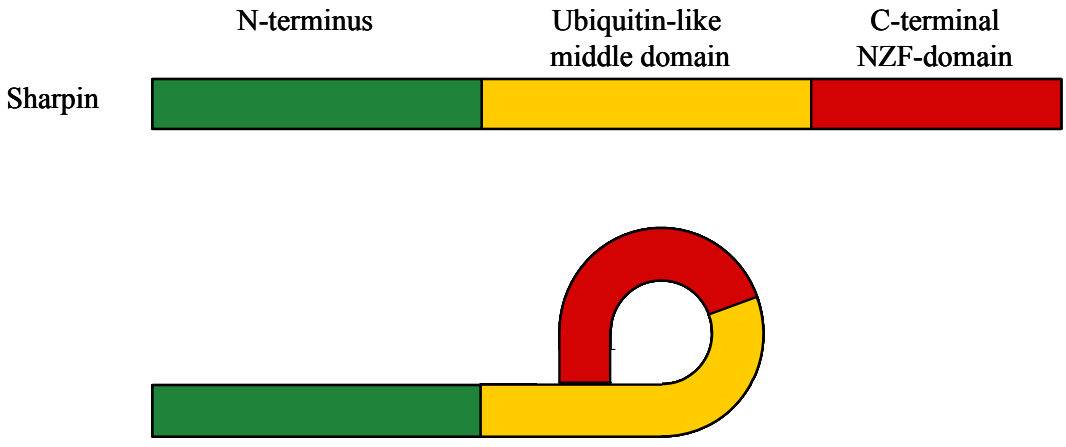

Diagram 3.1 Proposed Intramolecular Interaction of Sharpin
A schematic representation of the proposed intramolecular interaction of Sharpin. Using the yeast two-hybrid system the C-terminal NZF-domain of Sharpin has been shown to have affinity for the ubiquitin-like middle domain.

The cDNA coding for the ubiquitin-like domain from the middle part of the Sharpin molecule was cloned into pACT and the cDNA coding for the C-terminal NZF-UBA domain was cloned into pGBKT7. After cotransformation and selection, a single colony was serially diluted and plated onto QDO agar. Up to a 10^{-3} dilution, growth occurred, clearly demonstrating that the two domains interacted with each other.

3.3. Sharpin/Shank Interaction

3.3.1. Effect of MG132 on Coprecipitation of Sharpin and Shank

Figure 3.13 shows experiments confirms previous findings by Mameza (2003), who had previously shown that the N-terminus of Shank (1-171 aa) can form an intramolecular interaction with the ankyrin repeat domain of Shank.

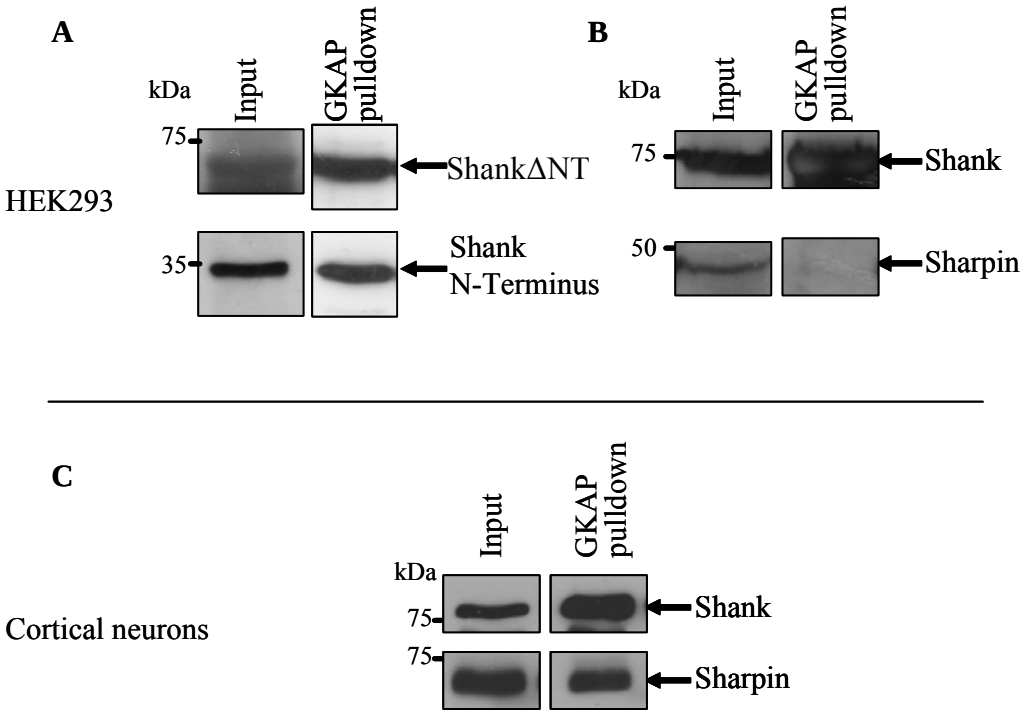

Figure 3.13 Shank-Sharpin Interaction in HEK293 Cells and Neurons
A) A construct encoding Flag-tagged, N-terminally deleted Shank (aa 194-774) and one consisting only of the N-terminus of Shank (aa 72-174) fused in frame with EGFP were coexpressed in HEK293 cells. Using GKAP-coupled sepharose, the N-terminally deleted Shank was precipitated from lysates. Precipitated ShankΔNT and co-precipitated ShankNT were detected with α-FLAG and α-EGFP antibodies, respectively. B) A GKAP pull-down was performed with lysates of HEK293 cells coexpressing Shank (aa 72-774) with c-myc-tagged Sharpin. Shank and Sharpin were detected with α-Shank and α-c-myc antibodies, respectively. C) EGFP-tagged Sharpin and flag-tagged Shank (aa 72-774) constructs were transfected in cortical neurons (DIV 7). In GKAP pull-downs from lysates prepared 48 h post transfection, Sharpin and Shank were immunoblotted with α-EGFP and α-FLAG antibody, respectively.

This interaction was confirmed here by coprecipitation of a construct that only comprised the aminoterminus of Shank with an N-terminally deleted Shank construct (see panel A of Figure 3.13). On the other hand, Lim *et al*. (2001) had previously also described binding of Sharpin to Shank mediated by the N-terminal ankyrin repeat domain of Shank. In an attempt to also reproduce this interaction, a GKAP pull-down was performed with lysates of HEK293 cells cotransfected with cDNAs for Shank (aa 72-774) and Sharpin. However, as shown in panel B of Figure 3.13, no Sharpin band was found in such pull-downs. Since failure to detect an interaction could be due to the cellular background, binding of Sharpin to the N-terminal ankyrin repeat domain of Shank was also assessed in primary cortical neurons. When an EGFP-tagged Sharpin construct was coexpressed with Shank in cortical neurons, an interaction between both proteins was readily detectable. Taken to together, these results suggested that the Shank/Sharpin interaction may be dependent on the cellular context or on a certain stimulus. In order to test this, HEK293 cells overexpressing Shank and Sharpin were treated with various chemicals. Among the stimuli tested were ionomycin, which raises intracellular Ca^{2+} levels, PMA (phorbol 12-myristate-13-acetate), which activates protein kinase C, stauroporine, a broad kinase inhibitor, and the proteasome inhibitor MG132. After treating the cells for 16 h with the proteasome inhibitor MG132 at 10 µM final concentration, we observed a strong increase in the interaction between Shank and Sharpin.

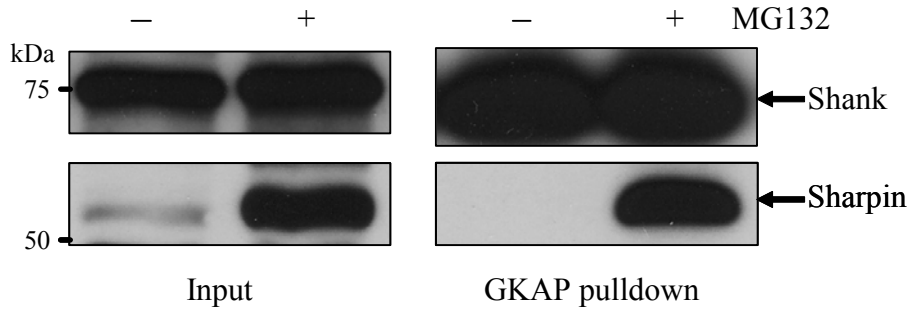

Figure 3.14 Shank/Sharpin Interaction in the Presence of Proteasome Inhibitor

Sharpin and a N-terminal Shank construct (aa 72-774) were co-overexpressed in HEK293 cells, and the cells were treated with 10 µM MG132 as before. GKAP pull-downs were performed with the lysates. MG132 not only increased the protein level of Sharpin dramatically, but also the amount of Sharpin that coprecipitated with Shank.

As shown in Figure 3.14, the amount of Sharpin present in whole cell lysate as well as in GKAP pull-downs increased dramatically by MG132 treatment, whereas levels of Shank protein remained unchanged. This cannot be due to differences in transfection efficiency between the treated and untreated samples, as the cells for both samples originated from the same transfection plate. If Sharpin were normally rather instable in the cellular environment, disrupting the steady state equilibrium between its permanent degradation by the proteasome and replenishment by *de novo* synthesis with a proteasome inhibitor could explain the massive accumulation of Sharpin seen after MG132 addition. However, the experiments described in Section 3.1 demonstrate that, even when the expression of Sharpin was stabilized by fusing it to the PDZ domain of Shank1, its interaction with OS-9 still required the presence of proteasome inhibitors. Therefore the most plausible explanation seems that Sharpin interacts with its partners in a transient complex that is stabilized by inactivation of the proteasome.

3.3.2. Protein Stability Analyses of Sharpin and Shank

3.3.2.1. Pulse-Chase Experiments in HEK293 Cells

The hypothesis outlined above assumes that the Sharpin pool in cells is normally rapidly turned over. In order to test this, the half-life of Sharpin was determined in a pulse-chase experiment. To this end, Sharpin was overexpressed in HEK293 cells and an *in vivo* pulse labeling of cellular proteins was performed using radiolabeled ^{35}S-methionine as described in Section 2.2.4.8. After different chase periods with medium containing non-radiolabeled methionine, Sharpin was immunoprecipitated with anti-c-myc antibody from the cell lysates. Figure 3.15 illustrates that radiolabeled Sharpin had almost completely disappeared from the cells within 6 h of the chase period. By quantifying of the immunoprecipitated protein bands in panel A the half-life of Sharpin was calculated to be approximately 1.5 h. A similar value was also obtained in two other, independently performed experiments. So Sharpin is indeed a very short-lived protein in HEK293 cells and the large effect of MG132 treatment on its cellular abundance suggests that proteasomal degradation is a major contributing factor to its rapid turn-over in HEK293 cells.

In order to also determine the half-life of Shank and to test whether Sharpin affects the cellular turn-over rate of Shank, a similar pulse-chase experiment as described above was performed using HEK293 cells transfected with a HA-tagged Shank expression plasmid either alone or together with a full length Sharpin construct.

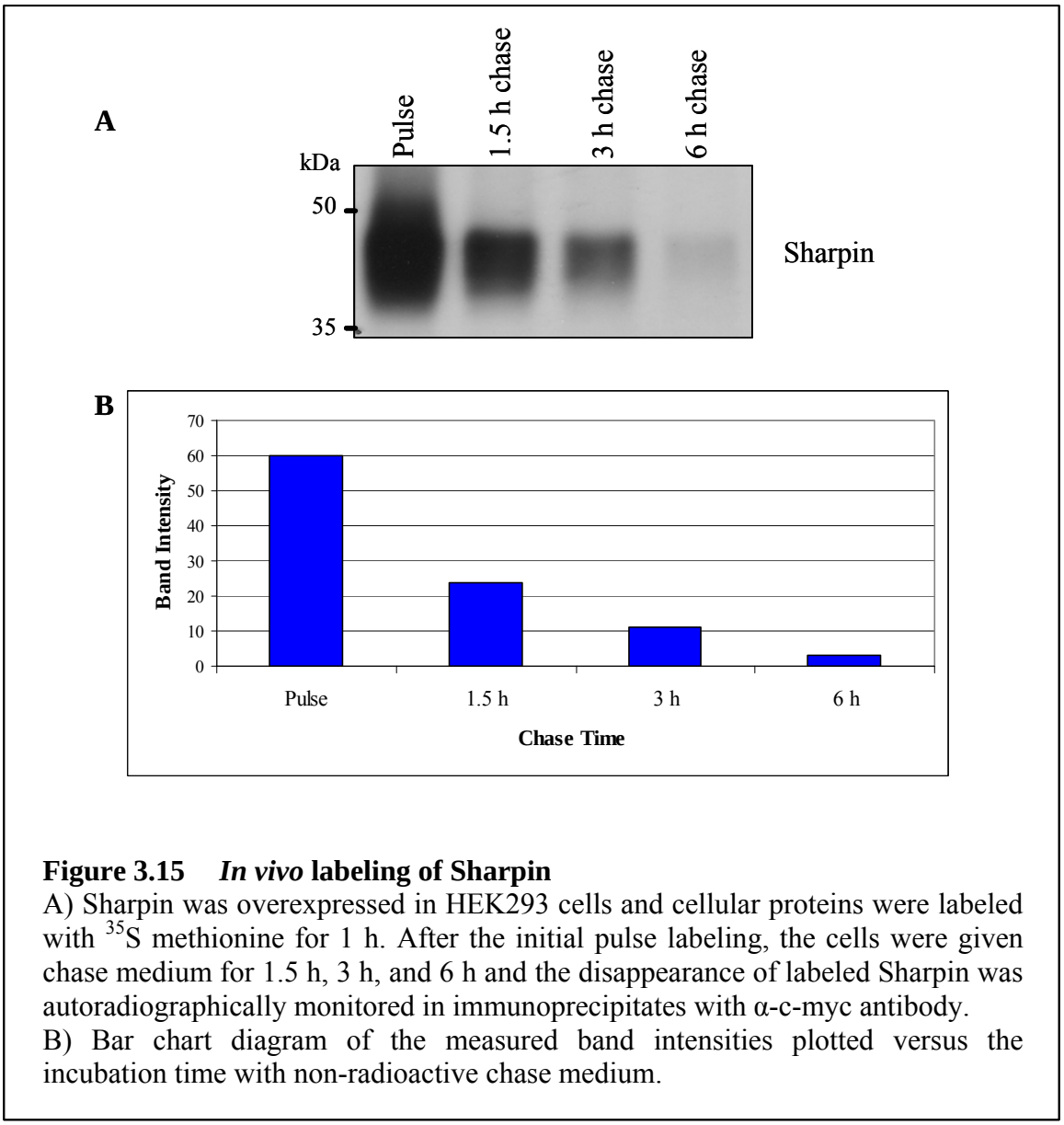

Figure 3.15 ***In vivo*** **labeling of Sharpin**
A) Sharpin was overexpressed in HEK293 cells and cellular proteins were labeled with ^{35}S methionine for 1 h. After the initial pulse labeling, the cells were given chase medium for 1.5 h, 3 h, and 6 h and the disappearance of labeled Sharpin was autoradiographically monitored in immunoprecipitates with α-c-myc antibody.
B) Bar chart diagram of the measured band intensities plotted versus the incubation time with non-radioactive chase medium.

Shank was immunoprecipitated with an α-HA-antibody and autoradiographically quantified. Cotransfection of Sharpin together with Shank resulted in a ~50% decrease of labeled Shank in comparison to transfection of Shank alone (compare the bars labeled “pulse” +/- Sharpin in panel B of Figure 3.16). However, the kinetic of disappearance of radiolabeled Shank was

unchanged by the presence of Sharpin. The amount of labeled Shank protein declined by roughly 30% within a 6 h chase period, whether Sharpin had been cotransfected or not. The results outlined above demonstrate that Shank is a much more stable protein in HEK293 cells than Sharpin ($t_{1/2}$ >6h versus $t_{1/2}$ = 1.5 h, respectively) and that in these cells coexpression of Sharpin does not significantly alter the half-life of Shank.

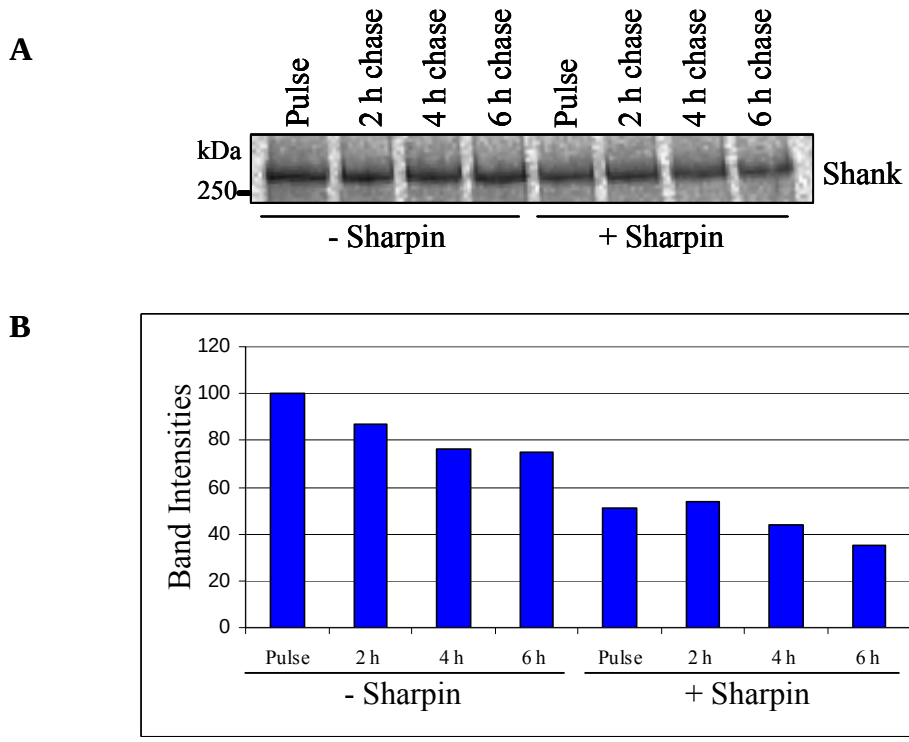

Figure 3.16 ***In vivo*** **labeling of Shank**
A pulse-chase experiment as described above was also performed for over-expressed Shank with and without cotransfection of Sharpin. A) Autoradiograph of α-HA immunoprecipitated, radiolabeled Shank. B) Bar chart diagram of the measured band intensities plotted against the chase duration.

3.3.2.2. Cycloheximide Experiments with Cortical Neurons

In order to determine, whether endogenous Sharpin is also a short-lived protein in cortical neurons, its stability was assessed by treating neurons with cycloheximide. This inhibitor of protein translation was added to the medium of cortical neurons (DIV 14) at different time periods before lysis (between 0.5 and 32 h).

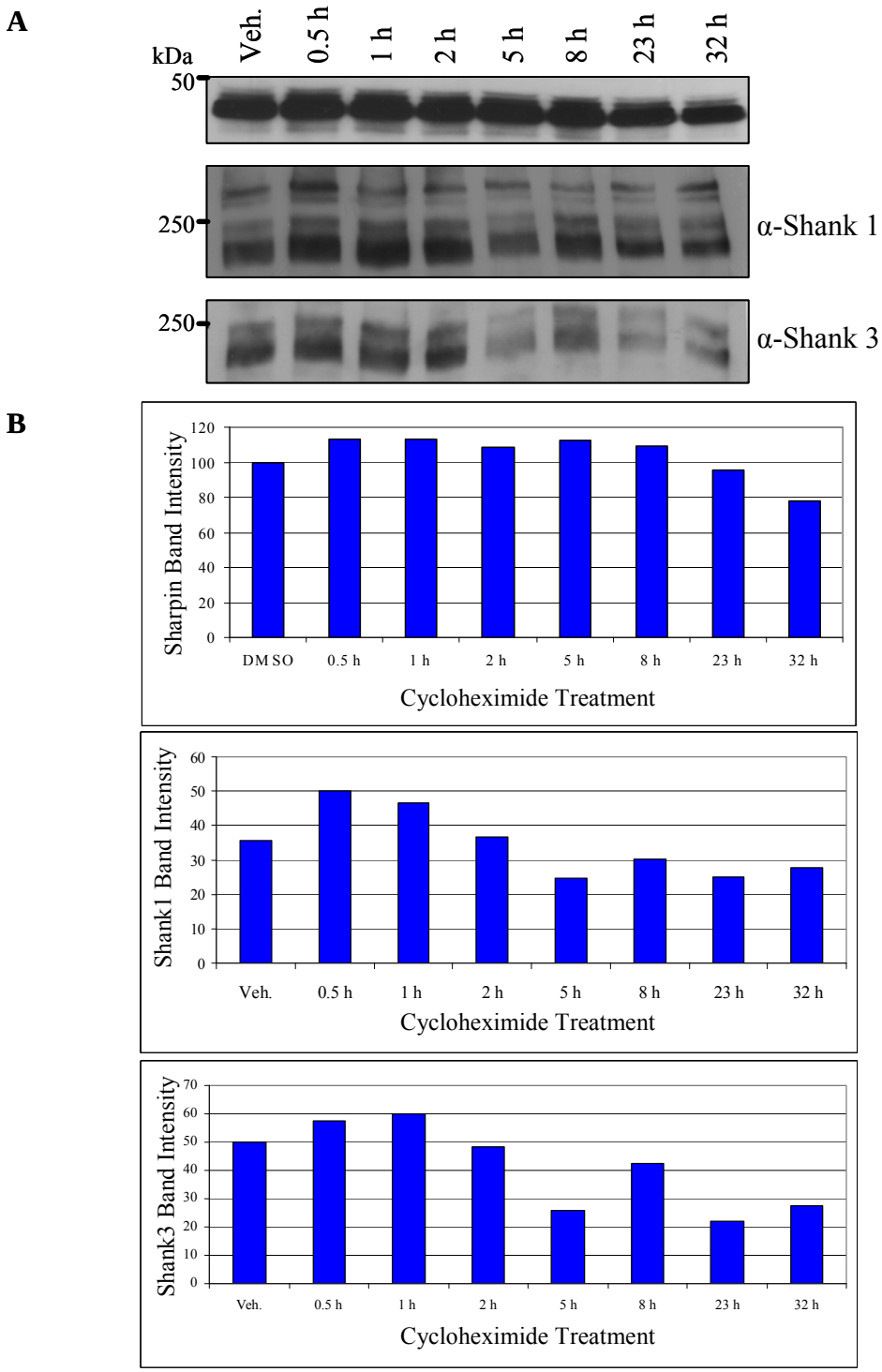

Figure 3.17 Sharpin Stability in Cortical Neurons
A) Cortical neurons (DIV 14) were treated with 10 µg/ml cycloheximide or vehicle for the time periods indicated. After that the neurons were lysed and equal amounts of protein for each sample were analyzed by Western blot with specific antibodies against Sharpin, Shank1 and Shank3, respectively. **B)** The intensities of the bands in panel A were quantified and plotted against the treatment duration.

Cell lysates were then immunoblotted with antibodies against Sharpin, Shank1 and Shank3. As shown in Figure 3.17, endogenous Sharpin was quite stable in cortex neurons. Even 32 h after blocking *de novo* protein synthesis, the Sharpin level in neurons had only declined by about 20 %. In contrast, the levels of Shank1 and Shank3 protein declined within 5 h after cycloheximide addition by about 50 %, and then remained flat for the rest of the time period analyzed. In summary, the turn-over rates of Sharpin and Shank seem highly dependent on the cellular background and their order of stability is completely reversed in cortical neurons as compared to HEK293 cells. However, it cannot be ruled out that the observed discrepancy can also be due to the difference in methods used for assessing protein stability in neurons versus HEK293 cells (cycloheximide treatment versus pulse-chase labeling).

3.3.3. Postsynaptic Density Analyses

3.3.3.1. Effect of Bicuculline and MG132 on Shank1 Levels in PSD

According to Ehlers (2003), when cortical neurons are treated for 48 h with 40 µM bicuculline, a $GABA_A$ receptor antagonist that increases excitatory synaptic activity, there is a decrease in the amount of Shank1 in PSD preparations compared to unstimulated controls. This decrease of Shank protein in overstimulated synapses is dependent upon proteasome function, because the author showed that the amount of Shank1 remains unchanged, when the neurons are concomitantly treated with proteasome inhibitor. Since Sharpin could be involved in targeting Shank1 for proteasomal degradation in response to synaptic overstimulation of neurons, we tried to confirm the results published by Ehlers (2003) using his protocol for preparing PSD from cultured cortical neurons.

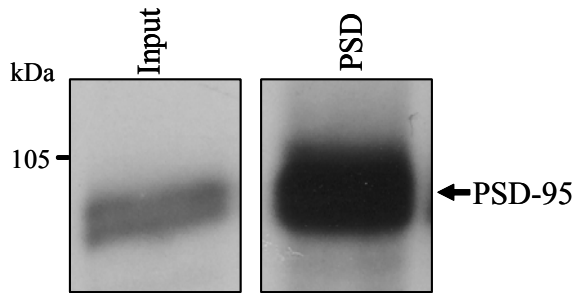

Figure 3.18 Verification of PSD Enrichment
PSD was prepared from cultured cortical neurons (DIV 14). Aliquots of the un-purified input material and the purified PSD preparation are compared by Western blotting with a specific antibody against the PSD marker protein-PSD-95.

Figure 3.18 documents successful enrichment of PSD proteins using this protocol by showing a substantial increase in the PSD marker protein PSD-95 in an aliquot of the purified PSD fraction versus an aliquot of the unpurified starting material. Next PSD-enriched fractions from bicuculline-treated and untreated samples were compared for changes in Shank1 content. Three preparations of cortical neuron PSDs were immunoblotted using an α-Shank1 antibody and each preparation was analyzed twice independently.

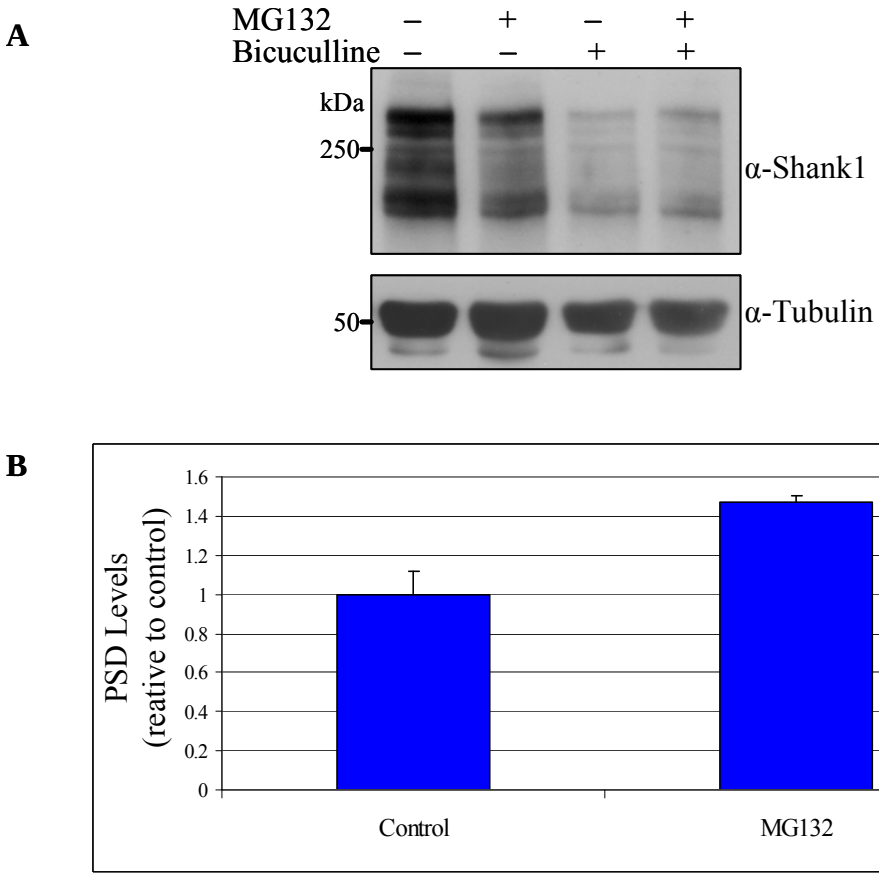

Figure 3.19 PSD Preparations Analyzed for Shank1
A) Cortical neurons (DIV 14) were treated as indicated above with 40 µM bicuculline for 48 h and 10 µM MG132 for 16 h prior to harvesting. Post-synaptic densities were prepared and analyzed by immunoblotting with the α-Shank1 antibody. **B)** A qualitative evaluation of the data shown in panel A. The effect of MG132 treatment on the ratio of Shank1 protein levels in the PSD in the presence of bicuculline versus in the absence of bicuculline. The data is given as mean ± SEM.

The Shank1 band intensities were normalized to tubulin as a loading control. A substantial decrease in the amount of Shank1 present in PSDs from the bicuculline treated neurons

could be verified (Compare the first and third lane in panel A of Figure 3.19). Proteasome inhibition with MG132 partially prevented this decrease (compare the third and fourth lane in panel A of Figure 3.19). There was a statistically significant reduction of Shank protein levels in PSDs after bicuculline treatment in the absence of MG132 ($p=0.016$), whereas there was only a statistically non-significant trend toward lower Shank protein levels in PSDs after bicuculline treatment of MG132 inhibited cells ($p=0.11$) As illustrated by panel B of Figure 3.19, the ratio of the Shank1 levels in PSDs in the presence versus absence of bicucullin treatment was improved by approximately 50%, when cells were concomitantly treated with MG132. This seems primarily due to MG132 treatment partially preventing bicuculline-induced Shank1 degradation in PSD, rather then a general increase in Shank levels in the presence of proteasome inhibitor, because repeated experiments showed that in the absence of bicuculline treatment, proteasome inhibition with MG132 alone did not cause a detectable increase in the amount of Shank1 present in the PSD fraction.

3.3.3.2. MG132-Induced Sharpin Accumulation in the PSD

The purified PSD fractions were also immunoblotted with an antibody against Sharpin. When the intensities of the bands from the vehicle control samples and the proteasome inhibitor treated samples are compared (see Figure 3.20; third and fourth lane of the top blot in panel A), a strong increase in the amount of Sharpin present in the PSD is evident. Quantification of the Sharpin band intensities normalized to the tubulin loading control revealed that the amount of Sharpin found in the PSD after proteasome inhibition had more than doubled. This 115% increase was statistically significant ($p=0.0448$, Student's t-Test). The fact that at the same time there was no substantial increase in the Sharpin levels detected in the unpurified input material after MG132 treatment (compare first and second lane of the top blot in panel A of Figure 3.20) suggests that proteasome inhibition increased the localization of Sharpin in the PSD rather than the overall Sharpin protein level in the neurons.

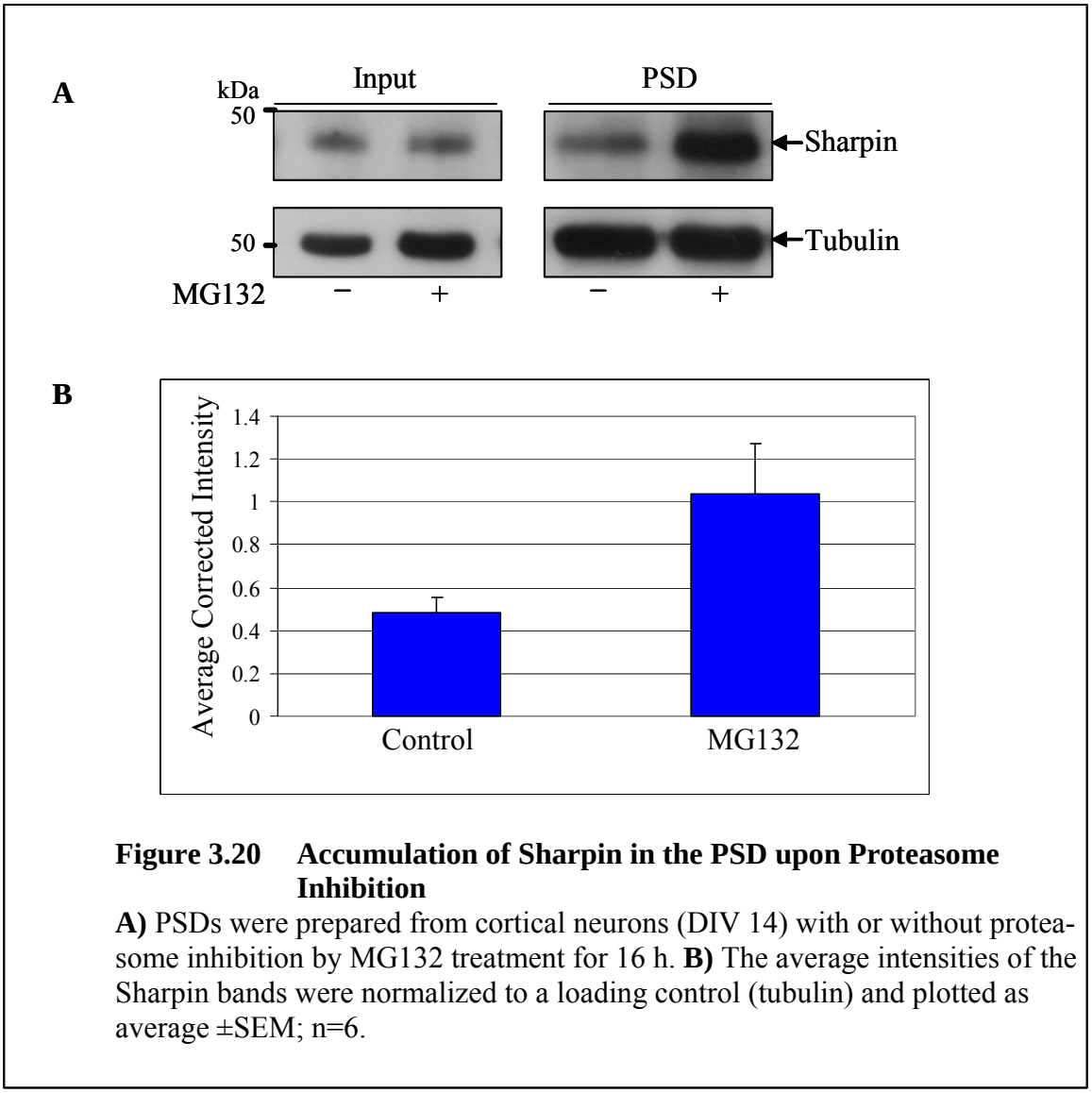

Figure 3.20 Accumulation of Sharpin in the PSD upon Proteasome Inhibition

A) PSDs were prepared from cortical neurons (DIV 14) with or without proteasome inhibition by MG132 treatment for 16 h. **B)** The average intensities of the Sharpin bands were normalized to a loading control (tubulin) and plotted as average ±SEM; n=6.

3.3.4. Immunocytochemical Analyses

3.3.4.1. MG132-Induced Change in the Subcellular Localization of Sharpin

The massive accumulation of Sharpin in the PSD region upon proteasome inhibition of cortical neurons was also investigated by immunocytochemistry. To this end, cultured cortical neurons (DIV 7) were transfected with a flag-tagged Sharpin vector. The next day vehicle or MG132 (10 µM final concentration) were added. Another 24 h later the neurons were fixed with 4% PFA. Sharpin was detected using the α-Sharpin antibody followed by an Alexa 488(green)-labeled secondary anti-rabbit antibody. In order to quantify this effect, 70 neurons from untreated and MG132-treated samples were scored positive or negative for cytoplasmic localization of Sharpin based upon the criterion, whether staining intensity was greater in the cytosol or nucleus, respectively. As illustrated in Figure 3.21, the number of cells with Sharpin accumulated in their cytoplasm increased approximately six fold in the presence of the proteasome inhibitor.

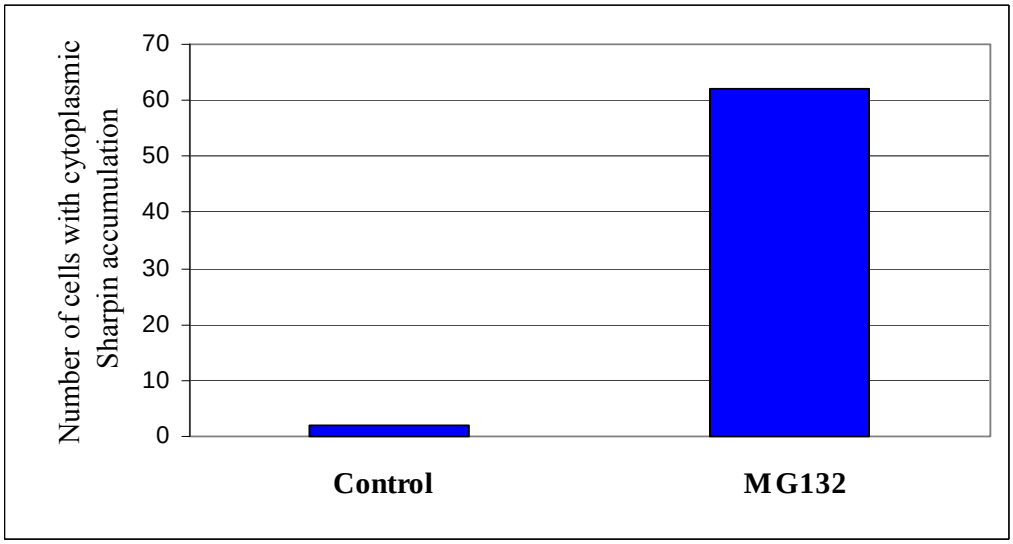

Figure 3.21 Quantification of the Change in Sharpin Localization
Neurons immunostained with α-Sharpin antibody (as shown in Figure 3.22 below) were analyzed for subcellular distribution of Sharpin. For both treatment groups, 70 neurons were scored and the number of cells that stained positive for Sharpin primarily in the cytoplasm is graphed.

Figure 3.22 shows representative pictures of DAPI and α-Sharpin antibody stained cortical neurons. While in vehicle-treated control neurons some cytosolic distribution of Sharpin is

visible, the majority of Sharpin molecules are clearly localized in the nucleus. This was confirmed by co-staining with DAPI (4',6-diamidino-2-phenylindole). Upon proteasome inhibition, however, most of the Sharpin molecules were exported from the nucleus and accumulated in the cell soma and in the dendrites.

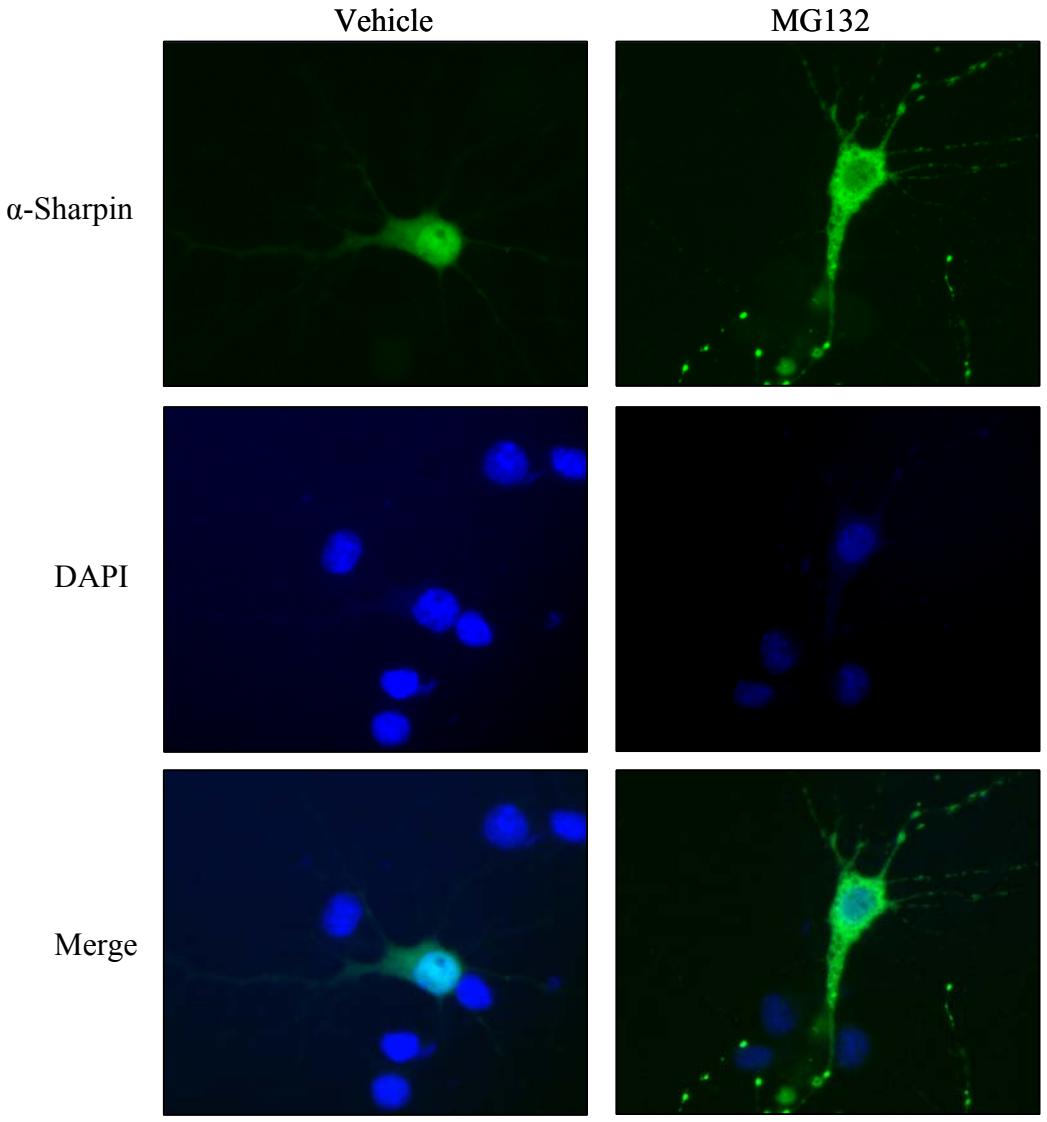

Figure 3.22 Intracellular Localization of Sharpin
Flag-tagged Sharpin was overexpressed in cortical neurons (DIV 7), 10 µM of proteasome inhibitor (MG132) was added on day 8 and the cells were fixed in 4% PFA on day 9. Sharpin was detected using an α-Sharpin primary antibody and an anti-rabbit Alexa 488 secondary antibody. The nuclei were visualized with DAPI staining.

It has been reported in the literature that proteasome inhibitor treatment induces cellular side effects like ER stress and apoptosis (Paschen and Mengesdorf, 2003, Suh *et al*., 2005). Looking at the morphology of the proteasome treated neurons, the irregular accumulation of proteins in aggregrates along the dendrites could represent an apoptotic feature known as blebbing. In order to determine, whether or not the treated cells are undergoing apoptosis, a method described by Aharoni *et al*. (1997) was employed to visualize apoptotic cells by DAPI staining of the nucleus. Under a fluorescence microscope nuclei of apoptotic cells can be clearly distinguished from those of healthy cells by DNA fragmentation and nuclear condensation. As shown in Figure 3.23, the nuclei of vehicle control and MG132 treated cells are indiscernible and appear to be normal and healthy in both cases, when compared to the DAPI staining pattern of an apoptotic nucleus.

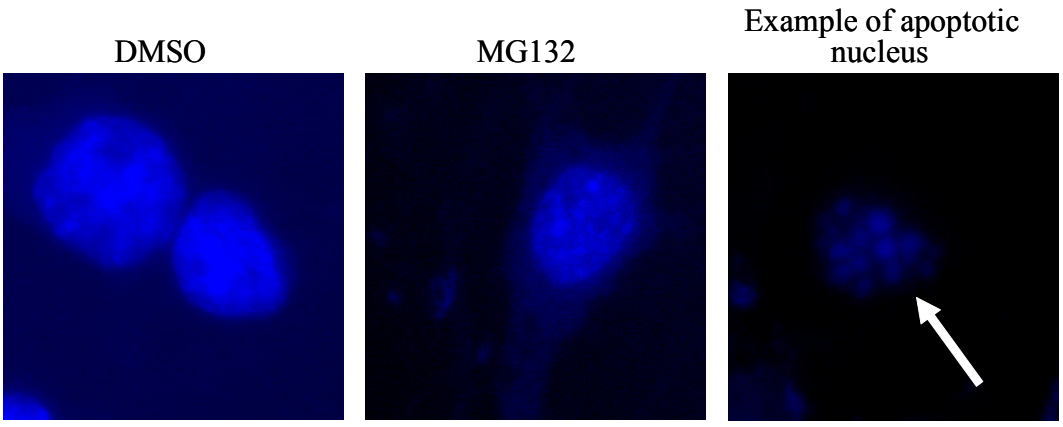

Figure 3.23 Morphological Comparison of DAPI-stained Nuclei
The nuclei of the same cells as depicted in Figure 3.22 are shown here for comparison to a nucleus from an apoptotic cell. While the nucleus of the apoptotic cell on the right is clearly fragmentated, the nuclei of the DMSO as well as the MG132 treated cells look morphologically normal and healthy.

Lack of DNA-fragmentation suggested by the DAPI staining method illustrated in Figure 3.23 was independently confirmed by a DNA fragmentation assay. After treatment for 16 h with vehicle or MG132, cortical neurons (DIV 9) were lysed in TTE Buffer. Fragmented DNA was precipitated using glycogen as a carrier and analyzed by agarose gel electrophoresis.

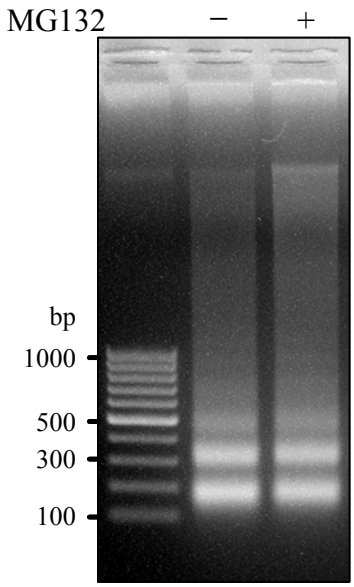

Figure 3.24 DNA Fragmentation Assay
Cortical neurons (DIV 8) were treated for 16 h with proteasome inhibitor prior to lysis. Using glycogen as a carrier, fragmented DNA was precipitated and separated on a 2 % agarose gel. A characteristic ladder of fragmented DNA bands indicates some degree of apoptosis, but no increase is seen with MG132 treatment.

While some degree of DNA fragmentation was observed in both samples, there was no significant increase in the extent of DNA fragmentation by MG132 versus control (compare the third and second lane in Figure 3.24).

3.3.4.2. MG132-Induced Sharpin/Shank Colocalization in Dendritic Aggregates

As shown above in Figure 3.22, the amount of Sharpin staining in the cytoplasm and dendrites increased, when neurons were treated with proteasome inhibitor. Also the amount of Sharpin in PSD preparations was shown here to increase in MG132-treated cortical neurons (see Figure 3.20). Both these observations raise the question as to whether proteasome inhibition increases cellular co-localization of Sharpin with Shank1. To test this possibility, DIV-7 cortical neurons cotransfected with Shank1 and Sharpin expression constructs were immunofluorescently labeled with α-Shank1 and α-Sharpin antibodies.

Figure 3.25 shows that in cells treated with DMSO both antibodies show weak, but homogeneously distributed staining of cytoplasm and dendrites, while the nucleus stains strongly for both Sharpin and Shank1. As the neurons in this experiment were only cultured for 9 days they had not yet developed mature spines; therefore the typical spine puncta, normally seen when neurons are stained for Shank, are not seen here. In contrast to the homogeneous staining of the dendrites in vehicle-treated neurons, irregularly shaped aggregates that strongly stained for Shank became visible in the dendrites of neurons that were treated with proteasome inhibitor (see panel A in Figure 3.25). Furthermore, it appears that Shank and Sharpin colocalize in these areas. This can be seen better in the enlarged views of the boxed areas that are shown in horizontal orientation directly underneath panel A of Figure 3.25.

Panel B of Figure 3.25 depicts a shorter exposure of a proteasome inhibitor treated cell costained with DAPI and α-Sharpin antibody to illustrate the marked decrease in nuclear Sharpin staining compared to the DMSO-treated cells in the top row of panel A. The DAPI-staining also confirms that there were no signs of nuclear fragmentation in the same cell.

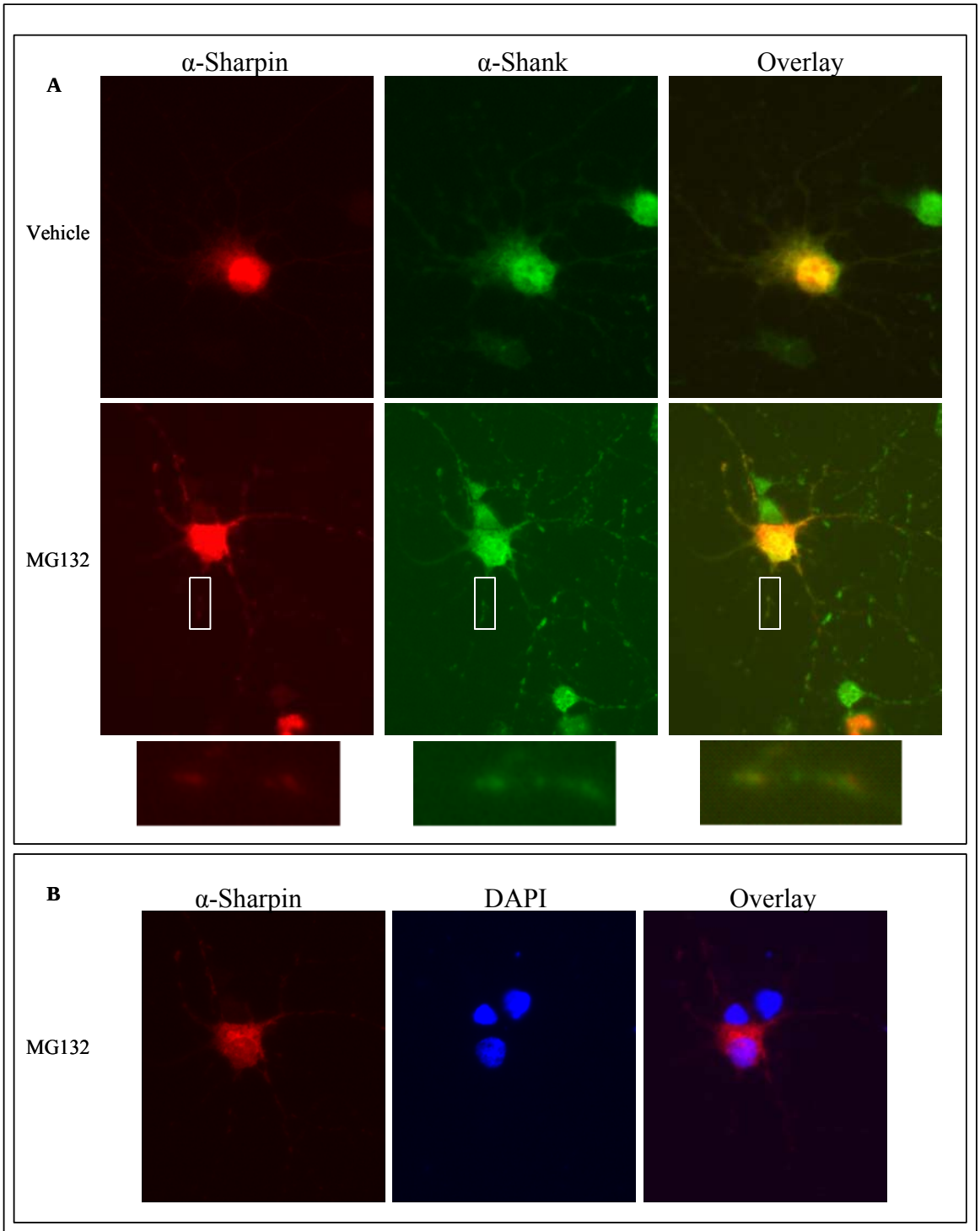

Figure 3.25 Colocalization of Shank1 and Sharpin
A) Shank1 and Sharpin were overexpressed in cortical neurons (DIV 7). Proteasome inhibitor was added on day 8 for 16 h before fixing the cells with 4 % PFA. Sharpin and Shank were detected with α-c-myc and α-Shank1 antibodies, respectively. The white boxes depict regions that are shown enlarged at the bottom of panel A. B) A shorter exposure of an MG132-treated cell from panel A shown to illustrate the much reduced Sharpin staining in the nucleus. The DAPI staining also reveals that there were no signs of nuclear fragmentation.

Chapter 4 Discussion

In the brain synapses are constantly being modified or remodeled depending upon neuronal activity. This activity-dependent ability of synapses to change has been termed synaptic plasticity, and lies at the foundation of most learning, memory, and synaptic development models (Abbott and Nelson, 2000). The synapse may undergo short-term modifications lasting only up to a few minutes. These modifications are generally of a post-translational nature like changes in the phosphorylation status of protein components. On the other hand, long-term modifications may last from a few hours to a number of years. These persistent modifications require more stable changes that involve the transcription of new mRNAs, synthesis of new proteins, and potentially new synaptic growth. Until recently these were the main paradigms for changes in synaptic architecture, but an increasing number of studies implicating local protein degradation by the proteasome in synaptic plasticity has reshaped this view (Hegde, 2004) and has directed more attention to ubiquitination as another important posttranslational modification that influences the remodeling of synapses. It appears that synergistic action between protein synthesis and protein degradation is crucial for synaptic plasticity, Fonseca *et al*. (2006) have shown that balance between the synthesis and degradation of PSD proteins is a key factor for the late phase of long-term potentiation, which results in enhanced synaptic transmission.

Sharpin was originally identified by Lim *et al*. (2001) as a protein that interacted with Shank. It was subsequently shown to interact and colocalize with Shank1 at the synapses of hippocampal neurons. Interestingly, *in silico* analysis of Sharpin using bioinformatics tools like MotifScan and SMART identifies two relevant ubiquitin signaling motifs: a type 2 ubiquitin-like domain (Ubl) in the middle of the protein and a NZF ubiquitin binding domain at its C-terminus. NZF domains have been reported to mediate binding to mono- and poly-ubiquitin side chains of proteins, suggesting that Sharpin might specifically interact with proteins that are modified by ubiquitination. To date, 16 different ubiquitin binding domains (UBD) have been identified. These can be categorized into three main groups: helical ubiquitin-binding domains, ZnF domains, and Ubc-related domains (Hurley *et al*. 2006). The NZF domain of Sharpin belongs to the ZnF domain group. Experiments performed in the course of this thesis provided clear evidence that Sharpin is indeed involved in some aspect

of the ubiquitin pathway. *In vitro* pull down assays confirmed that Sharpin interacts with monoubiquitin. Monoubiquitination has been shown to act as a signal for diverse processes like endocytosis, protein trafficking, and gene silencing (Pickart and Fushman, 2004). Consequently, proteins that interact with ubiquitin, termed ubiquitin binding proteins or ubiquitin receptors, regulate important cell signaling mechanisms, for instance via translocation of ubiquitin-conjugated proteins to the proteasome or via endocytosis of cell surface receptors. Using the yeast-two hybrid system, I was able to prove that ubiquitin binding of Sharpin occurs through its NZF domain. The C-terminal glycine (Gly76) residue of ubiquitin can be attached to lysine residues of target proteins through an isopeptide bond. To form a polyubiquitin chain, subsequent molecules of ubiquitin can be attached to this starter molecule through linkages with one of seven lysine residues. The type of ubiquitin chain linkage is known to be a key factor in the recognition of these chains by different ubiquitin binding proteins, which in turn determines the functional consequences of the modification. Proteins modified with Lys 48-linked polyubiquitin chains are generally targeted to the proteasome for degradation. The ubiquitin binding proteins that shuttle substrates to the proteasome primarily recognize Lys 48 chains consisting of at least four ubiquitin moieties or more (Thrower *et al*., 2000; Hofmann and Pickart, 2001). In contrast to this, proteins modified by Lys 63-linked ubiquitin chains rather play a role in DNA damage tolerance, kinase activation, protein trafficking, and translation (Pickart, 2004). As Sharpin was shown here to interact with both of these types of ubiquitin side chains as well as with unconjugated monoubiquitin, the functional role of this interaction cannot be easily predicted. In fact, it can also not be ruled out that Sharpin only interacts with the single monoubiquitin molecule that is found at the end of each of the two types of polyubiquitin chains.

Many of the proteins that, like Sharpin, have been described to contain both a UBD and a Ubl domain are known to act as ubiquitin receptors that translocate ubiquitin-conjugated proteins to the 26S proteasome for degradation. The Rad23 and Dsk2 families of substrate adaptors for the proteasome are the best described examples for this. These proteins have a C-terminal UBA domain that binds to the ubiquitinated substrate and an N-terminal Ubl motif that interacts with the Rpn1 or Rpn2 subunit of the 19S regulatory particle of the 26S proteasome. By analogy, Sharpin could simultaneously bind proteasome targets via its C-terminal NZF domain and a subunit of the proteasome through the Ubl domain that, in case of

Sharpin is not located at its N-terminus, but rather in the middle of the molecule. An obvious target protein marked by Sharpin for degradation would be Shank1, since Ehlers (2003) had previously shown that Shank1 is highly ubiquitinated and degraded in a neuronal activity-dependent fashion in cortical neurons. Therefore, the hypothesis was tested, whether Sharpin interacts specifically with ubiquitinated Shank and promotes its degradation by the ubiquitin proteasome system (UPS). This hypothesis would predict that high levels of Sharpin expression adversely affect protein stability of Shank. A pulse-chase experiment in HEK293 cells revealed, however, that this is not the case. In fact, there was no difference in the turn-over rate of Shank, whether it was overexpressed alone or co-overexpressed with Sharpin. This result could also indicate that another protein involved in Sharpin-mediated Shank degradation is limited or missing in HEK293 cells. Therefore, it was further investigated, if Sharpin could promote the degradation of endogenous PSD proteins in cortical neurons. To this end, PSDs were isolated from cultured cortical neurons with or without proteasome inhibitor treatment. Western blot analysis of PSD preparations clearly demonstrated an increase in the amount of endogenous Sharpin present in the PSD prepared from neurons treated with proteasome inhibitor compared to PSD from untreated control cells. However, none of the other proteins that were analyzed by Western blot showed significant accumulation in the PSD after proteasome inhibition. Therefore, at this time it is not clear, whether Sharpin accumulates in the PSD, because its complex formation with a yet unidentified PSD component that it would normally target for UPS degradation is stabilized by proteasome inhibition or whether instead the transport of Sharpin to the PSD is somehow enhanced in the presence of proteasome inhibitor.

Although a role for Sharpin in enhancing the degradation of co-overexpressed Shank1 in HEK293 cells or in controlling the degradation of any of the analyzed PSD proteins in neurons could not be shown, I was able to link Sharpin to the UPS through its coprecipitation with the ubiquitin binding proteins Rad23 and S5a. Rad23 binds to the 19S regulatory particle subunits and S5a itself is a component of the 19S proteasome regulatory particle. Many of the polyubiquitinated target proteins of Rad23 and S5A that coprecipitate in GST-pull-down assays show a characteristic band smear toward higher molecular weights, when analyzed by Western blotting. In contrast to this, immunodetection of coprecipitating Sharpin gave a single band at its normal molecular weight position indicating that Sharpin in

these complexes was not polyubiquitinated. There are two possible explanations of this result. One possibility could be that Sharpin interacts with ubiquitin chains of other substrate proteins that are coprecipitated with the S5a or Rad23 beads. This would explain, why Sharpin is found in the precipitate, and yet it is not ubiquitinated. The other possibility could be that Sharpin interacts directly with S5a or Rad23 through its Ubl domain. A direct interaction between the Ubl domain of Sharpin and these two ubiquitin receptors would also explain the Sharpin pull-down in the absence of polyubiquitination of Sharpin. In order to test, whether there is a direct interaction between S5a and the ubiquitin-like domain of Sharpin, the yeast-two hybrid system was employed. Using various truncated constructs of Sharpin, including one that consisted mainly of its ubiquitin-like domain with few adjacent areas, no interaction was seen with S5a. This strongly argues against the latter model outlined above, although it cannot be entirely excluded that the residual adjacent areas of the truncated construct somehow interfered with S5A binding. Unfortunately, the interaction between full-length Sharpin and S5a could not be tested in this system, since the expression of full length Sharpin was by itself sufficient to fully activate the promoter that drives the yeast auxotrophy markers.

Rpt1 is another proteasome subunit that Sharpin coprecipitated with, when the two proteins were cotransfected in HEK 293 cells. This interaction was not an artifact of co-over-expression, since it was only seen in lysates from cells treated with proteasome inhibitor. The AAA-ATPase Rpt1 forms part of the hexameric ring of the 19S regulatory particle of the 26S proteasome. It has recently been shown to be necessary for cotranslational protein degradation, a process that occurs simultaneously with the translation of proteins. Due to their lack of secondary and tertiary structure, nascent polypeptides leaving the ribosome, may mimic unfolded proteins by exposing hydrophobic residues, which may be recognized by the UPS, thereby targeting the corresponding proteins for degradation as they are being synthesized (Turner and Varshavsky, 2000). Chuang *et al*. (2005) have shown that the translation elongation factor 1A (eEF1A), which mediates cotranslational degradation of nascent protein, interacts with Rpt1. Furthermore they demonstrated that degradation of these proteins is inhibited in yeast cells that have a temperature sensitive mutation in Rpt1 preventing its interaction with eEF1A. In the experiments described in this thesis, I used the yeast Rpt1 cDNA, however similar findings are to be expected with its mammalian homolog

given the high degree of structural and functional conservation between the regulatory particles from yeast and mammals throughout the course of evolution. In fact, the yeast Rpt1 ATPase has 76% identity with its human homolog S7 (Glickman *et al*., 1998). Furthermore, Bingol and Schuman (2006) have shown that an ectopically expressed yeast Rpt1-GFP fusion protein was incorporated into the proteasome of mammalian cells with approximately 77% efficiency compared to the endogenous subunit. Thus the interaction between Sharpin and Rpt1 shown here could indicate that Sharpin plays a role in cotranslational degradation of certain target proteins. Due to constant rapid degradation of these protein complexes, the steady-state level of Sharpin associated with proteasome subunits might be undetectably small under normal conditions and only upon proteasome inhibition enough of these transient complexes would accumulate to allow detection by coprecipitation analysis. While binding of Sharpin with Rpt1 suggests a role for Sharpin in cotranslational protein degradation, additional functions of the Sharpin/Rpt1 complex could also be envisioned, since Rpt3 and Rpt6, two close homologs of Rpt1, have recently been shown to also have non-proteasome-related functions in the nucleus of cells (Hedge, 2004).

Similar findings as reported here for Sharpin have recently also been published by Seibenhener *et al*. (2004) for the protein sequestosome 1/p62 (p62). This protein has first been found to interact with $p56^{lck}$ and the atypical protein kinase Cζ. The authors mentioned above showed that p62 also interacts with ubiquitin chains and the proteasome. Using similar techniques as applied in the work presented here, they also demonstrated that p62 precipitates in an S5a pull-down assay, but runs as a single band in Western blots indicating that, like Sharpin, p62 in S5A pull-downs is not polyubiquitinated. Moreover, the authors demonstrate that p62, like Sharpin, interacts with Rpt1 in a stimulus-dependent manner. As mentioned above Rpt1 is part of the 19S regulatory particle and has been implicated in cotranslational UPS degradation. Seibenhener *et al*. (2004) also show that p62 has a preference for binding to Lys63-linked ubiquitin chains. This is somewhat unexpected since Lys63-linked chains are primarily associated with non-proteasome related functions in the cell. However, there have been reports of Lys63-linked substrates degraded by the UPS (Hofmann and Pickart, 2001).

In the study presented here, it was shown that the interaction between Sharpin and several of its binding partners in HEK293 is increased after treatment with proteasome inhibitor. This is true for its previously described interaction with Shank1 as well as for its binding to the novel interacting partners found in the course of this work: OS-9, EDD1 (discussed below), and Rpt1. These interactions did not seem to be dependent on polyubiquitination, as the analysis by Western blotting showed individual bands for each of the coprecipitated proteins instead of a typical polyubiquitin smear pattern. The fact that the interaction between these proteins only occurred in the presence of proteasome inhibitor could be explained, if Sharpin was stabilized under those conditions allowing the interaction to be detected. However, using a Sharpin construct that was intrinsically more stable due to the presence of a PDZ-tag at its C-terminus, showed that complex formation still only occurred in HEK293 cells treated with proteasome inhibitor. Taken together, this leads to the conclusion that the interaction in HEK293 cells between Sharpin and its interacting partners may be due to a secondary effect of proteasome inhibition like the formation of protein aggregates, the induction of oxidative stress, or induction of the heat shock protein response (Bush *et al*. 1997).

In immunocytochemical analyses of cortical neurons overexpressing Sharpin, the majority of the anti-Sharpin antibody staining was seen in the nucleus of transfected neurons (DIV 9). When such neurons were incubated with proteasome inhibitor prior to fixing, the intercellular localization of Sharpin changed so that the majority of the fluorescence signal was seen in the cytoplasm. The cytoplasmic staining pattern of Sharpin strongly resembled staining patterns reported for ER marker proteins, however costaining with antibodies for such ER markers was not possible due to poor sensitivity of the available anti-ER marker antibodies. Strong anti-Sharpin staining was also observed in the dendrites of the treated neurons, where it appeared to form aggregate-like inclusions. In fact these inclusions may be true aggregates, as it has been shown that inhibition of the proteasome leads to the accumulation of ubiquitinated proteins in aggregrates (Bence *et al*. 2001). In neurons cotransfected with Sharpin and Shank1 or Sharpin and OS-9 both proteins colocalized in dendritic aggregate-like formations. It would be interesting to determine, whether these same inclusions are also stained by anti-ubiquitin antibodies as this would provide additional evidence that they are aggregates of ubiquitinated proteins. In addition to ubiquitinated

proteins, aggregrates have also been shown to colocalize with non-ubiquitinated proteins like proteasomes, heat shock proteins, and unfolded proteins (Wigley *et al*. 1999; Garcia-Mata *et al*. 1999).

Interestingly, in coprecipitation studies with cortex neurons the interaction between overexpressed Shank and Sharpin occurred regardless of proteasome inhibition. This starkly contrasts to the results obtained in HEK293 cells where the interaction between Shank and Sharpin was only seen after proteasome inhibition. In these cells some important factors may be missing for this interaction to occur.

Although the Ubl domain is best described for its interaction with 19S regulatory particle subunits of the proteasome (Rpn1 and 2), there have been recent reports that Ubl domains also interact with non-proteasome proteins. For example the Ubl domain of Rad23 has been shown by Kim *et al*. (2004) to interact with the E4 ubiquitination enzyme Ufd2. This enzyme elongates ubiquitin side chains by adding further ubiquitin residues to an existing ubiquitin moiety on a substrate protein (Koegl *et al*., 1999). It was shown that the Ubl of Rad23 interacts with either the E4 enzyme or with Rpn1, but not with both at the same time. The authors propose that the mutually exclusive interaction of the Rad23 Ubl domain with either Ufd2 or Rpn1 allows for regulation of the transport of substrates from the ubiquitination machinery to the proteasome without inadvertent degradation of the ubiquitinating enzymes themselves. Another example of an alternative function for a Ubl domain interaction can be found in the context of the regulation of epidermal growth factor receptor (EGFR) endocytosis. Parkin is a Ubl domain containing E3 ubiquitin ligase (Sakata, 2003). The Ubl domain of Parkin has been shown to interact with the ubiquitin interacting motif (UIM) of the epidermal-growth-factor receptor pathway substrate 15 (Eps15). Eps 15 is a crucial protein in the clathrin-mediated endocytic pathway and is involved in the early stages of clatherin coated vesicle formation (Benmerah, 1995). Through binding of Parkin's Ubl domain its adjacent RING domain is brought into close proximity with Eps15, thus allowing Parkin to ubiquitinate Eps15 (Fallon et al. 2006). Since Ubl containing proteins can interact with E3 ligases like Parkin, the possibility that Sharpin may also be part of a ligase complex or interact with an E3 ligase directly was investigated. To this end a yeast-two hybrid screen was performed using the region of Sharpin that includes the Ubl domain as

bait. In this screen the E3 ligase EDD1 was one of the proteins identified. The interaction between the Ubl domain of Sharpin and EDD1 occurs in the region of EDD1 that contains part of its HECT (homology to E6-AP carboxyl terminus) domain. This interaction was further confirmed by coprecipitation studies in HEK293 cells. However, coprecipitation was again only observed in the presence of proteasome inhibitor suggesting that the interaction is transient as long as the UPS is functional, but becomes more stable when further processing is blocked.

Another protein identified in this same yeast-two hybrid screen was OS-9. Again confirmation of this interaction in HEK293 cells was possible, but only after treatment with proteasome inhibitor. Mammalian OS-9 has originally been identified as a protein of unknown function that is upregulated in osteosarcoma. Its yeast homolog (yOS-9) has been described to play a role in endoplasmic reticulum associated protein degradation (ERAD). This highly controlled cellular degradation process removes incorrectly folded proteins from the ER. While target selection occurs by a quality control system residing in the ER, elimination of the target proteins is ultimately performed by the cytoplasmic UPS. It is one of the unique features of ERAD that it requires retrotranslocation of the target proteins from the ER to the cytoplasm. However, in mammals a role for OS-9 in ERAD has not yet been confirmed. A recent publication by Baek et al. (2005) suggests that OS-9 plays a role in the hypoxia response of mammalian cells by mediating hydroxylation and degradation of HIF1-α and it may also be involved in subcellular HIF1-α transport.

After the experimental work for this thesis was completed, a new paper by Seymour *et al*. (2007) shed new light on a role for Sharpin in the non-canonical NF-κB signaling pathway. The authors reported that spontaneous mutations that cause the chronic proliferative dermatitis (*cpdm*) phenotype in mice actually occur in the Sharpin gene. In two independently arising mouse models for this disease, C57BL/KaLawRij-*cpdm/ cpdm* and OBy.OcB3-$cpdm^{Dem}$/ $cpdm^{Dem}$, it was shown that frame-shift mutations in exon 1 resulting in premature stop codons within the Sharpin coding region caused this disease. In the C57BL/KaLawRij-*cpdm/ cpdm* mice the deletion of a single base pair shifts the reading frame and results in the translation of a truncated Sharpin protein that stops after the addition of 3 nonsense amino acids at position 68. A deletion of 14 base pairs is responsible for the

reading frame shift in the OBy.OcB3-*cpdm*^{Dem}/ *cpdm*^{Dem} mice. This mutation generates a protein that is only 44 amino acids in length and deviates from the Sharpin amino acid sequence after the sixth amino acid. Both of these mutations in the coding region of Sharpin result in a complete loss of functional Sharpin gene product in these mutant mice.

cpdm/ cpdm mutant mice were originally described by an inflammation of the stratified squamous cell epithelia of skin, lungs, lymph nodes, tongue, esophagus and forestomach caused by esosinophil infiltration. These mice also have enlarged spleens and dermatitis caused by an increase of granulocytes in these tissues (HogenEsch *et al*., 1999; Gijbels *et al*., 1996). In addition, there is an increased expression of the type 2 helper T cell (T_H2) cytokines interleukin-4 (IL), IL-5, and IL-13, which are involved in the humoral immune system, as well as an impaired production of the type 1 helper T cell (T_H1) cytokine interferon-γ, which regulates the cellular immune response (HogenEsch *et al*., 2001). Furthermore, there are acute structural abnormalities in the immune system of these Sharpin-deficient animals. Peyer's patches are absent in *cpdm/ cpdm* mice (HogenEsch *et al*., 1999). Peyer's patches are oval areas of lymphoid tissue found in the wall of the small intestine primarily in the ileum. Here they play a humoral role in the body's primary defense to intestinal antigens. Peyer's patches contain naïve B cells, follicular dendritic cells (FDCs), and areas rich in T cells (Doe, 1989; Spahn and Kucharzik, 2004). Other secondary organs in the immune system like the spleen, lymph nodes, and nasal-associated lymphoid tissue were present in *cpdm/ cpdm* mice, but these tissues had poorly defined follicles and lacked germinal centers and FDCs (HogenEsch *et al*., 1999). Due to their lack of germinal centers and FDCs, *cpdm/ cpdm* mice have a lower serum concentration of immunoglobin (Ig) G, IgA, and IgE compared to control mice, although IgM concentration was normal (HogenEsch *et al*., 1999).

The phenotype seen in *cpdm/ cpdm* mice is very similar to phenotypes seen in knock-out mice in which genes of the NF-κB pathway have been deleted. NF-κB signaling can occur through two pathways – one is termed the canonical and the other the non-canonical pathway. The canonical pathway of NF-κB signaling, which results in the activation of NF-κB/p50 (NF-κB1), is essential for the innate immune response. In comparison, the non-canonical pathway, which leads to the activation of NF-κB/p52 (NF-κB2), is crucial for the

development of lymphoid organs and the adaptive immune response. In order to determine the functions of the many proteins involved in the NF-κB pathways, many groups have generated mouse models specifically lacking these gene products. Upon analysis of these animals, it became clear that the canonical and non-canonical pathways play different roles in the development of the immune system and that the genesis of secondary lymphoid organs involves intricate signaling mechanisms. Table 4.1 gives an overview of the phenotypes of knock-out mice lacking genes of various NF-κB signaling components.

Table 4.1 Phenotypes of Gene Knock-out Mice and Naturally Occurring Mutations from the NF-κB pathways

Mouse mutant	Peyer's patches	FDCs	Lymph nodes	GCs	Spleen morphology	Marginal zone	Immune response	1º B cell Follicles	LymphoΦ organ infiltration	Ref.
cpdm/cpdm	-	-	abnormal	-	abnormal	-	↓ IgA,G,E	P/D sp ln	+	a
Non-canonical NFκB pathway										
Ltα$^{-/-}$	-	-	-[1]	-	abnormal	-	↓ IgA	-	+	b,c,d,e,f
Ltβ$^{-/-}$	-	-	-[2]	-sp, +mln	abnormal	abnormal	↓ IgA	-	+	d,e,f
Ltβr$^{-/-}$	-	-	-	-[3]	abnormal	-	↓[4]	-	+	g
Nfκb2$^{-/-}$ *p52/p100*	-	-	abnormal	-	abnormal	abnormal	↓ IgG1, G2b,A	-	N/R	h,i
aly/aly NIK^{G855R}	-	-	-	-	abnormal	-	↓ IgM ⇓ IgG,A	-	N/R	j,k,l,m,n
relB$^{-/-}$	-	-	-	-	abnormal	abnormal	N/R	N/R	+	o,p,q,r
Ikkα$^{-/-}$ r/c[5]	-[6]			-	abnormal		↓IgM,G,A			s,t,u
Canonical NFκB pathway										
Tnfα$^{-/-}$	+[7]	-	+[8]	-	abnormal	enlarged	normal IgA	-	-	d,v,w
Tnfr1$^{-/-}$*p55*	+[7]	-	+[8]	-	abnormal	abnormal	normal IgA	-	-	d,v,w
Tnfr2$^{-/-}$*p75*	+	+	+	+	normal	N/R	N/R	+	normal	d,x
Nfκb1$^{-/-}$ *p50/p105*	+	+	+	+	N/R	abnormal	↓IgG1,E,A[9]	+	N/R	q,y

As shown in Table 4.1, all of the proteins with a phenotype similar to that seen in mice containing a spontaneous Sharpin mutation are components of the non-canonical NF-κB signaling cascade.

The NF-κB (Rel) family of transcription factors consists of RelA, RelB, c-Rel, NF-κB/p50, and NF-κB/p52. NF-κB family members all contain a highly conserved REL-homology domain (RHD) that is necessary for dimerization, nuclear translocation, and DNA binding. In the cytoplasm, NF-κB dimers are inhibited by interaction with an IκB protein. There are five IκB proteins, including NF-κB/p105 and NF-κB/p100 themselves. IκB proteins contain an ankyrin repeat domain that inhibits the NF-κB proteins by interacting with their RHD

Table 4.1 Phenotypes of Gene Knock-out Mice and Naturally Occurring Mutations from the NF-κB Pathways

[1]Few abnormal structures present in mesenteric fat were reported.
[2]Lacked peripheral lymph nodes, but mesenteric and cervical lymph nodes were present.
[3]Aberrant formation of GCs.
[4]Impaired affinity maturation in GCs.
[5]*Ikkα*$^{-/-}$ mice die *in utero*. Single-cell suspensions of fetal livers harvested from embryonic day 16 mice were injected into the tail vein of lethally irradiated 8-week-old C57BL/6-CD45.1 female hosts thus producing *Ikkα*$^{-/-}$ bone marrow chimeras.
[6] Ikkα^{AA} (Ser176Ala and Ser180Ala) knock-in mice were used to determine the role in Peyer's patch formation.
[7] Present in reduced numbers and are smaller than controls, have architectural abnormalities compared to controls.
[8] Present, but have architectural abnormalities compared to controls.
[9]These mice have a decrease in T cell dependent antibody response.

Abbreviations: cpdm, chronic proliferative dermatitis; GCs, germinal centers; Ig, immunoglobin; ln, lymph node, LymphoΦ, Lymphocyte; Lt, lymphotoxin; mln, mesenteric lymph nodes; nfκb, nuclear factor κB; NIK, NF-kappaB-inducing kinase; N/R, not reported; P/D, poorly defined, r/c radiation chimeras; *r*, receptor; sp, spleen; Tfnr1, tumor necrosis factor receptor p55; ↓ decreased; ⇓ highly decreased

[a]HogenEsch *et al*., 1999; [b]De Togni *et al*., 1994; [c]Banks *et al*., 1995; [d]von Boehmer, 1997; [e]Koni *et al*., 1997; [f]Alimzhanov *et al*., 1997; [g]Fütterer *et al*., 1998; [h]Franzoso *et al*., 1998; [i]Paxian *et al*., 2002; [j]Koike *et al*., 1996; [k]Shinkura *et al*., 1996; [l]Miyawaki *et al*., 1994; [m]Yamada *et al*., 2000; [n]Shinkura *et al*., 1999; [o]Barton *et al*., 2000; [p]Yilmaz *et al*., 2003; [q]Weih *et al*., 2001; [r]Weih *et al*., 1995; [s]Senftleben *et al*., 2001; [t]Matsushima *et al*., 2001; [u]Kaisho et al., 2001; [v]Pasparakis *et al*., 1997; [w]Mayrhofer, 1997; [x]Erickson *et al*., 1994; [y]Sha *et al*., 1995

domain and masking the nuclear locatization signal (NLS). The C-terminal IκB-like ankyrin repeat domains of NF-κB/p105 and NF-κB/p100 are degraded by the proteasome producing the active forms NF-κB/p50 (NF-κB1) and NF- κB/p52 (NF-κB2), respectively. In the canonical pathway processing of NF-κB/p105 to NF-κB/p50 by the proteasome occurs constitutively in cells. The activation of NF-κB/p50 is regulated by an inhibitory interaction with IκBα that masks the NLS and retains the NF-κB/p50-RelA heterodimer in the cytoplasm. In contrast to this, processing of NF-κB/p100 to NF-κB/p52 by the proteasome is tightly regulated and occurs only upon activation by IKKα-mediated phosphorylation. Ultimately, activation of the canonical and non-canonical NF-κB pathways results in the release of NF-κB heterodimers from inhibition and subsequent translocation to the nucleus where they promote transcription of genes involved in many cellular responses. As part of an autoregulatory feedback mechanism they also activate transcription of genes that inhibit the NF-κB pathways (Bonizzi and Karin, 2004; Hayden *et al*., 2006; Xiao *et al*., 2006).

An overview of both NF-κB signaling cascades is schematically depicted in Figure 4.1. As the canonical NF-κB pathway has been discovered first and is important for TNFα (tumor necrosis factor α) signaling, this cascade has been the focus of much research and is exemplary shown on the left in Figure 4.1, although nuclear translocation of NF-κB1 in this pathway can also be induced by other plasma membrane receptors and ligands. Binding of a TNFα homotrimer induces trimerization of TNFR1. This initiates the recruitment of TNFR-associated death domain protein (TRADD), which in turn recruits TNF-receptor-associated factor (TRAF) 2 or 5 to the cytoplasmic C-termini of the receptors. TRAF 2 or 5 are E3 ligases and appear to function interchangeably. Once recruited to TRADD they oligomerize and autoactivate by transubiquitination. Activated TRAF6 in collaboration with Ubc13/Eev1A promotes Lys63-linked polyubiquination of RIP1 (serine/threonine kinase receptor interacting protein 1), which acts as a scaffold for components of the IKK complex. This complex is composed of four kinases: IKKα, IKKβ, IKKγ, and TAK1 (TGF-β-activated kinase1). Lys63-linked chains attached to RIP1 have been shown to play a pivotal role for the phosphorylation of the IKK complex. Upon activation, the IKK complex in turn phosphorylates IκBα, the inhibitor of the NF-κB/p50-RelA heterodimer, which is a signal for its ubiquitination and subsequent degradation by the UPS. Once freed of its inhibitor NF-κB/p50-RelA can translocate to the nucleus (Adhikari *et al*. 2007; Beinke and Ley, 2004;

Bonizzi and Karin, 2004; Chen, 2005; Hayden *et al*., 2006; Kanayama *et al*., 2004; Scheiderheit, 2006; Tian *et al*., 2007; Xiao *et al*., 2006).

While the canonical pathway was discovered almost twenty years ago, the non-canonical pathway has only been unraveled in 2001 (Sen and Baltimore, 1986; Senftleben *et al*., 2001). Therefore the signaling cascade involved in activation of NF-κB/p52 is much less well understood. The non-canonical pathway is also stimulated by different ligand/ recaptor combinations. The right side of Figure 4.1 depicts as an example its activation by the lymphotoxin beta receptor (LTβR) and its ligand lymphotoxin ($LT\alpha_1\beta_{2)}$. Sharpin appears to be a crucial component of this pathway. The ligand binding and trimerization of LTβR by $LT\alpha_1\beta_2$ has been shown to activate the NF-κB-inducing kinase (NIK). The exact signaling events leading to NIK activation are not clear at the moment. NIK appears to be recruited to LTβR through an interaction with TRAF 2 or TRAF 5, however, this recruitment alone is probably not enough to induce NIK activation. The stability of NIK seems to be highly regulated by another TRAF protein. In the absence of stimulation, TRAF 3 has been shown to interact with NIK and promote the ubiquitination and degradation of NIK by the UPS. Indeed, upon stimulation of the non-canonical pathway, the expression of NIK becomes more stable due to the degradation of TRAF 3 (Beinke and Ley, 2004; Hauer et al., 2005; Liao *et al*., 2004; Xiao *et al*., 2006). Stabilized NIK activates IKKα and also acts as a docking protein by mediating the interaction between IKKα and the NF-κB/p100-RelB heterodimer. After being brought into close proximity IKKα activates NF-κB/p100 by phosphorylation, which in turn triggers its ubiquitination by the SCF-βTrCP ligase resulting in partial degradation of NF-κB/p100 to NF-κB/p52 by the proteasome. After proteasome processing, the NF-κB/p52-RelB heterodimer can translocate to the nucleus. (Bienke and Ley, 2004; Senftleben *et al*., 2001; Xiao *et al*., 2001; Xiao *et al*., 2004; Xiao *et al*., 2006).

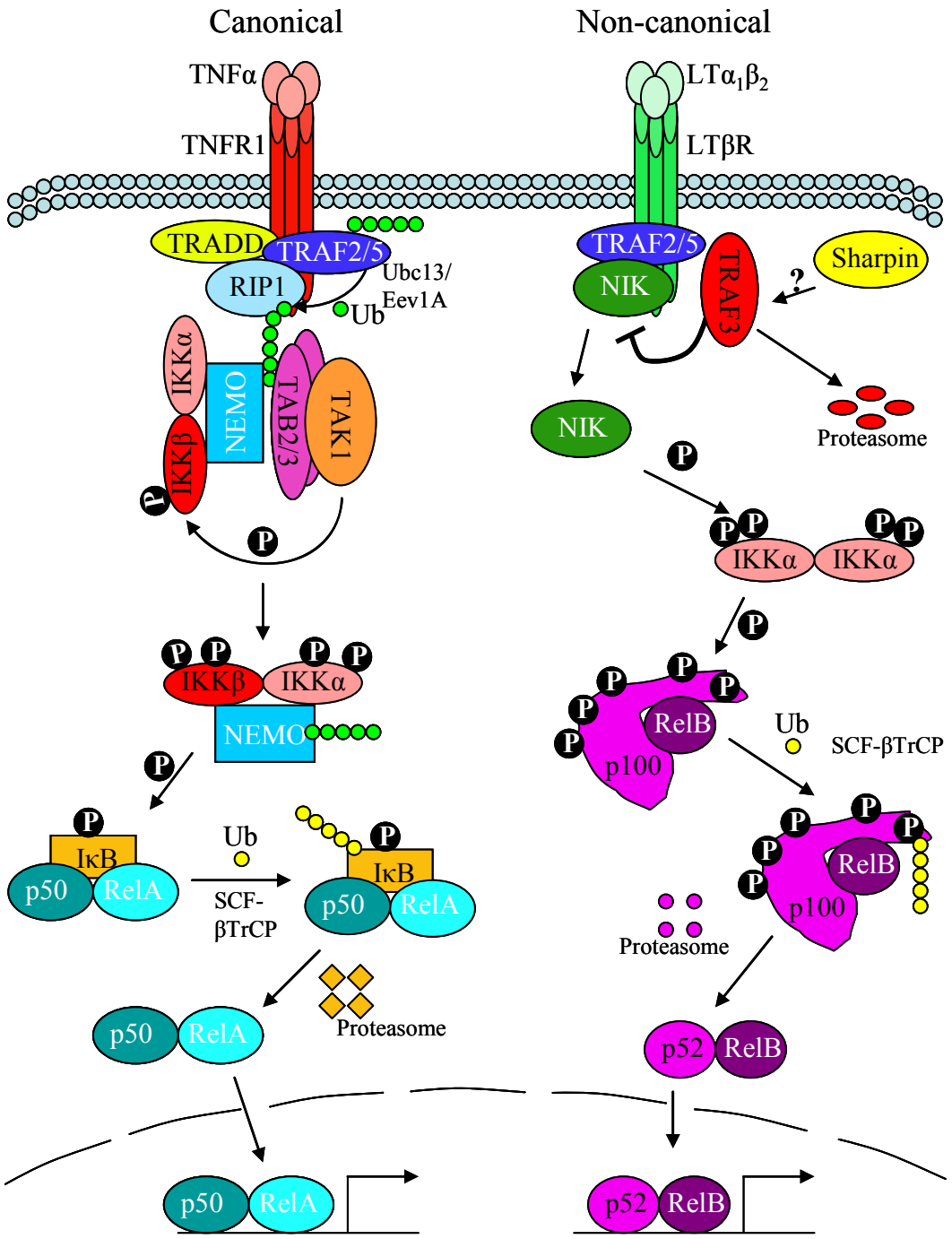

Figure 4.1 NF-κB Signaling Pathways
A schematic diagram of the activation of the transcription factors NF-κB/p50 and NF-κB/p52 is depicted. In both pathways, receptor activation leads to the translocation of the NF-κB transcription factors to the nucleus. These pathways are highly regulated by both phosphorylation and ubiquitination. Refer to the above text for further details on the signaling cascades. Ubiquitin (Ub) chains depicted in green represent Lys63 linkages and chains depicted in yellow represent Lys48 linkages.

Because mice deficient in various components of the non-canonical pathway that leads to NF-κB/p52 activation have a similar phenotype as *cpdm/cpdm* mice with a spontaneous mutation in the Sharpin gene, Sharpin is very likely to play a role in the non-canonical NF-κB signaling pathway. As shown in this study, Sharpin can bind to ubiquitin through its NZF domain and interacts with the ubiquitin ligase EDD1. It may also play a role in shuttling proteins to the UPS for degradation, since it coprecipitates with S5a and Rpt1. Therefore it is feasible that Sharpin binds to a signaling component of the non-canonical pathway and assists in the degradation of that protein. Recently, Tian *et al*. (2007) have shown that RBCK1 interacts with TAB2 and TAB3, which are proteins in the canonical NF-κB pathway that form a complex with TAK and recognize the polyubiquitin chains of RIP1. The protein RBCK1 (RBCC protein interacting with protein kinase C1) exhibits 45% homology with the region of Sharpin that contains the type 2 Ubl and the NZF domains (Lim *et al*. 2001). In addition to the region homologous to Sharpin, RBCK1 also contains a RING-IBR (Really interesting new gene - in-between-RINGS) region. Proteins containing this region have been shown to be E3 ubiquitin ligases (Marin and Ferrus, 2002). TAB2 and TAB3, have very similar structures at the N-terminus. They have a ubiquitin binding domain called CUE (coupling of ubiquitin conjugation to endoplasmic reticulum degradation). At the C-terminus they also have a coiled-coil (CC) and an NZF domain. The region of RBCK1 that has homology to Sharpin was shown to interact with the C-terminal CC and NZF region of TAB 2 and TAB 3. This interaction was shown to induce the degradation of TAB2 and TAB3 by the UPS. Furthermore, overexpression of RBCK1 inhibited the TAB2 and TAB3 mediated activation of NF-κB by TNFα and IL-1. Conversely, silencing of RBCK1 by RNAi technology enhanced the activation of NF-κB by TNFα and IL-1 (Tian *et al*. 2007). To date, there has been no report of TAB proteins involved in the non-canonical pathway, but similar molecular mechanisms might also play a role here.

Despite many structural similarities between Sharpin and RBCK1, a major functional difference between the two proteins is that Sharpin seems to play an activating role in the non-canonical pathway, whereas RBCK1 has a negative regulatory role in the canonical pathway. The phenotype of Sharpin mutant mice points towards a role in the activation of NF-κB2. A point in the non-canonical signaling cascade, where Sharpin might play such a role could be in promoting the degradation of TRAF3. As mentioned before TRAF3 inhibits

NIK activity by constitutively targeting NIK for degradation by the UPS. Upon activation of the non-canonical pathway TRAF3, itself, is degraded by the proteasome resulting in increased levels of NIK protein and activity (Liao *et al*. 2004). A role for Sharpin in shuttling the NIK inhibitor TRAF3 to the proteasome for instance would fit with the inhibition of the non-canonical NF-κB seen in the *cpdm/cpdm* mice. Alternatively or additionally, Sharpin may play a role in the activation of TRAF2 or 5. A similar mechanism as outlined above has been described for sequestosome 1/p62 (Siebenhener *et al*., 2007).

Since the NF-κB signaling pathway was originally described in the field of immunology, the majority of information known about this pathway is tied into immune response and inflammation. However, more recently NF-κB signaling has also been described in other areas of biology like the nervous system. NF-κB is a ubiquitiously expressed transcription factor and its activity has been detected in various areas of the central nervous system (CNS), in particular in the hippocampus and cortex. In these brain regions, NF-κB can be activated in response to many different stimuli that induce synaptic plasticity like glutamate, depolarization, changes in intracellular Ca^{2+}, neuropeptides, N-CAM (neural cell-adhesion molecule), as well as the cytokines TNFα and IL-1, and oxidative stress. Neuronal activity of the NF-κB pathway has been shown to play a role in learning and memory. In neurons, NF-κB is present at both sides of the synapse. A current model for NF-κB signaling in neurons assumes activation of NF-κB at the synapse and retrograde transport of activated NF-κB to the nucleus for gene transcription. This model ties the activity of synapses to the transcription of genes for long-term changes in the synapse. To date, most studies have only focused on the activetion of the canonical NF-κB/p105-p50 pathway in neuronal activity (Kaltschmidt *et al*., 2005; Romano *et al*., 2006; Mémet, 2006). Recently, Hu *et al*. (2005) have proposed a novel role for NIK in neurons. In contrast to its normal function in the non-canonical pathway, NIK may activate the canonical NF-κB pathway in neurons. A novel protein, NIBP (NIK and IKKβ binding protein) was shown to concomitantly interact with both NIK and IKKβ. NIBP expression enhanced NF-κB activation, most likely by mediating the activation of IKKβ by NIK. Moreover, in PC12 cells NIK induced neurite outgrowth and protected the cells from apoptosis (Foehr *et al*., 2000). Neuronal expression of NF-κB/p100-p52 has been detected (Franzén *et al*., 2003). Taking in consideration all the observations summarized above, future studies of a potential role for Sharpin in the non-

canonical pathway in the CNS are certainly warranted. The recent finding that Sharpin plays an integral role in the non-canonical pathway will greatly aid elucidating its role in neurons, since it offers a number of cellular read-outs for Sharpin function. Experiments that investigate, how overexpression of wildtype Sharpin or of deletion mutants of Sharpin affect NF-κB2 processing and activation in neurons seem feasible now. It would also be interesting to see, if Sharpin can indeed promote the degradation of TRAF3 in neurons. This could be monitored by a decrease in TRAF3 levels and a concomitant increase in the expression of NIK as well as in the processing and nuclear translocation of NF-κB2.

Chapter 5 Summary

Sharpin is a protein which has been initially described as an interacting protein for the post-synaptic protein Shank. Shank functions as a scaffold protein at the glutamatergic synapse in neurons of the central nervous system. However, as Sharpin is widely expressed, and even in neurons is not exclusively localized to synaptic sites, it is likely that the cellular function of Sharpin is not limited to a role at the synapse.

This work set out to identify and characterize novel protein-protein interactions of Sharpin in order to shed some light on its potential cellular functions. Sharpin contains two domains that in the context of other proteins have previously been described to play a role in the ubiquitin proteasome system (UPS): a Npl4 zinc finger (NZF) domain and a type 2 ubiquitin-like domain (Ubl). The NZF domain of Sharpin was shown here to bind to ubiquitin in a yeast two-hybrid system. The interaction was demonstrated for monoubiquitin as well as for Lys48- and Lys63-linked polyubiquitin chains. Interestingly, in a yeast two-hybrid screen with the Ubl domain of Sharpin (aa 171-304) as bait, OS-9, a protein upregulated in osteosarcoma, and the E3 ubiquitin ligase EDD1 were identified here as novel interaction partners of Sharpin. In human cells, all these interactions of Sharpin (including the interaction with Shank) were confirmed but required previous inhibition of the proteasome by MG132. Subcellular fractionation revealed that Sharpin/OS-9 complexes were predominantly present in the fractions with the highest amount of proteasome subunits again linking this interaction to UPS function. Sharpin also interacted with coexpressed Rpt1, a 19S proteasome subunit. MG132 treatment of cultured cortical neurons resulted in a substantially increased amount of endogenous Sharpin present in postsynaptic density preparations. Under these conditions, also the subcellular localization of ectopically expressed Sharpin changed significantly. A reduction in the nuclear localization of Sharpin was accompanied by its accumulation in the cytoplasm, where it was found colocalized with Shank1 in aggregate-like structures. Taken together the results presented in this work suggest a possible shuttling role for Sharpin in the UPS. Via its interaction with OS-9, Sharpin could be involved in regulating the ubiquitination and degradation of components of the hypoxia response pathway. Based on the recent identification of a mouse line which suffers from severe immunological deficits due to a spontaneous mutation in the Sharpin gene, it can also be speculated that Sharpin similarly plays a role as a ubiquitin shuttling protein for components of the non-canonical NF-κB signaling pathway.

Chapter 6 References

Abbott LF, Nelson SB (2000) Synaptic plasticity: Taming the beast. Nat Neurosci 3 Suppl:1178-1183.

Adhikari A, Xu M, Chen ZJ (2007) Ubiquitin-mediated activation of TAK1 and IKK. Oncogene 26:3214-3226.

Aguilar RC, Wendland B (2003) Ubiquitin: Not just for proteasomes anymore. Curr Opin Cell Biol 15:184-190.

Aharoni D, Meiri I, Atzmon R, Vlodavsky I, Amsterdam A (1997) Differential effect of components of the extracellular matrix on differentiation and apoptosis. Curr Biol 7:43-51.

Alam SL, Sun J, Payne M, Welch BD, Blake BK, Davis DR, Meyer HH, Emr SD, Sundquist WI (2004) Ubiquitin interactions of NZF zinc fingers. EMBO J 23:1411-1421.

Alimzhanov MB, Kuprash DV, Kosco-Vilbois MH, Luz A, Turetskaya RL, Tarakhovsky A, Rajewsky K, Nedospasov SA, Pfeffer K (1997) Abnormal development of secondary lymphoid tissues in lymphotoxin beta-deficient mice. Proc Natl Acad Sci U S A 94:9302-9307.

Arnason T, Ellison MJ (1994) Stress resistance in saccharomyces cerevisiae is strongly correlated with assembly of a novel type of multiubiquitin chain. Mol Cell Biol 14:7876-7883.

Aunis D, Bader MF (1988) The cytoskeleton as a barrier to exocytosis in secretory cells. J Exp Biol 139:253-266.

Baek JH, Mahon PC, Oh J, Kelly B, Krishnamachary B, Pearson M, Chan DA, Giaccia AJ, Semenza GL (2005) OS-9 interacts with hypoxia-inducible factor 1alpha and prolyl hydroxylases to promote oxygen-dependent degradation of HIF-1alpha. Mol Cell 17:503-512.

Banks TA, Rouse BT, Kerley MK, Blair PJ, Godfrey VL, Kuklin NA, Bouley DM, Thomas J, Kanangat S, Mucenski ML (1995) Lymphotoxin-alpha-deficient mice. effects on secondary lymphoid organ development and humoral immune responsiveness. J Immunol 155:1685-1693.

Baron MK, Boeckers TM, Vaida B, Faham S, Gingery M, Sawaya MR, Salyer D, Gundelfinger ED, Bowie JU (2006) An architectural framework that may lie at the core of the postsynaptic density. Science 311:531-535.

Barton D, HogenEsch H, Weih F (2000) Mice lacking the transcription factor RelB develop T cell-dependent skin lesions similar to human atopic dermatitis. Eur J Immunol 30:2323-2332.

Bays NW, Gardner RG, Seelig LP, Joazeiro CA, Hampton RY (2001) Hrd1p/Der3p is a membrane-anchored ubiquitin ligase required for ER-associated degradation. Nat Cell Biol 3:24-29.

Beinke S, Ley SC (2004) Functions of NF-kappaB1 and NF-kappaB2 in immune cell biology. Biochem J 382:393-409.

Bence NF, Sampat RM, Kopito RR (2001) Impairment of the ubiquitin-proteasome system by protein aggregation. Science 292:1552-1555.

Benmerah A, Gagnon J, Begue B, Megarbane B, Dautry-Varsat A, Cerf-Bensussan N (1995) The tyrosine kinase substrate eps15 is constitutively associated with the plasma membrane adaptor AP-2. J Cell Biol 131:1831-1838.

Bennett V, Baines AJ (2001) Spectrin and ankyrin-based pathways: Metazoan inventions for integrating cells into tissues. Physiol Rev 81:1353-1392.

Bhamidipati A, Denic V, Quan EM, Weissman JS (2005) Exploration of the topological requirements of ERAD identifies Yos9p as a lectin sensor of misfolded glycoproteins in the ER lumen. Mol Cell 19:741-751.

Bingol B, Schuman EM (2006) Activity-dependent dynamics and sequestration of proteasomes in dendritic spines. Nature 441:1144-1148.

Blichenberg A, Schwanke B, Rehbein M, Garner CC, Richter D, Kindler S (1999) Identification of a cis-acting dendritic targeting element in MAP2 mRNAs. J Neurosci 19:8818-8829.

Bockers TM, Mameza MG, Kreutz MR, Bockmann J, Weise C, Buck F, Richter D, Gundelfinger ED, Kreienkamp HJ (2001) Synaptic scaffolding proteins in rat brain. ankyrin repeats of the multidomain shank protein family interact with the cytoskeletal protein alpha-fodrin. J Biol Chem 276:40104-40112.

Bockmann J, Kreutz MR, Gundelfinger ED, Bockers TM (2002) ProSAP/Shank postsynaptic density proteins interact with insulin receptor tyrosine kinase substrate IRSp53. J Neurochem 83:1013-1017.

Boeckers TM, Winter C, Smalla KH, Kreutz MR, Bockmann J, Seidenbecher C, Garner CC, Gundelfinger ED (1999) Proline-rich synapse-associated proteins ProSAP1 and ProSAP2 interact with synaptic proteins of the SAPAP/GKAP family. Biochem Biophys Res Commun 264:247-252.

Bonizzi G, Karin M (2004) The two NF-kappaB activation pathways and their role in innate and adaptive immunity. Trends Immunol 25:280-288.

Brakeman PR, Lanahan AA, O'Brien R, Roche K, Barnes CA, Huganir RL, Worley PF (1997) Homer: A protein that selectively binds metabotropic glutamate receptors. Nature 386:284-288.

Bush KT, Goldberg AL, Nigam SK (1997) Proteasome inhibition leads to a heat-shock response, induction of endoplasmic reticulum chaperones, and thermotolerance. J Biol Chem 272:9086-9092.

Chen L, Madura K (2002) Rad23 promotes the targeting of proteolytic substrates to the proteasome. Mol Cell Biol 22:4902-4913.

Chen L, Shinde U, Ortolan TG, Madura K (2001) Ubiquitin-associated (UBA) domains in Rad23 bind ubiquitin and promote inhibition of multi-ubiquitin chain assembly. EMBO Rep 2:933-938.

Chen X, Vinade L, Leapman RD, Petersen JD, Nakagawa T, Phillips TM, Sheng M, Reese TS (2005) Mass of the postsynaptic density and enumeration of three key molecules. Proc Natl Acad Sci U S A 102:11551-11556.

Chen ZJ (2005) Ubiquitin signalling in the NF-kappaB pathway. Nat Cell Biol 7:758-765.

Chuang SM, Chen L, Lambertson D, Anand M, Kinzy TG, Madura K (2005) Proteasome-mediated degradation of cotranslationally damaged proteins involves translation elongation factor 1A. Mol Cell Biol 25:403-413.

Ciechanover A, Brundin P (2003) The ubiquitin proteasome system in neurodegenerative diseases: Sometimes the chicken, sometimes the egg. Neuron 40:427-446.

Ciechanover A, Finley D, Varshavsky A (1984) Ubiquitin dependence of selective protein degradation demonstrated in the mammalian cell cycle mutant ts85. Cell 37:57-66.

Cline H (2003) Synaptic plasticity: Importance of proteasome-mediated protein turnover. Curr Biol 13:R514-6.

Colledge M, Snyder EM, Crozier RA, Soderling JA, Jin Y, Langeberg LK, Lu H, Bear MF, Scott JD (2003) Ubiquitination regulates PSD-95 degradation and AMPA receptor surface expression. Neuron 40:595-607.

DE ROBERTIS ED, BENNETT HS (1954) A submicroscopic vesicular component of schwann cells and nerve satellite cells. Exp Cell Res 6:543-545.

De Togni P, Goellner J, Ruddle NH, Streeter PR, Fick A, Mariathasan S, Smith SC, Carlson R, Shornick LP, Strauss-Schoenberger J (1994) Abnormal development of peripheral lymphoid organs in mice deficient in lymphotoxin. Science 264:703-707.

Deng L, Wang C, Spencer E, Yang L, Braun A, You J, Slaughter C, Pickart C, Chen ZJ (2000) Activation of the IkappaB kinase complex by TRAF6 requires a dimeric ubiquitin-conjugating enzyme complex and a unique polyubiquitin chain. Cell 103:351-361.

Devi VS, Binz HK, Stumpp MT, Pluckthun A, Bosshard HR, Jelesarov I (2004) Folding of a designed simple ankyrin repeat protein. Protein Sci 13:2864-2870.

DiAntonio A, Haghighi AP, Portman SL, Lee JD, Amaranto AM, Goodman CS (2001) Ubiquitination-dependent mechanisms regulate synaptic growth and function. Nature 412:449-452.

Doe WF (1989) The intestinal immune system. Gut 30:1679-1685.

Du Y, Weed SA, Xiong WC, Marshall TD, Parsons JT (1998) Identification of a novel cortactin SH3 domain-binding protein and its localization to growth cones of cultured neurons. Mol Cell Biol 18:5838-5851.

Ehlers MD (2003) Activity level controls postsynaptic composition and signaling via the ubiquitin-proteasome system. Nat Neurosci 6:231-242.

Elsasser S, Finley D (2005) Delivery of ubiquitinated substrates to protein-unfolding machines. Nat Cell Biol 7:742-749.

Elsasser S, Chandler-Militello D, Muller B, Hanna J, Finley D (2004) Rad23 and Rpn10 serve as alternative ubiquitin receptors for the proteasome. J Biol Chem 279:26817-26822.

Enenkel C, Lehmann A, Kloetzel PM (1998) Subcellular distribution of proteasomes implicates a major location of protein degradation in the nuclear envelope-ER network in yeast. EMBO J 17:6144-6154.

Erickson SL, de Sauvage FJ, Kikly K, Carver-Moore K, Pitts-Meek S, Gillett N, Sheehan KC, Schreiber RD, Goeddel DV, Moore MW (1994) Decreased sensitivity to tumour-necrosis factor but normal T-cell development in TNF receptor-2-deficient mice. Nature 372:560-563.

Fallon L, Belanger CM, Corera AT, Kontogiannea M, Regan-Klapisz E, Moreau F, Voortman J, Haber M, Rouleau G, Thorarinsdottir T, Brice A, van Bergen En Henegouwen,P.M., Fon EA (2006) A regulated interaction with the UIM protein Eps15 implicates parkin in EGF receptor trafficking and PI(3)K-akt signalling. Nat Cell Biol 8:834-842.

Farinha CM, Amaral MD (2005) Most F508del-CFTR is targeted to degradation at an early folding checkpoint and independently of calnexin. Mol Cell Biol 25:5242-5252.

Finley D, Sadis S, Monia BP, Boucher P, Ecker DJ, Crooke ST, Chau V (1994) Inhibition of proteolysis and cell cycle progression in a multiubiquitination-deficient yeast mutant. Mol Cell Biol 14:5501-5509.

Foehr ED, Bohuslav J, Chen LF, DeNoronha C, Geleziunas R, Lin X, O'Mahony A, Greene WC (2000) The NF-kappa B-inducing kinase induces PC12 cell differentiation and prevents apoptosis. J Biol Chem 275:34021-34024.

Fonseca R, Vabulas RM, Hartl FU, Bonhoeffer T, Nagerl UV (2006) A balance of protein synthesis and proteasome-dependent degradation determines the maintenance of LTP. Neuron 52:239-245.

Franzen B, Duvefelt K, Jonsson C, Engelhardt B, Ottervald J, Wickman M, Yang Y, Schuppe-Koistinen I (2003) Gene and protein expression profiling of human cerebral endothelial cells activated with tumor necrosis factor-alpha. Brain Res Mol Brain Res 115:130-146.

Franzoso G, Carlson L, Poljak L, Shores EW, Epstein S, Leonardi A, Grinberg A, Tran T, Scharton-Kersten T, Anver M, Love P, Brown K, Siebenlist U (1998) Mice deficient in nuclear factor (NF)-kappa B/p52 present with defects in humoral responses, germinal center reactions, and splenic microarchitecture. J Exp Med 187:147-159.

Friedmann E, Salzberg Y, Weinberger A, Shaltiel S, Gerst JE (2002) YOS9, the putative yeast homolog of a gene amplified in osteosarcomas, is involved in the endoplasmic reticulum (ER)-golgi transport of GPI-anchored proteins. J Biol Chem 277:35274-35281.

Futterer A, Mink K, Luz A, Kosco-Vilbois MH, Pfeffer K (1998) The lymphotoxin beta receptor controls organogenesis and affinity maturation in peripheral lymphoid tissues. Immunity 9:59-70.

Garcia-Mata R, Bebok Z, Sorscher EJ, Sztul ES (1999) Characterization and dynamics of aggresome formation by a cytosolic GFP-chimera. J Cell Biol 146:1239-1254.

Gijbels MJ, Zurcher C, Kraal G, Elliott GR, HogenEsch H, Schijff G, Savelkoul HF, Bruijnzeel PL (1996) Pathogenesis of skin lesions in mice with chronic proliferative dermatitis (cpdm/cpdm). Am J Pathol 148:941-950.

Glickman MH, Ciechanover A (2002) The ubiquitin-proteasome proteolytic pathway: Destruction for the sake of construction. Physiol Rev 82:373-428.

Glickman MH, Rubin DM, Fried VA, Finley D (1998) The regulatory particle of the saccharomyces cerevisiae proteasome. Mol Cell Biol 18:3149-3162.

Gosslau A, Ruoff P, Mohsenzadeh S, Hobohm U, Rensing L (2001) Heat shock and oxidative stress-induced exposure of hydrophobic protein domains as common signal in the induction of hsp68. J Biol Chem 276:1814-1821.

Haas S, Hilla A, Lessner G (2005) ECL-blots hausgemacht. 1.

Haglund K, Dikic I (2005) Ubiquitylation and cell signaling. EMBO J 24:3353-3359.

Hauer J, Puschner S, Ramakrishnan P, Simon U, Bongers M, Federle C, Engelmann H (2005) TNF receptor (TNFR)-associated factor (TRAF) 3 serves as an inhibitor of TRAF2/5-mediated activation of the noncanonical NF-kappaB pathway by TRAF-binding TNFRs. Proc Natl Acad Sci U S A 102:2874-2879.

Hayden MS, West AP, Ghosh S (2006) NF-kappaB and the immune response. Oncogene 25:6758-6780.

Hegde AN (2004) Ubiquitin-proteasome-mediated local protein degradation and synaptic plasticity. Prog Neurobiol 73:311-357.

Henderson MJ, Russell AJ, Hird S, Munoz M, Clancy JL, Lehrbach GM, Calanni ST, Jans DA, Sutherland RL, Watts CK (2002) EDD, the human hyperplastic discs protein, has a role in progesterone receptor coactivation and potential involvement in DNA damage response. J Biol Chem 277:26468-26478.

Henderson MJ, Munoz MA, Saunders DN, Clancy JL, Russell AJ, Williams B, Pappin D, Khanna KK, Jackson SP, Sutherland RL, Watts CK (2006) EDD mediates DNA damage-induced activation of CHK2. J Biol Chem 281:39990-40000.

Hershko A (1988) Ubiquitin-mediated protein degradation. J Biol Chem 263:15237-15240.

Hicke L (2001) A new ticket for entry into budding vesicles-ubiquitin. Cell 106:527-530.

Hicke L (1997) Ubiquitin-dependent internalization and down-regulation of plasma membrane proteins. FASEB J 11:1215-1226.

Hicke L, Schubert HL, Hill CP (2005) Ubiquitin-binding domains. Nat Rev Mol Cell Biol 6:610-621.

Hofmann RM, Pickart CM (2001) In vitro assembly and recognition of lys-63 polyubiquitin chains. J Biol Chem 276:27936-27943.

HogenEsch H, Janke S, Boggess D, Sundberg JP (1999) Absence of peyer's patches and abnormal lymphoid architecture in chronic proliferative dermatitis (cpdm/cpdm) mice. J Immunol 162:3890-3896.

HogenEsch H, Torregrosa SE, Boggess D, Sundberg BA, Carroll J, Sundberg JP (2001) Increased expression of type 2 cytokines in chronic proliferative dermatitis (cpdm) mutant mice and resolution of inflammation following treatment with IL-12. Eur J Immunol 31:734-742.

Hu WH, Pendergast JS, Mo XM, Brambilla R, Bracchi-Ricard V, Li F, Walters WM, Blits B, He L, Schaal SM, Bethea JR (2005) NIBP, a novel NIK and IKK(beta)-binding protein that enhances NF-(kappa)B activation. J Biol Chem 280:29233-29241.

Huang C, Ni Y, Wang T, Gao Y, Haudenschild CC, Zhan X (1997) Down-regulation of the filamentous actin cross-linking activity of cortactin by src-mediated tyrosine phosphorylation. J Biol Chem 272:13911-13915.

Hurley JH, Lee S, Prag G (2006) Ubiquitin-binding domains. Biochem J 399:361-372.

Imai Y, Soda M, Takahashi R (2000) Parkin suppresses unfolded protein stress-induced cell death through its E3 ubiquitin-protein ligase activity. J Biol Chem 275:35661-35664.

Innocenti M, Gerboth S, Rottner K, Lai FP, Hertzog M, Stradal TE, Frittoli E, Didry D, Polo S, Disanza A, Benesch S, Di Fiore PP, Carlier MF, Scita G (2005) Abi1 regulates the activity of N-WASP and WAVE in distinct actin-based processes. Nat Cell Biol 7:969-976.

Jordan BA, Fernholz BD, Boussac M, Xu C, Grigorean G, Ziff EB, Neubert TA (2004) Identification and verification of novel rodent postsynaptic density proteins. Mol Cell Proteomics 3:857-871.

Kaisho T, Takeda K, Tsujimura T, Kawai T, Nomura F, Terada N, Akira S (2001) IkappaB kinase alpha is essential for mature B cell development and function. J Exp Med 193:417-426.

Kaltschmidt B, Widera D, Kaltschmidt C (2005) Signaling via NF-kappaB in the nervous system. Biochim Biophys Acta 1745:287-299.

Kanayama A, Seth RB, Sun L, Ea CK, Hong M, Shaito A, Chiu YH, Deng L, Chen ZJ (2004) TAB2 and TAB3 activate the NF-kappaB pathway through binding to polyubiquitin chains. Mol Cell 15:535-548.

Kang Y, Zhang N, Koepp DM, Walters KJ (2007) Ubiquitin receptor proteins hHR23a and hPLIC2 interact. J Mol Biol 365:1093-1101.

Kessels MM, Engqvist-Goldstein AE, Drubin DG, Qualmann B (2001) Mammalian Abp1, a signal-responsive F-actin-binding protein, links the actin cytoskeleton to endocytosis via the GTPase dynamin. J Cell Biol 153:351-366.

Kim I, Mi K, Rao H (2004) Multiple interactions of rad23 suggest a mechanism for ubiquitylated substrate delivery important in proteolysis. Mol Biol Cell 15:3357-3365.

Kishino T, Lalande M, Wagstaff J (1997) UBE3A/E6-AP mutations cause angelman syndrome. Nat Genet 15:70-73.

Kitada T, Asakawa S, Hattori N, Matsumine H, Yamamura Y, Minoshima S, Yokochi M, Mizuno Y, Shimizu N (1998) Mutations in the parkin gene cause autosomal recessive juvenile parkinsonism. Nature 392:605-608.

Klebe RJ, Harriss JV, Sharp ZD, Douglas MG (1983) A general method for polyethylene-glycol-induced genetic transformation of bacteria and yeast. Gene 25:333-341.

Koegl M, Hoppe T, Schlenker S, Ulrich HD, Mayer TU, Jentsch S (1999) A novel ubiquitination factor, E4, is involved in multiubiquitin chain assembly. Cell 96:635-644.

Koike R, Nishimura T, Yasumizu R, Tanaka H, Hataba Y, Hataba Y, Watanabe T, Miyawaki S, Miyasaka M (1996) The splenic marginal zone is absent in alymphoplastic aly mutant mice. Eur J Immunol 26:669-675.

Koni PA, Sacca R, Lawton P, Browning JL, Ruddle NH, Flavell RA (1997) Distinct roles in lymphoid organogenesis for lymphotoxins alpha and beta revealed in lymphotoxin beta-deficient mice. Immunity 6:491-500.

Kornau HC, Schenker LT, Kennedy MB, Seeburg PH (1995) Domain interaction between NMDA receptor subunits and the postsynaptic density protein PSD-95. Science 269:1737-1740.

Kostova Z, Wolf DH (2003) For whom the bell tolls: Protein quality control of the endoplasmic reticulum and the ubiquitin-proteasome connection. EMBO J 22:2309-2317.

Laemmli UK (1970) Cleavage of structural proteins during the assembly of the head of bacteriophage T4. Nature 227:680-685.

Lee S, Tsai YC, Mattera R, Smith WJ, Kostelansky MS, Weissman AM, Bonifacino JS, Hurley JH (2006) Structural basis for ubiquitin recognition and autoubiquitination by rabex-5. Nat Struct Mol Biol 13:264-271.

Liao EH, Hung W, Abrams B, Zhen M (2004) An SCF-like ubiquitin ligase complex that controls presynaptic differentiation. Nature 430:345-350.

Lilley BN, Ploegh HL (2004) A membrane protein required for dislocation of misfolded proteins from the ER. Nature 429:834-840.

Lim S, Sala C, Yoon J, Park S, Kuroda S, Sheng M, Kim E (2001) Sharpin, a novel postsynaptic density protein that directly interacts with the shank family of proteins. Mol Cell Neurosci 17:385-397.

Litovchick L, Friedmann E, Shaltiel S (2002) A selective interaction between OS-9 and the carboxyl-terminal tail of meprin beta. J Biol Chem 277:34413-34423.

Lodish H, Berk A, Zipursky SL, Matsudaira P, Baltimore D, Darnell J (2000) Molecular cell biology.

Mameza M (2003) Weschelwirkung PSD protein aus mensch und der ratte. .

Marin I, Ferrus A (2002) Comparative genomics of the RBR family, including the parkinson's disease-related gene parkin and the genes of the ariadne subfamily. Mol Biol Evol 19:2039-2050.

Matsushima A, Kaisho T, Rennert PD, Nakano H, Kurosawa K, Uchida D, Takeda K, Akira S, Matsumoto M (2001) Essential role of nuclear factor (NF)-kappaB-inducing kinase and inhibitor of kappaB (IkappaB) kinase alpha in NF-kappaB activation through lymphotoxin beta receptor, but not through tumor necrosis factor receptor I. J Exp Med 193:631-636.

Mayrhofer G (1997) Peyer's patch organogenesis--cytokines rule, OK? Gut 41:707-709.

Memet S (2006) NF-kappaB functions in the nervous system: From development to disease. Biochem Pharmacol 72:1180-1195.

Meusser B, Hirsch C, Jarosch E, Sommer T (2005) ERAD: The long road to destruction. Nat Cell Biol 7:766-772.

Meyer HH, Wang Y, Warren G (2002) Direct binding of ubiquitin conjugates by the mammalian p97 adaptor complexes, p47 and Ufd1-Npl4. EMBO J 21:5645-5652.

Miller J, Gordon C (2005) The regulation of proteasome degradation by multi-ubiquitin chain binding proteins. FEBS Lett 579:3224-3230.

Miyawaki S, Nakamura Y, Suzuka H, Koba M, Yasumizu R, Ikehara S, Shibata Y (1994) A new mutation, aly, that induces a generalized lack of lymph nodes accompanied by immunodeficiency in mice. Eur J Immunol 24:429-434.

Naisbitt S, Kim E, Tu JC, Xiao B, Sala C, Valtschanoff J, Weinberg RJ, Worley PF, Sheng M (1999) Shank, a novel family of postsynaptic density proteins that binds to the NMDA receptor/PSD-95/GKAP complex and cortactin. Neuron 23:569-582.

Olazabal IM, Machesky LM (2001) Abp1p and cortactin, new "hand-holds" for actin. J Cell Biol 154:679-682.

PALAY SL (1958) The morphology of synapses in the central nervous system. Exp Cell Res 14:275-293.

Paschen W, Mengesdorf T (2003) Conditions associated with ER dysfunction activate homer 1a expression. J Neurochem 86:1108-1115.

Pasparakis M, Alexopoulou L, Grell M, Pfizenmaier K, Bluethmann H, Kollias G (1997) Peyer's patch organogenesis is intact yet formation of B lymphocyte follicles is defective in peripheral lymphoid organs of mice deficient for tumor necrosis factor and its 55-kDa receptor. Proc Natl Acad Sci U S A 94:6319-6323.

Patrick GN (2006) Synapse formation and plasticity: Recent insights from the perspective of the ubiquitin proteasome system. Curr Opin Neurobiol 16:90-94.

Patrick GN, Bingol B, Weld HA, Schuman EM (2003) Ubiquitin-mediated proteasome activity is required for agonist-induced endocytosis of GluRs. Curr Biol 13:2073-2081.

Paxian S, Merkle H, Riemann M, Wilda M, Adler G, Hameister H, Liptay S, Pfeffer K, Schmid RM (2002) Abnormal organogenesis of peyer's patches in mice deficient for NF-kappaB1, NF-kappaB2, and bcl-3. Gastroenterology 122:1853-1868.

Penengo L, Mapelli M, Murachelli AG, Confalonieri S, Magri L, Musacchio A, Di Fiore PP, Polo S, Schneider TR (2006) Crystal structure of the ubiquitin binding domains of rabex-5 reveals two modes of interaction with ubiquitin. Cell 124:1183-1195.

Peng J, Kim MJ, Cheng D, Duong DM, Gygi SP, Sheng M (2004) Semiquantitative proteomic analysis of rat forebrain postsynaptic density fractions by mass spectrometry. J Biol Chem 279:21003-21011.

Peng J, Schwartz D, Elias JE, Thoreen CC, Cheng D, Marsischky G, Roelofs J, Finley D, Gygi SP (2003) A proteomics approach to understanding protein ubiquitination. Nat Biotechnol 21:921-926.

Pickart CM (2004) Back to the future with ubiquitin. Cell 116:181-190.

Pickart CM (2000) Ubiquitin in chains. Trends Biochem Sci 25:544-548.

Pickart CM, Eddins MJ (2004) Ubiquitin: Structures, functions, mechanisms. Biochim Biophys Acta 1695:55-72.

Pickart CM, Fushman D (2004) Polyubiquitin chains: Polymeric protein signals. Curr Opin Chem Biol 8:610-616.

Proepper C, Johannsen S, Liebau S, Dahl J, Vaida B, Bockmann J, Kreutz MR, Gundelfinger ED, Boeckers TM (2007) Abelson interacting protein 1 (abi-1) is essential for dendrite morphogenesis and synapse formation. EMBO J 26:1397-1409.

Qualmann B, Boeckers TM, Jeromin M, Gundelfinger ED, Kessels MM (2004) Linkage of the actin cytoskeleton to the postsynaptic density via direct interactions of Abp1 with the ProSAP/Shank family. J Neurosci 24:2481-2495.

Quitsch A, Berhorster K, Liew CW, Richter D, Kreienkamp HJ (2005) Postsynaptic shank antagonizes dendrite branching induced by the leucine-rich repeat protein densin-180. J Neurosci 25:479-487.

Romano A, Freudenthal R, Merlo E, Routtenberg A (2006) Evolutionarily-conserved role of the NF-kappaB transcription factor in neural plasticity and memory. Eur J Neurosci 24:1507-1516.

Romorini S, Piccoli G, Jiang M, Grossano P, Tonna N, Passafaro M, Zhang M, Sala C (2004) A functional role of postsynaptic density-95-guanylate kinase-associated protein complex in regulating shank assembly and stability to synapses. J Neurosci 24:9391-9404.

Sakata E, Yamaguchi Y, Kurimoto E, Kikuchi J, Yokoyama S, Yamada S, Kawahara H, Yokosawa H, Hattori N, Mizuno Y, Tanaka K, Kato K (2003) Parkin binds the Rpn10 subunit of 26S proteasomes through its ubiquitin-like domain. EMBO Rep 4:301-306.

Sambrook J, Fritsch EF, Maniatis T (1989) Molecular cloning - A laboratory manual. cold spring harbor laboratory press. .

Schauber C, Chen L, Tongaonkar P, Vega I, Lambertson D, Potts W, Madura K (1998) Rad23 links DNA repair to the ubiquitin/proteasome pathway. Nature 391:715-718.

Scheidereit C (2006) IkappaB kinase complexes: Gateways to NF-kappaB activation and transcription. Oncogene 25:6685-6705.

Seibenhener ML, Babu JR, Geetha T, Wong HC, Krishna NR, Wooten MW (2004) Sequestosome 1/p62 is a polyubiquitin chain binding protein involved in ubiquitin proteasome degradation. Mol Cell Biol 24:8055-8068.

Sen R, Baltimore D (1986) Inducibility of kappa immunoglobulin enhancer-binding protein nf-kappa B by a posttranslational mechanism. Cell 47:921-928.

Senftleben U, Cao Y, Xiao G, Greten FR, Krahn G, Bonizzi G, Chen Y, Hu Y, Fong A, Sun SC, Karin M (2001) Activation by IKKalpha of a second, evolutionary conserved, NF-kappa B signaling pathway. Science 293:1495-1499.

Seymour RE, Hasham MG, Cox GA, Shultz LD, Hogenesch H, Roopenian DC, Sundberg JP (2007) Spontaneous mutations in the mouse sharpin gene result in multiorgan inflammation, immune system dysregulation and dermatitis. Genes Immun 8:416-421.

Sha WC, Liou HC, Tuomanen EI, Baltimore D (1995) Targeted disruption of the p50 subunit of NF-kappa B leads to multifocal defects in immune responses. Cell 80:321-330.

Shang J, Korner C, Freeze H, Lehrman MA (2002) Extension of lipid-linked oligosaccharides is a high-priority aspect of the unfolded protein response: Endoplasmic reticulum stress in type I congenital disorder of glycosylation fibroblasts. Glycobiology 12:307-317.

Sheng M, Kim E (2000) The shank family of scaffold proteins. J Cell Sci 113 (Pt 11):1851-1856.

Shimura H, Hattori N, Kubo S, Mizuno Y, Asakawa S, Minoshima S, Shimizu N, Iwai K, Chiba T, Tanaka K, Suzuki T (2000) Familial parkinson disease gene product, parkin, is a ubiquitin-protein ligase. Nat Genet 25:302-305.

Shinkura R, Matsuda F, Sakiyama T, Tsubata T, Hiai H, Paumen M, Miyawaki S, Honjo T (1996) Defects of somatic hypermutation and class switching in alymphoplasia (aly) mutant mice. Int Immunol 8:1067-1075.

Shinkura R, Kitada K, Matsuda F, Tashiro K, Ikuta K, Suzuki M, Kogishi K, Serikawa T, Honjo T (1999) Alymphoplasia is caused by a point mutation in the mouse gene encoding nf-kappa b-inducing kinase. Nat Genet 22:74-77.

Soltau M, Richter D, Kreienkamp HJ (2002) The insulin receptor substrate IRSp53 links postsynaptic shank1 to the small G-protein cdc42. Mol Cell Neurosci 21:575-583.

Spahn TW, Kucharzik T (2004) Modulating the intestinal immune system: The role of lymphotoxin and GALT organs. Gut 53:456-465.

Spence J, Gali RR, Dittmar G, Sherman F, Karin M, Finley D (2000) Cell cycle-regulated modification of the ribosome by a variant multiubiquitin chain. Cell 102:67-76.

Staub O, Rotin D (2006) Role of ubiquitylation in cellular membrane transport. Physiol Rev 86:669-707.

Stryer L (1995) Biochemistry.

Sugiyama Y, Kawabata I, Sobue K, Okabe S (2005) Determination of absolute protein numbers in single synapses by a GFP-based calibration technique. Nat Methods 2:677-684.

Suh J, Lee YA, Gwag BJ (2005) Induction and attenuation of neuronal apoptosis by proteasome inhibitors in murine cortical cell cultures. J Neurochem 95:684-694.

Sun L, Chen ZJ (2004) The novel functions of ubiquitination in signaling. Curr Opin Cell Biol 16:119-126.

Takeuchi M, Hata Y, Hirao K, Toyoda A, Irie M, Takai Y (1997) SAPAPs. A family of PSD-95/SAP90-associated proteins localized at postsynaptic density. J Biol Chem 272:11943-11951.

Thrower JS, Hoffman L, Rechsteiner M, Pickart CM (2000) Recognition of the polyubiquitin proteolytic signal. EMBO J 19:94-102.

Tian Y, Zhang Y, Zhong B, Wang YY, Diao FC, Wang RP, Zhang M, Chen DY, Zhai ZH, Shu HB (2007) RBCK1 negatively regulates tumor necrosis factor- and interleukin-1-triggered NF-kappaB activation by targeting TAB2/3 for degradation. J Biol Chem 282:16776-16782.

Tobaben S, Sudhof TC, Stahl B (2000) The G protein-coupled receptor CL1 interacts directly with proteins of the shank family. J Biol Chem 275:36204-36210.

Tu JC, Xiao B, Yuan JP, Lanahan AA, Leoffert K, Li M, Linden DJ, Worley PF (1998) Homer binds a novel proline-rich motif and links group 1 metabotropic glutamate receptors with IP3 receptors. Neuron 21:717-726.

Tu JC, Xiao B, Naisbitt S, Yuan JP, Petralia RS, Brakeman P, Doan A, Aakalu VK, Lanahan AA, Sheng M, Worley PF (1999) Coupling of mGluR/Homer and PSD-95 complexes by the shank family of postsynaptic density proteins. Neuron 23:583-592.

Turner GC, Varshavsky A (2000) Detecting and measuring cotranslational protein degradation in vivo. Science 289:2117-2120.

von Boehmer H (1997) Lymphotoxins: From cytotoxicity to lymphoid organogenesis. Proc Natl Acad Sci U S A 94:8926-8927.

Wahlman J, DeMartino GN, Skach WR, Bulleid NJ, Brodsky JL, Johnson AE (2007) Real-time fluorescence detection of ERAD substrate retrotranslocation in a mammalian in vitro system. Cell 129:943-955.

Wang B, Alam SL, Meyer HH, Payne M, Stemmler TL, Davis DR, Sundquist WI (2003) Structure and ubiquitin interactions of the conserved zinc finger domain of Npl4. J Biol Chem 278:20225-20234.

Wang HR, Zhang Y, Ozdamar B, Ogunjimi AA, Alexandrova E, Thomsen GH, Wrana JL (2003) Regulation of cell polarity and protrusion formation by targeting RhoA for degradation. Science 302:1775-1779.

Weih DS, Yilmaz ZB, Weih F (2001) Essential role of RelB in germinal center and marginal zone formation and proper expression of homing chemokines. J Immunol 167:1909-1919.

Weih F, Carrasco D, Durham SK, Barton DS, Rizzo CA, Ryseck RP, Lira SA, Bravo R (1995) Multiorgan inflammation and hematopoietic abnormalities in mice with a targeted disruption of RelB, a member of the NF-kappa B/Rel family. Cell 80:331-340.

Wente W, Efanov AM, Treinies I, Zitzer H, Gromada J, Richter D, Kreienkamp HJ (2005) The PDZ/coiled-coil domain containing protein PIST modulates insulin secretion in MIN6 insulinoma cells by interacting with somatostatin receptor subtype 5. FEBS Lett 579:6305-6310.

Wigley WC, Fabunmi RP, Lee MG, Marino CR, Muallem S, DeMartino GN, Thomas PJ (1999) Dynamic association of proteasomal machinery with the centrosome. J Cell Biol 145:481-490.

Xiao G, Fong A, Sun SC (2004) Induction of p100 processing by NF-kappaB-inducing kinase involves docking IkappaB kinase alpha (IKKalpha) to p100 and IKKalpha-mediated phosphorylation. J Biol Chem 279:30099-30105.

Xiao G, Harhaj EW, Sun SC (2001) NF-kappaB-inducing kinase regulates the processing of NF-kappaB2 p100. Mol Cell 7:401-409.

Xiao G, Rabson AB, Young W, Qing G, Qu Z (2006) Alternative pathways of NF-kappaB activation: A double-edged sword in health and disease. Cytokine Growth Factor Rev 17:281-293.

Yamada T, Mitani T, Yorita K, Uchida D, Matsushima A, Iwamasa K, Fujita S, Matsumoto M (2000) Abnormal immune function of hemopoietic cells from alymphoplasia (aly) mice, a natural strain with mutant NF-kappa B-inducing kinase. J Immunol 165:804-812.

Yamagishi A, Masuda M, Ohki T, Onishi H, Mochizuki N (2004) A novel actin bundling/filopodium-forming domain conserved in insulin receptor tyrosine kinase substrate p53 and missing in metastasis protein. J Biol Chem 279:14929-14936.

Yao I, Hata Y, Hirao K, Deguchi M, Ide N, Takeuchi M, Takai Y (1999) Synamon, a novel neuronal protein interacting with synapse-associated protein 90/postsynaptic density-95-associated protein. J Biol Chem 274:27463-27466.

Ye Y, Meyer HH, Rapoport TA (2001) The AAA ATPase Cdc48/p97 and its partners transport proteins from the ER into the cytosol. Nature 414:652-656.

Ye Y, Shibata Y, Yun C, Ron D, Rapoport TA (2004) A membrane protein complex mediates retro-translocation from the ER lumen into the cytosol. Nature 429:841-847.

Yi JJ, Ehlers MD (2005) Ubiquitin and protein turnover in synapse function. Neuron 47:629-632.

Yilmaz ZB, Weih DS, Sivakumar V, Weih F (2003) RelB is required for peyer's patch development: Differential regulation of p52-RelB by lymphotoxin and TNF. EMBO J 22:121-130.

Young P, Deveraux Q, Beal RE, Pickart CM, Rechsteiner M (1998) Characterization of two polyubiquitin binding sites in the 26 S protease subunit 5a. J Biol Chem 273:5461-5467.

Zhang H, Maximov A, Fu Y, Xu F, Tang TS, Tkatch T, Surmeier DJ, Bezprozvanny I (2005) Association of CaV1.3 L-type calcium channels with shank. J Neurosci 25:1037-1049.

Zhao Y, Hegde AN, Martin KC (2003) The ubiquitin proteasome system functions as an inhibitory constraint on synaptic strengthening. Curr Biol 13:887-898.

Zigmond MJ, Bloom FE, Landis SC, Roberts J.L., Squire, L.R. (1999) Fundamental neuroscience.

Zitzer H, Richter D, Kreienkamp HJ (1999a) Agonist-dependent interaction of the rat somatostatin receptor subtype 2 with cortactin-binding protein 1. J Biol Chem 274:18153-18156.

Zitzer H, Honck HH, Bachner D, Richter D, Kreienkamp HJ (1999b) Somatostatin receptor interacting protein defines a novel family of multidomain proteins present in human and rodent brain. J Biol Chem 274:32997-33001.

Appendix

List of Primers Used in this Study

Construct	Sequence 5'-3'
SharpinFL	for cccaagcttgccgccaccatgtcgccgcccgccggc
	rev ggaattcggtggaagttgcagtaaggg
Sharpin NT	for cccaagcttgccgccaccatgtcgccgcccgccggc
	rev ggaattcctagagaagaaaaaagttcaaaggtc
pCMV PDZ Nterm	for aaggatccatggatgggattggc
	rev aagaattccctggtgaccatcac
Rpt1	for aactcgagaccatgggtcaaagtcag
	rev aaaaagcttaagagatagacccctc
Sharpin PDZ	for aaaaagcttatgtcgccgcccgcc
	rev aaagtcgacggtggaagttgcagtaag
EDD1	for aagaatccgccaccatgatgtctgctcgaggg
	rev actcgagcacaaaaccaaaattcttgg
OS-9	for aactcgaggatccatatggcggcggaggcgc *
	rev ttgctagcgtcgacgaagtcaaactcatcc
S5a	for aagaattcatggtgttggaaagcactatgg
	rev aactcgagtcacttcttgtcttcctccttc
Asp58Ala	for gctgtctgcttacaacattc
	rev atgttgtaagcagacagcg
Ile44Ala	for gattggcctttgccggtaag
	rev taccggcaaaggccaatc
Ubiquitin	for aggaattcagattttcgtcaagactttg
	rev agcctcgagttaaccacctcttagccttag
pACTM	for aagaattcatgccgccatggagctggctacacacctg
	rev aagaattcatgccgccatgggacacagccctcaacactcc

* PCR product was generated with these primers, but the OS-9 signal peptide was subsequently removed using an internal Hind III site.

for = forward primer
rev = reverse primer

Biography

The author of this thesis was born in Mt. Clemens, Michigan, USA. After receiving her Bachelors degree from the University of Michigan (Dearborn Campus), she worked for four years in the laboratory of Morris White at the Joslin Diabetes Center, a Harvard Medical School affiliation, in Boston, Massachusetts. After a one year stay in Robert Schwinger's laboratory at the university clinic in Köln, she decided to obtain a Ph.D. degree. To this end she first set about acquiring a German diploma degree in biology from the University of Hamburg. In 2004, she then began work for this Ph.D. thesis in the laboratory of Privatdozent Dr. Hans-Jürgen Kreienkamp.

Acknowledgements

I would like to thank Dr. Hans-Jürgen Kreienkamp for giving me the opportunity to complete my Ph.D. thesis in his laboratory, for being a great boss, and for dealing with my somewhat hectic tendencies.

I would also like to thank Prof. Dietmar Richter and Prof. Andreas Gal for generously allowing me to work in their respective institutes, the former Institut für Zellbiochemie und Klinische Neurobiologie and the Institut für Humangenetik.

I thank Prof. Bretting for kindly agreeing to review this written thesis on the part of the Biology Department from the Universität Hamburg and I also highly appreciate the willingness of all members of my defence committee to sacrifice time and effort for their participation in my disputation.

In addition, many thanks to present and former members of the Kreienkamp lab for their assistance and ideas: Kerstin Berhörster, Katrin Falley, Tarja Kokkola, Chong Wee Liew, Marie Mameza, Arne Quitsch, Corinna Sawallisch, Sabine Sieber, Mattias Vöckel, and last and most importantly Hans-Hinrich Hönck.

Lastly, I would like to thank my family for being a constant source of support in all of my endeavours and my husband for his proofreading services and constant support throughout the past few years.